Synthesis of Polymeric Nanoparticles for the Controlled Release of Hydrophobic and Hydrophillic Theraputic Compounds

by

Jiang Xu

A thesis

presented to the University Of Waterloo

in fulfillment of the

thesis requirement for the degree of

Doctor of Philosophy

in

Chemical Engineering (Nanotechnology)

Waterloo, Ontario, Canada, 2016

AUTHOR'S DECLARATION

I hereby declare that I am the sole author of this thesis. This is a true copy of the thesis, including any required final revisions, as accepted by my examiners.

I understand that my thesis may be made electronically available to the public.

ABSTRACT

Polymeric nanoparticle (NP) drug carriers present a promising technology for controlled release since they are capable of improving the encapsulation efficiency and stability of the drugs inside the NPs and also able to provide effective drug levels over a longer period of time, compared to traditional therapy. However, before the NP drug delivery technology becomes a reality, important parameters of NPs like size, drug loading ability and sustained release kinetics must be well investigated and optimized in order to minimize the adverse effects of chemotherapeutic compounds and prolong the drug releasing profile in a controlled manner.

In order to accomplish this objective, this thesis proposed two novel methods for synthesis of NPs as drug delivery carriers, with assistance from bulk and microfluidic technologies, for hydrophobic and hydrophilic drugs, individually.

For encapsulation of hydrophobic drugs, a modified flow focusing method was developed on a glass capillary microfluidic platform. Unlike conventional microfluidic flow focusing using two miscible phases, an insoluble component (DCM) was introduced into the dispersed phase to form a partially water-miscible precursor, and a transformation phenomenon of "jet—micro droplets--nanoparticles" was firstly observed instead of the "jet—micro droplets" or "jet—nanoparticles" from traditional flow focusing. Using Doxorubicin as a drug model, size-tunable Doxorubicin-PLGA NPs (80~170 nm) were synthesized by adjusting the flow rates, polymer concentration and the volume fraction of DCM in dispersed phase with an excellent monodispersity (PDI=0.1~0.2) which was superior to those from conventional flow focusing. We also found that drug loading content increased when volume ratio of DCM/DMSO in dispersed phase increased, with a considerable mass loading ratio up to 26.3%. In addition, Doxorubicin-PLGA NPs synthesized with DCM/DMSO precursor exhibited a slower drug release profile than those synthesized with pure DMSO precursor.

This modified flow focusing method can also be extended to encapsulate inorganic compounds, such as iron oxide (Fe_2O_3) for a combination of chemotherapy and thermo-therapy, and showed a better loading ability of Fe_2O_3 than conventional research using

pure DMSO. This method successfully combined the advantages from previous classical drug encapsulation techniques: small particle size, ease to operation—like nanoprecipitation; monodispersity, high drug encapsulation efficiency—like emulsion-based methods, provided us a promising tool for preparing nanoparticle carriers for multiple drug loading of both organic drugs and inorganic compounds

For encapsulation and release of hydrophilic drugs, a modified bulk drop-wise nanoprecipiation method was designed by separating drug and polymer into aqueous and DMSO phases, respectively. In this case, we successfully solved the problem of the poor solubility of hydrophilic drug in organic solvents, for which reason the traditional nanoprecipitation method was limited to the application of hydrophilic drug encapsulation. Monodisperse ciprofloxacin-loaded PLA (poly (D,L-lactide))-Dextran and PLGA-PEG (poly (lactide-co-glycolide)-block-poly (ethylene glycol)) NPs were prepared of a tunable size range (80~200 nm). The drug loading ability, up to 18.6% (w/w), was found having an excellent linear correlation with the original feed of the ciprofloxacin drug, which indicated that drug content encapsulated by the NPs could be precisely controlled and an *in-vitro* sustained release was achieved up to 95.4% in 6 days.

This thesis demonstrated the design and mechanism of different drug encapsulation and release systems; and synthesis, characterization, and optimization of drug-loaded polymeric nanoparticles. Our novel drug delivery systems significantly improved the encapsulation efficiency of various therapeutic compounds and exhibited a sustained-release profile. These nano-drug-delivery systems exploited intrinsic properties of NPs for controlled release, and will not only benefit the field of nanobiomedicine, but also could be further applied to food, flavor, fragrance and cosmetics industry.

ACKNOWLEDGEMENTS

If I may get serious for a moment, this Ph.D. has been one of my most crazy rides, with all its ups and downs. From October 1st, 2012 to today, nearly 4 years, more than 1300 days, this long, tough but wonderful Ph.D. journey finally comes to its end. Looking back on this period, I would like to thank all the people involved in these past 4 years with me. You are the very important and indispensable reason that why I can finish this thesis.

First and foremost, I would like to thank my two supervisors, Prof. Annie Colin and Prof. Frank Gu, for their guidance and help. From Prof. Annie Colin, I have not only learned knowledge and research skills in the labs, but also gained encouragements, recommendations and advices for my career path. I am deeply impressed me by her critical research attitude and extensive expertise, and touched by her kindness and warm instructions in my daily life. With her help, I have grown up as an independent researcher from that fresh man in microfluidic field, in these 4 years. I also enjoy the time in Prof. Frank Gu' lab, where I got basic training and fundamental knowledge of controlled release. One-to-one talk with him has been always relaxing but inspiring, and he keeps encouraging me to deeply dig into my research and do something new. I deeply appreciate the open but critical, bold but prudential research spirit they brought to me, which benefited me so much in my Ph.D. study.

I would also like to thank my committee members, Prof. Juewen Liu, Prof. Michael Pope, Prof. Tsui Ting from University of Waterloo, for their guidance and supervision of my Ph.D. comprehensive exam. Their fruitful comments and suggestions helped me modify my research routine and shaped my thesis. In addition, I would like to express my appreciation to the French jury, Prof. Jerome Bibette, Prof. Marie Caroline Julien, Prof. Sébastien Lecommandoux, for reading this thesis and sharing their opinions. I would also like to deeply acknowledge Prof. Olivier Sandre, for his help about the drug encapsulation and release test in LCPO. Without his enthusiastic instructions and encouragement, this project can't be finished smoothly.

It is lucky for me to have experience of studying and working in different countries

and groups during my Ph.D, and I get a chance to know these lovely lab members and friends. I am especially graceful to the co-op student, Ms. Yuyan Chen; the current and former graduate students in Waterloo, Dr. Shengyan Liu, Erin Bedford, Jasper Huang, Paul Chen, Tim LeShuk, Sarah LeBlanc, Peter Lin, Stuart Linley and Dr. Mohit Verma; the friends and colleagues in Bordeaux, Dr. Shusheng Zhang, Dr. Uyxing Vongsaysy, Dr. Mylène Le Borgne, Dr. Edgar Cao, Mehdi Neqal, Dr Julien Rolly, Dr. Hongyu Chen, Dr. Pierre Guillot, Dr. Steven Meeker, Dr. Vincent Miralles, Dr. Patrick Maestro, Gerald Clisson, Dr. Lingguo Du, Hao Pan, Yu Zhou, Tianjiao Cai, Qianwen Wu, Xuejiao Yin and Dr. Na Liu. Their friendship and support accompanied my entire Ph.D. study.

Family is always my warmest haven. I am extremely grateful for my parents and my girlfriend for their endless encouragement and constant support. In addition, I would like to dedicate this thesis to my beloved grandfather who warmed and sweetened my entire childhood, but passed away twelve years ago because of liver cancer. This is the most important reason for me to select drug release area as the topic of my thesis. I wish I could contribute something to cancer treatment for human beings, even if just a little bit.

Finally, I want to thank for the financial support provided by the Erasmus Mundus Scholarship from the European Commission, the UW Graduate Research Studentship, and the UW Graduate Scholarship. Additionally, I am also grateful for the accommodation and technical support from Lab of Future of the industrial partner Solvay.

TABLE OF CONTENTS

List of Figures

List of Tables

Chapter 1 INTRODUCTION

1.1 Overview

Drug delivery system (DDS) plays an increasingly important role in treatments for various diseases nowadays[1], which can be performed through different organs like eye, nose, ear canal, vagina, rectum and mouth or through dental, transdermal, subcutaneous, intramuscular injection or implantation. Drugs from DDS is released or absorbed in a controlled rate and so that could be maintained at a safe, stable and efficient concentration. Currently, combination of DDS and nanomedicine attracts growing attentions from researchers with the advancement of nanotechnology to solve a number of existing challenges. Biocompatible polymeric nanoparticles (PLGA, PLA[2] and their copolymers, etc.) are considered to be promising drug delivery carriers since they are capable of encapsulating bioactive agents for therapeutic proposes and their high area-to-volume ratio ensures a great potential to conduct an effective release[3]. In addition, NPs could improve the stability of drugs and tiny NPs of sub-100nm range are able to circulate with blood and accumulate in tumor areas by the enhanced permeability and retention (EPR) effect.

Drugs can be distinguished as two categories: hydrophobic and hydrophilic, and different encapsulation techniques are chosen according to this property to fabricate drug-loaded NPs. However, problems like low encapsulation efficiency, low controllability over the size and drug loading ability of particles and complex protocols still exist in the encapsulation methods for both hydrophobic and hydrophilic drugs which need to be optimized before their further biomedical applications.

(1) Conventional nanoprecipitation method, mixing one miscible fluid in water, mainly used for encapsulation of hydrophobic drugs, could bring us very small NPs. But we have to bear the consequences that relatively low encapsulation efficiency and board distribution of the nanoparticles during the bulk mixing procedure. Microfluidic technology is previous used to solve this problem, however, partially: The droplet-based microfluidics is able to produce homogenous O/W emulsion, yet of micro sizes; flow-focusing microfluidics is able to produce smaller particles, yet relatively lower

encapsulation efficiency. We are thus motived to combine the advantages of these two techniques together: fabricating highly uniform nanoparticles as drug delivery carriers and improving the encapsulation efficiency of hydrophobic drugs at the same time.

A modified microfluidic flow focusing technique has been proposed to solve this problem that we used a mixed solvent of DCM/DMSO instead of pure DMSO as a dispersed phase. With the diffusion of DMSO into water, the insoluble DCM was left with PLGA NPs so that monodisperse droplets were generated and these droplets could transfer to nanoparticles afterwards. In addition, since DCM has a strong surface tension with water, more hydrophobic drugs can be preserved when using Doxorubicin and Tamoxifen as drug model because DCM creates a good solvent condition inside the nanoparticles. By controlling the flow rates of Q_w and Q_{oil}, polymer concentration and volume fraction of DCM in dispersed phase, highly uniform PLGA NPs were synthesized with a precisely-tunable size.

(2) While nanoprecipitation technology is highly-efficient, easily-handled and rapid, it has, to date, had limited potential to encapsulate hydrophilic drugs due to the poor solubility of these drugs in organic solvents[4]. So the encapsulation of most hydrophilic drugs are accomplished by multiple-step-emulsion techniques e.g., tetanus toxoid encapsulated by solid-oil-water emulsion, methylene blue entrapped by emulsion solvent evaporation and water-oil-water encapsulation of insulin by double emulsions. However, the emulsion-based encapsulation methods also suffer from the weak controllability over the size of particles and complex preparation process.

Thus we developed a new modified drop-wise nanoprecipitation method, the biggest difference of which from the conventional one is the drug and polymer were separated into organic phase and aqueous phase individually. Monodispersed ciprofloxacin-loaded poly (D,L-lactide)-dextran and PLGA-PEG nanoparticles were formed through a simple drop-wise mixing process. The characterization of morphology and the encapsulation efficiency of PLA-DEX and PLGA-PEG NPs were assessed. In addition, the relationship of initial concentration of ciprofloxacin the mass loading ability of PLA-DEX and PLGA-PEG NPs were investigated and a cumulative release of ciprofloxacin was evaluated *in-vitro*.

(3) It is highly desirable that nanoparticle carriers can not only deliver anti-cancer drugs to tumor sites, but also provide thermotherapy[5] as a second treatment addition to chemotherapy. Currently, there is limited range of mature drug delivery systems that could satisfy: (i) multiple loading of drugs and magnetic contents; (ii) biocompatibility and non-toxicity; (iii) stability of drugs and inorganic components.

Nanoparticle drug delivery technology may provide a more efficient, harmless solution to overcome these problems. Dual loading of anti-cancer drugs and magnetic nanoparticles can be achieved within polymer carriers through simple procedures[6]. However, NPs prepared by chemically-conjugated[7] or conventional nanoprecipitation method[8] are limited by low loading ability of magnetic iron oxide nanoparticles, which directly affects its ability of transferring magnetic energy to heat energy, thus lower the effect of hyperthermia.

We were inspired by the great drug loading ability of modified microfluidic flow focusing method described in Section 1.1 (1), and therefore, applied it to dual loading of drug and iron oxide nanoparticles. PTMC-*b*-PGA polymer vesicles were prepared by the same microfluidic platform using a DCM/DMSO mixed precursor, with a uniform distribution. The morphology of the PTMC-*b*-PGA vesicles were measured and confirmed. The drug encapsulation efficiency of drug and iron oxide components were determined, individually. In addition, the influence parameters on the encapsulation efficiency and size of NPs, like polymer composition, flow ratio, initial drug feed were investigated.

1.2 SCOPE AND OBJECTIVES

The objective of this research is to synthesize functional polymeric nanoparticles for encapsulation and controlled release of therapeutic compounds. According to the different solubility of hydrophobic and hydrophilic drugs in aqueous and organic solvents, two different drug encapsulation methods should be developed, respectively, in order to modify the important properties of NPs such as size, encapsulation efficiency and sustained release ability for further biomedical application. So we divide our works

into two parts: for hydrophobic drugs and for hydrophilic drugs.

(i) For hydrophobic drugs, it is hypothesized that the encapsulation efficiency of hydrophobic drugs by nanoparticles from emulsion-based method is higher than that from nanoprecipitation method and nanoparticle synthesized by nanoprecipitation method may be smaller than that from emulsion-based method. There may be possibility to combine these two encapsulation methods together by microfluidic technology using a partially water-miscible precursor, and remain both of their advantages. A Microfluidic technology may serve as a promising tool to produce nanoparticles to encapsulate hydrophobic drugs. By achieving these desired properties, uniform nanoparticles may be synthesized around sub-200 nm size range and with a great encapsulation efficiency of hydrophobic drugs. In addition, previous literatures indicated that the encapsulation of iron oxide nanoparticles and be achieved in bulk emulsion or nanoprecpitation methods, which may open potential for dual loading of inorganic metal nanoparticles and organic drugs, and provide a fundament for combination of thermotherapy and chemotherapy. Further investigation is possibly about the mechanism of self-assembly behavior of nanoparticles by microfluidic flow focusing and controlling important parameters of the drug-loaded nanoparticles, such as size and distribution, encapsulation efficiency and release profiles.

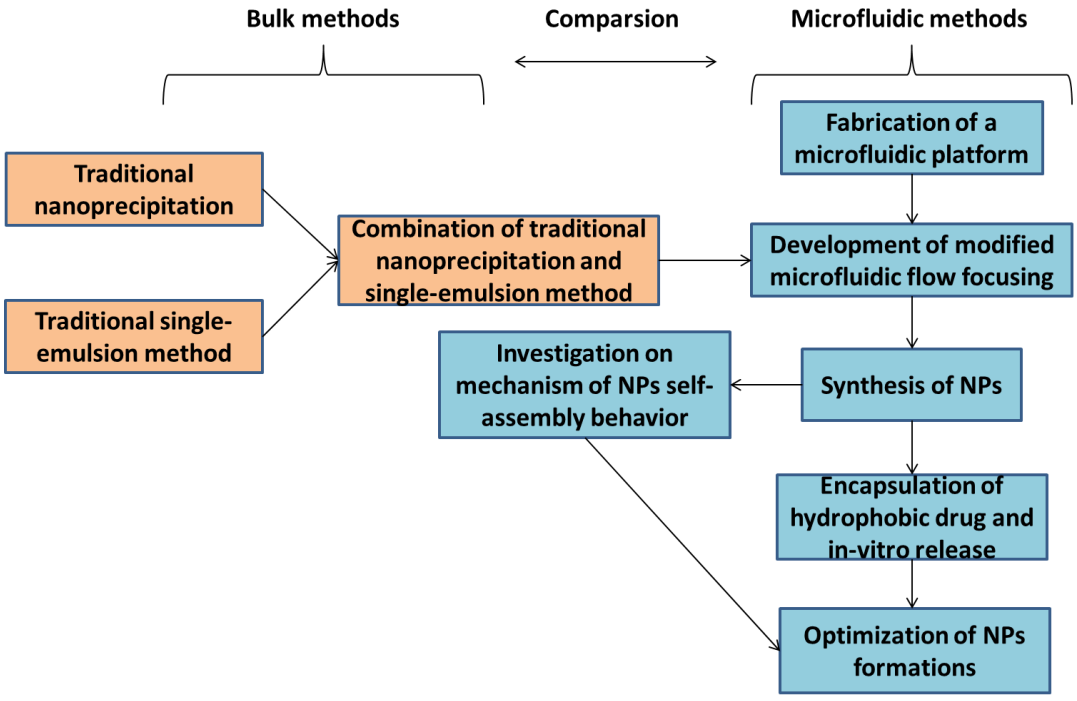

Figure 1. Summary of scope and objectives: Modified microfluidic flow focusing using a partially water-miscible precursor for encapsulation and controlled release of hydrophobic drugs

The work flow chart of this part is demonstrated in Figure 1 and the specific objectives to test the hypotheses are described below:

(1) Synthesize nanoparticles by traditional nanoprecipitation method, emulsion method and "emulsion + nanoprecipitation" method in bulk experiments, individually
(2) Characterize and compare size and distribution of nanoparticles, encapsulation efficiency and *in-vitro* release profiles by these three methods
(3) Design and fabricate a robust microfluidic platform using a partially water-miscible precursor to synthesize nanoparticles
(4) Investigate the formation process of nanoparticles and the impact factors over the size and distribution of nanoparticles
(5) Demonstrate encapsulation and *in-vitro* controlled release of hydrophobic drugs by the microfluidic platform
(6) Preform multiple loading of inorganic iron oxide nanoparticles and organic anti-cancer drugs
(7) Compare the results with different drugs, microfluidics, and bulk methods
(8) Modify parameters of NP formations to optimize its size and distribution, surface properties, encapsulation efficiency and controlled release.

(ii) For hydrophilic drugs, it is hypothesized that hydrophilic drugs dissolved in aqueous solvent can be encapsulated by polymer nanoparticles during the drop-wise nanoprecipitation. High drug/polymer ratio may lead to drug-loaded nanoparticles with a considerable drug loading ability. These drug-loaded nanoparticles may improve the stability of the drug and prolong the therapeutic release activity. Mechanism of the formation of drug-loaded nanoparticles is to be understood next. This modified drop-wise nanoprecipitation method may have potential to be extended to different polymeric nanomaterials and drugs and important parameters like particle size, distribution and

drug loading ability are possible to be tuned for optimization.

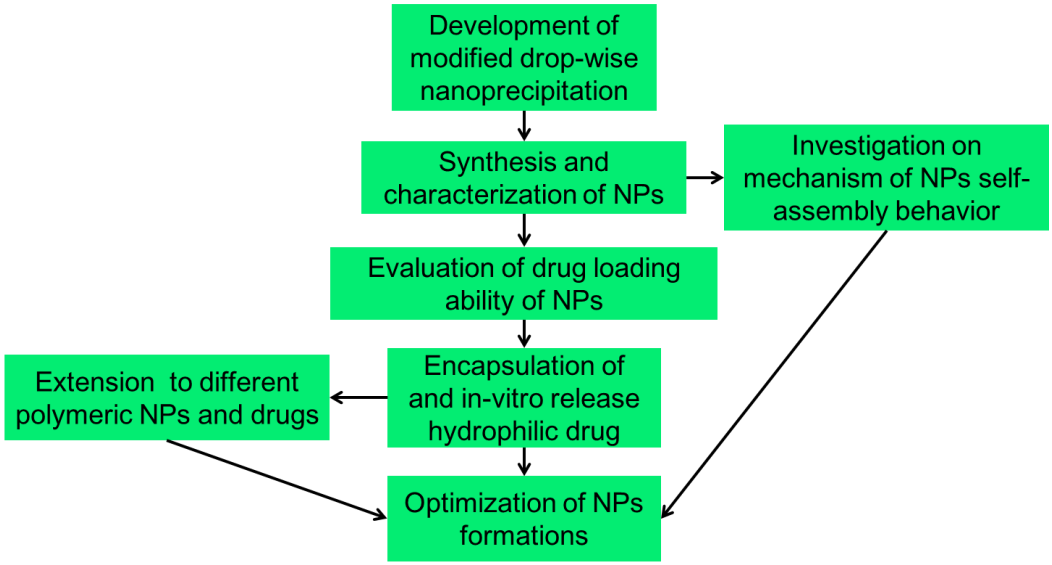

Figure 2. Summary of scope and objectives: Modified drop-wise nanoprecipitation for encapsulation and controlled release of hydrophilic drugs

The work flow chart of this part is demonstrated in Figure 2 and the specific objectives to test the hypotheses are described below:

(1) Synthesize drug-loaded nanoparticles by modified drop-wise nanoprecipitation

(2) Characterize the size and morphology of nanoparticles

(3) Perform encapsulation of hydrophilic drugs and evaluate the drug loading ability

(4) Demonstrate *in-vitro* release profiles and compare with ones from free drug group

(5) Modify the NP formations to optimize its size and distribution, surface properties, encapsulation efficiency and controlled release.

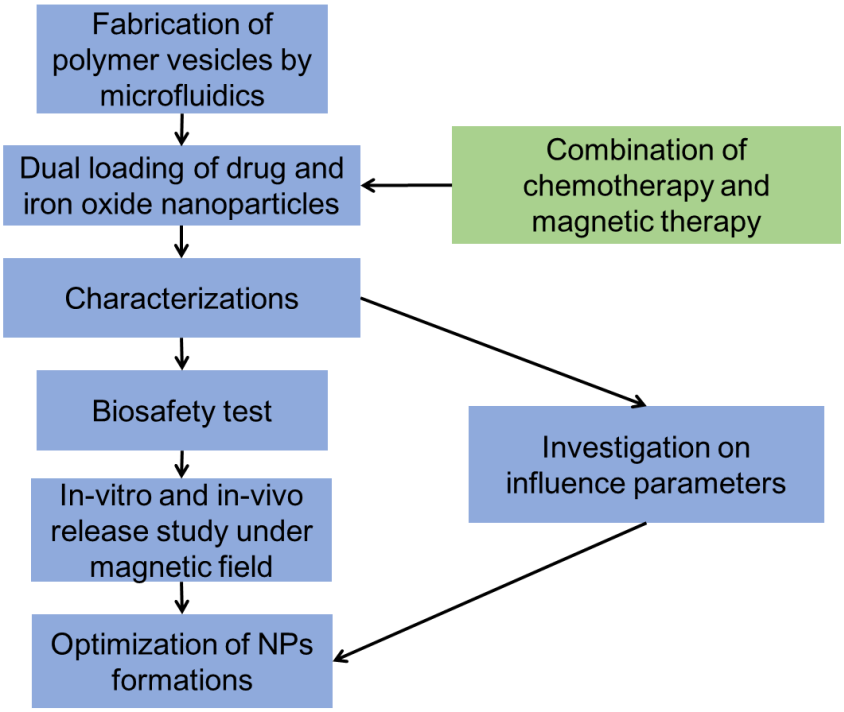

Figure 3. Summary of scope and objectives: Combination of chemotherapy and magnetic therapy, dual loading of drugs and iron oxide nanoparticles.

The work flow chart of this part is demonstrated in Figure 2 and the specific objectives to test the hypotheses are described below:

(1) Apply same microfluidic technology to fabricate uniform polymer vesicles using amphiphilic block polymers

(2) Dual encapsulate anti-cancer drugs and iron oxide nanoparticles

(3) Determine the morphology and structure of the drug/iron oxide-loaded vesicles

(4) Measure the encapsulation efficiency of drugs and iron oxide nanoparticles

(5) Test the biocompatibility of the drug/iron oxide-loaded vesicles in the cell culture

(6) Perform in-vitro and in-vivo drug release study under the magnetic field

(7) Investigate influence parameters on the drug loading ability, particle size, drug release rate, and hyperthermia effect for optimizations.

1.3 Thesis Outline

This thesis consists of one chapter of introduction of the Ph.D. research project, one

chapter of literature review, and followed by three research-based chapters and one chapter of conclusion and perspectives.

Chapter 1 outlines the background, existing problems to be solved, scopes, and objectives of this thesis

Chapter 2 reviews the current art states of developments of different encapsulation and release methods for hydrophobic, hydrophilic drugs, and combination of thermotherapy and chemotherapy, respectively.

Chapter 3 demonstrates the design and fabrication of a modified microfluidic platform using a partially water-miscible precursor to improve the encapsulation efficiency of hydrophobic drugs and drug loading ability of polymeric nanoparticles. Physical mechanism of evolution process of the partially water-miscible precursor in the microfluidic channel is firstly investigated. The effects of parameters on the formation of drug-loaded nanoparticles and release profiles are then discussed, including hydrophobicity of drugs, flow ratio, polymer concentration, drug/polymer feed ratio, and volume ratio of immiscible component.

Chapter 4 shows formation of drug-loaded NPs by the modified drop-wise nanoprecipitation to improve the loading ability of hydrophilic drugs. The self-assembly mechanism of hydrophilic drug-NPs is firstly investigated. Then the drug loading ability of different polymers and drug/polymer feed ratio are compared, and the effect of hydrophilicity of the co-polymers on the drug release rate are discussed as well

Chapter 5 utilizes the microfluidic technique developed in Chapter 3 to investigate the possibility of dual loading of inorganic iron oxide nanoparticles and organic therapeutics. The potential of this microfluidic method for multiple drug loading over conventional bulk methods, like monodispersity of NPs, smaller NP sizes, and higher drug loading content are illustrated. This chapter also provides proof-of-concept of combing magnetic therapy and chemotherapy using a facile microfluidic tool.

Chapter 6 concludes current achievements of this work so far and looks head the future perspectives of this thesis. One of the key avenues of this research is exploiting different drug encapsulation methods for fabricating drug-loading NPs with a considerable loading, according to the hydrophobicity or hydrophilicity of the drug.

Secondly, these methods are able to be extended to applications of various polymers, drugs, inorganic contents. Additionally, to industrialize and scale-up these encapsulation and release systems, an understanding of interactions of hydrophobic/hydrophilic drugs and NPs needs to be established

Chapter 2 LITERATURE REVIEW

2.1 Polymeric Nanoparticles (NPs)for drug delivery

Nano drug delivery system (DDS) refers to chemically and/or physically loading therapeutic compounds within nanomaterials, and forming a mixed system of drug and carriers. The main advantages of nano can be briefly concluded but not limited as: (1) increase the drug concentration in the target organs/tissues/cells to, thereby increasing drug utilization and treatment and lowering side effects[9, 10]; (2) improve the solubility of hydrophobic drugs in aqueous environment[1]; (3) able to deliver drug to targeted organs/tissues/cells[11]; (4) able to deliver biomacromolecules like DNA[12, 13, 14, 15]/RNA[16, 17, 18]/protein[19, 20, 21, 22] which are difficult for cells to uptake to active sites inside the cells. Thus, innovation and development of nano DDSs arise interests from biomedical scientists.

Biodegradable polymers are widely investigated and used for targeted drug delivery[23]. Because of their excellent biocompatibility and biodegradation, polymers like poly (lactic acid) (PLA)[24], poly (lactic-co-glycolic acid) (PLGA)[25] and their copolymers[26, 27], etc., are promising biomaterials that can be fabricated as microspheres and nanospheres[28] containing bioactive agents (drugs, proteins, DNA[12], etc.) for *in vivo* and *in vitro* therapeutic applications[29]. In the other hand, drug-loaded NPs provide us a novel perspective to overcome drawbacks of traditional approaches, such as drug solubility, toxicity[11] and *in vivo* half-life, in a sub-micron or a nano scale.

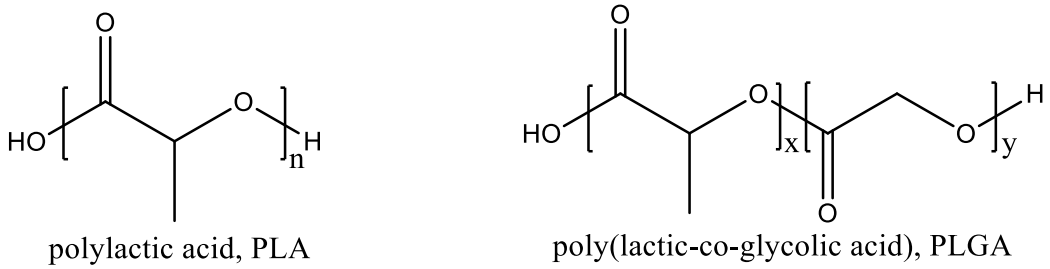

Figure 4. Molecular formula of PLA and PLGA

With various physical or chemical processes, biocompatible polymers could combine with most drugs by hydrophobic or electrostatic interactions and form functional NPs

of different structures, like micelles[30], core-shell, hydrogel[31], star, dendrimer, liposomes[32] and polymersomes[33, 34, 35] (Figure 5) and be stimuli-responsive[36, 37]. These NPs minimize the side effects of chemotherapeutic drugs and provide optimal drug levels for a longer period of time. The surface of NPs can also be coated or grafted with different functional groups (e.g. PEG[26], peptides[29]) in order to reduce its uptake by organs[38], improve its biocompatibility and bind targeting receptors[11].

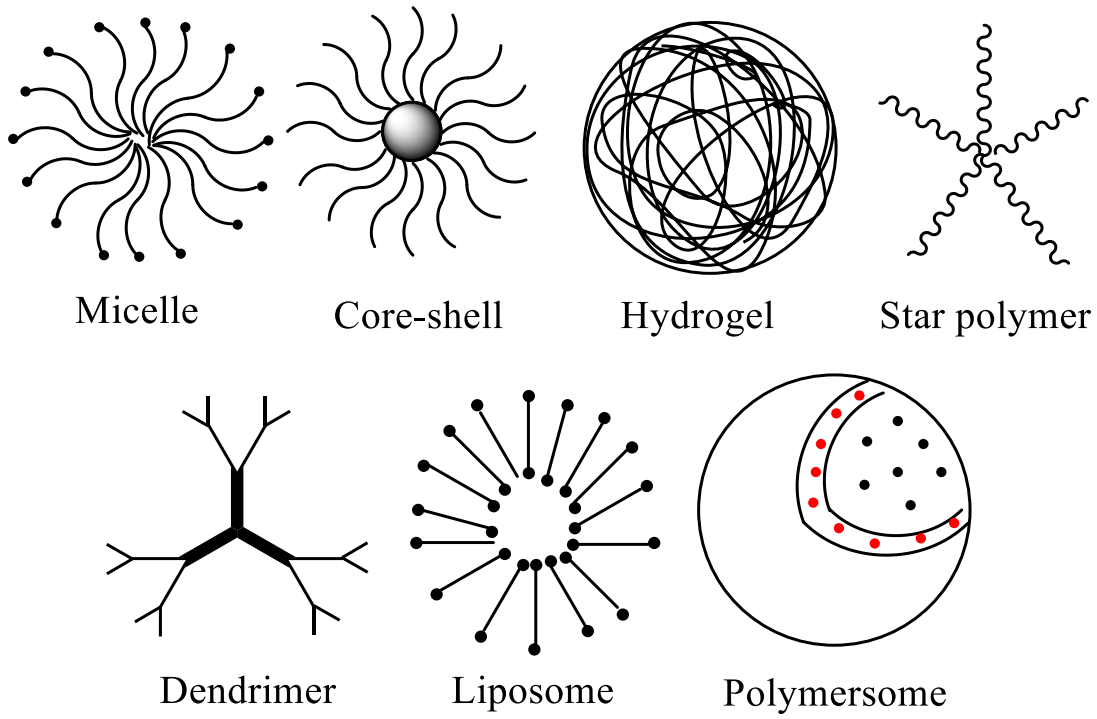

Figure 5. A schematic illustration of different structures of polymeric nanoparticles

However, several important parameters of NPs such as density of targeting receptors, drug loading ability, surface charges, morphology, hydrophilicity, etc. still need to be optimized[39], before targeted controlled release therapy becomes a reality.

2.2 Traditional bulk encapsulation methods of hydrophilic/hydrophobic drugs by NPs for drug delivery system

An increasing number of newly innovated drugs that are poorly soluble in common solvents arises a need to develop novel effective methods for encapsulation and delivery[40]. In this chapter, conventional bulk methods to prepare nanoparticle drug carriers will be reviewed and discussed about how they are performed, the reason that they are chosen for hydrophobic /hydrophilic drugs and their advantages and limitations.

2.2.1 Common encapsulation methods for hydrophobic drugs

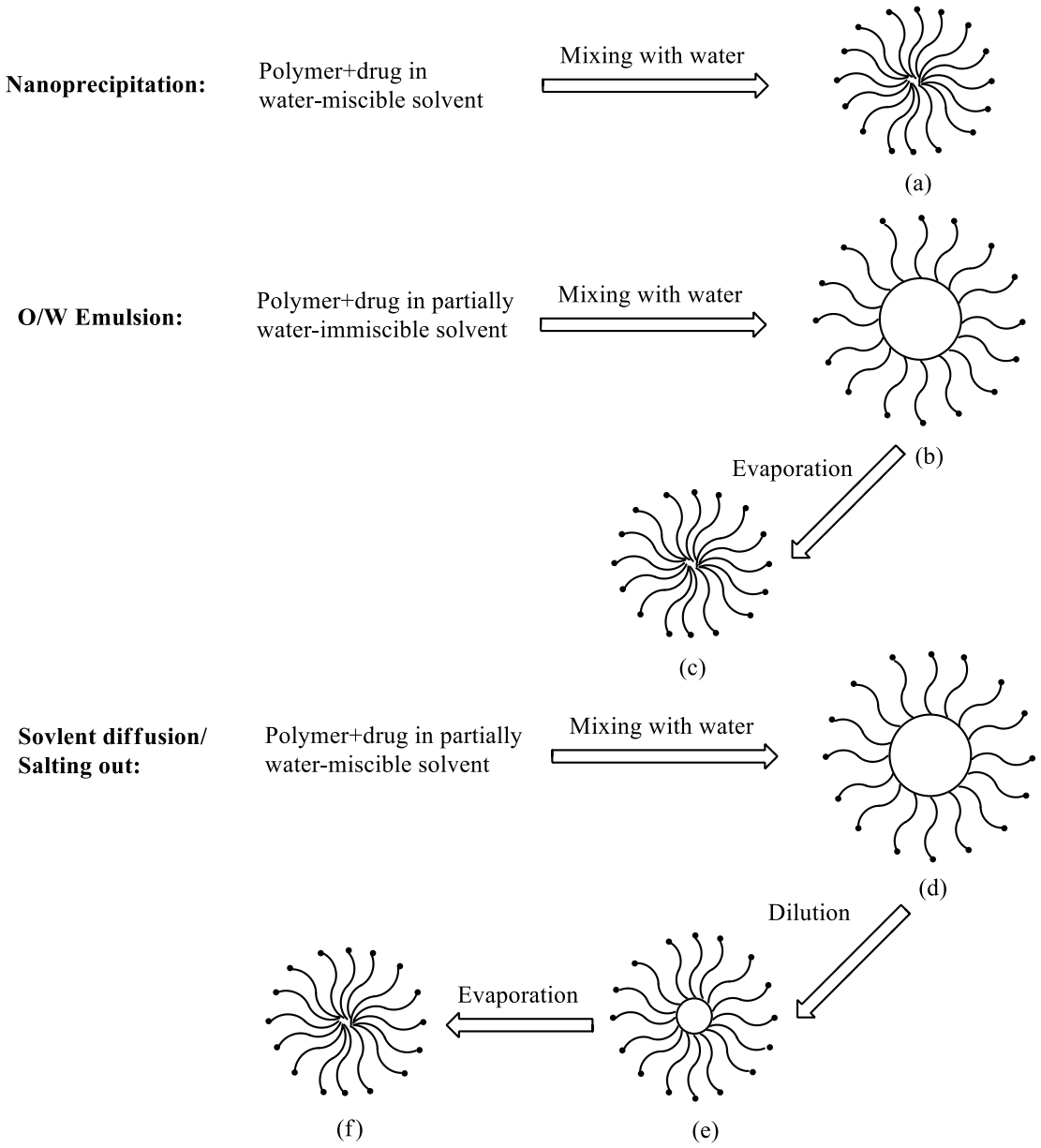

Figure 6. A brief flow chart of different encapsulation methods for hydrophobic drugs: (a). Formation of NPs after solvent evaporation, (b). Emulsion droplets containing water-immiscible contents, (c). Formation of NPs after solvent evaporation, (d). Emulsion droplets containing both water-miscible and water-immiscible contents, (e). Emulsion droplets containing water-immiscible contents after dilution, (f). Formation of NPs after solvent evaporation

2.2.1.1 Nanoprecipitation

Nanoprecipitation has grown up to one of the most commonly used methods for synthesis of polymeric hydrophobic drug-loaded NPs, which was firstly invented by H. Fessi et al[41] in the late 1980s. A typical process (Figure 6.a) of nanoprecipitation is like

this: polymer (or with drugs) were dissolved in same water-miscible organic solvents (dispersed phase) and then drop-wisely mixed with aqueous solution (continuous phase).The one-step formation of nanoparticles is due to the interfacial deposition of polymer (or with drugs) because of the interfacial solvent displacement between two different unstable liquid phases[41]. An incredibly amount of drugs (cyclosporine A, DOX, doctaxel, paclitaxel, etc.) and polymers (PLGA, PLA, PCL, PMMA, etc.) are able to be used to prepare NPs by nanoprecipitation. Important parameters of NPs, e.g. size, distribution, encapsulation efficiency, etc. can be easily tuned by controlling different experimental conditions of nanoprecipitation, such as O/W ratio[42], pH[43], polymer/drug ratio[44], block ratio of block polymers[45], solvent selection[46] and etc.

Since basically no external energy or surfactant is required for the formation of NPs, nanoprecipitation is indeed a facile and neat procedure. The solubility of drugs and the miscibility of solvents[46] with water are the dominating parameters for the results. The general encapsulation efficiency of hydrophobic drugs by nanoprecipitation method is less than 50%[47] and the loading ability is around 10% (weight ratio) [44]. In contrast, hydrophilic drug usually has a poor encapsulation efficiency by nanoprecipitation because it different solubility from polymer, though some attempts[48] are tried to improve its entrapment in NPs. In addition, the traditional nanoprecipitation is still currently limited inside labs due to its drop-wise operation, and the difficulties of extraction, recovery and reservation of NPs.

2.2.1.2 Oil/Water Single Emulsion

Emulsion-based methods are another kind of widely adapted techniques for hydrophobic drug encapsulation. Unlike nanoprecipitation procedure, water immiscible organic solvents are usually used in order to make emulsions. Compared to nanoprecipitation methods, NPs from emulsification procedure vary in particle size, drug-loading ability, etc. Different emulsion-based methods will be discussed in this and following sections.

O/W single emulsion is the most commonly used method to prepared NPs. It normally contains two steps (Figure 6.b, c): (1) Polymer and drug are dissolved in a volatile solvent (e.g. DCM, THF, etc.) and mixed with aqueous solution by sonication or high-speed stirring to form micro-sized or nano-sized emulsion; (2) The volatile solvent are removed gradually under evaporation.

Facile, rapid and easy to control, the O/W emulsion is regarded as a general method in drug delivery area that are suitable for many different kinds of solvents, such as ethyl acetate[49], DCM[50, 51, 52, 53]and chloroform[54],and polymers (e.g. Pluoronic F68&127[49], PS[54], PLGA[50, 51], PLA[50], PCL-PEG[15] and their copolymers[55]) and common drugs (DOX[56], docetaxel[57], paclitaxel[55], cyclosporinA[58], etc.). Multiple drug contents can be incorporated simultaneously[56]and high encapsulation efficiency (usually more than 80%, even close to 100%)[59] can be achieved as well. Conventional procedure may lead to unstable emulsion droplets so that surfactants like PVA[52, 53, 56] are required sometimes. Smaller emulsion particles are found having a "burst" sustained release[52] compared to larger ones, since smaller droplets suffer from a higher surface/volume ratio which accelerates the transportation of drugs, which means we need to find a balance point between the size and properties of NPs.

As for nanoprecipitation, the solubility of drugs also determines that the application of O/W single is mainly limited with hydrophobic drugs, however, , there are some efforts are made to break this boundary[60]. The residue of volatile solvent inside the NPs is a potential hazard for *in-vivo* therapy and the un-stability and polydispersity of emulsion droplet are the other issues to concern about.

2.2.1.3 Solvent Diffusion Emulsion

Solvent diffusion emulsion is another popularly used approach for preparation of nanoparticle drug carriers which was firstly reported by Y. Kawashima et al[61]in 1993. In this method, the polymer and drug are dissolved a partially water-miscible solvent (e.g. acetone+DCM[62]) which is pre-saturated by water, then drop-wisely added into

aqueous solution to form O/W emulsion droplets. The droplets are further diluted by an additional significant amount of water and the rapid diffusion of organic solvent into water induces the formation of NPs (Figure 6d, e, f). A typical solvent evaporation process is usually followed to get rid of the organics. In addition, different formation conditions of preparation could bring NPs with various properties, such as drug-loading ability, morphology and controlled release[13, 63, 64, 65, 66, 67, 68, 69].

This method is a further development of the conventional O/W single emulsion method[66], and could produce smaller NPs with a better monodispersity, which is superior to O/W single emulsion method and W/O/W double emulsion method, since less water-immiscible solvent is introduced into the emulsification thus it becomes easier to control. Generally, the solvent diffusion emulsion is thought of as a supplementary method to prepare hydrophobic drug-loaded NPs[70] besides nanoprecipitation method, however, both E.E. (less than 40%)[62] and drug loading content(less than 10%)[62] inside the nanospheres were still not satisfying. In addition, the large amount of additional diluting aqueous solution during the emulsification may limit its application for hydrophilic drug encapsulation[62]. In addition, the diluted emulsion also increases the difficulties of extraction of NPs and evaporation of volatile solvents.

2.2.1.4 Salting-out Emulsion

The organic solvent involved in salting-out emulsion method is totally miscible with water, like acetone. And the aqueous solution contains salts (magnesium chloride hexahydrate[68], calcium chloride[71], or magnesium acetate tetrahydrate[49])of a high concentration to prevent the diffusion of organic solvent into water. The polymer solution is firstly drop-wisely mixed with water and dispersed in forms of emulsion droplets, then the continuous phased is diluted greatly to induce the precipitation of polymer and drug and the formation of NPs (Figure 6.d,e,f).

So from the perspective of mechanism, salting-out emulsion can be seen as a

derivative of solvent-diffusion method and similarly, hydrophobic drug has much better encapsulation efficiency in salting-out emulsion because of the excess aqueous solution. Also, salting-out technique can be thought of as a modified nanoprecipitation method, however, with a "pause" first step (organic phase against highly-concentrated salt solution, almost no diffusion) and a rapid mixing second step. Compared with these two methods, NPs obtained by salting-out emulsion are usually larger than the ones from nanoprecipitation and smaller than the ones from solvent-diffusion[68], under same experimental conditions. A typical E.E. of this method is around 40% and mass loading ability is around 50%[72]. However, an additional purification step is normally required after salting out agent elimination[72], so is the removal of organic solvent[2]. Besides, a burst-release (>50%) usually happens in the very beginning stage of the release process[72], which means a bad control of the release rate. In addition, important issues like the concentration of salts, O/W ratio and selection of stabilizers are still need to be concerned in order to improve the salting-out emulsion method.

2.2.2 Common encapsulation methods for hydrophilic drugs

2.2.2.1 Water/Oil/Water Double Emulsion

W/O/W double emulsion is a further and supplementary development based on the O/W emulsion. A typical procedure to prepare W/O/W double emulsion (See Figure 7) is: (1) The hydrophilic drug and polymer are dissolved in aqueous solvent and organic solvent individually; (2) The first water-in-oil emulsion is prepared by mixing the two phases by sonication or high-speed shearing; (3) The water-in-oil emulsion is then poured into aqueous solution again to form water-oil-water double emulsion; (4) Microspheres or nanospheres can be produced after evaporation of organic solvent under reduced pressure or heating for further use.

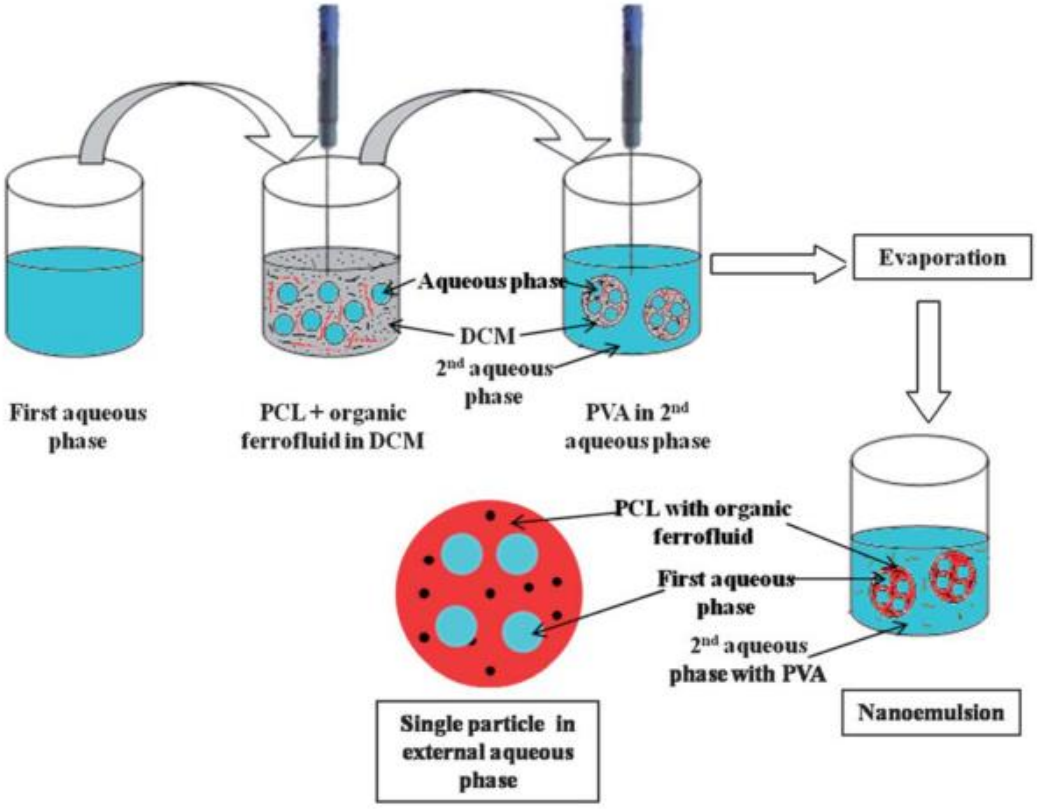

Figure 7. A typical process of double emulsion formation[73].

The double emulsion technique was firstly developed to encapsulate hydrophilic bioactives like proteins[71], insulin[59] and DNA[12], and it also can be applied to synthesize nanocomposites with inorganic materials[73]. Yet it also has potential encapsulation ability for hydrophobic drugs since it contain an organic core at the same time. Y.Y. Yang et al[74] reported a double-wall microspheres made of poly(orthoester) and PLGA with both good encapsulation efficiency of bovine serum albumin (BSA) and hydrophobic cyclosporin A (CyA). BSA and CyA are entrapped in shell and core, respectively, since their different solubility and both two drugs can be completely released.

The size and morphology or double emulsion NPs can be tuned by modifying the composition of polymers[75], O/W ratio[76], etc. and high encapsulation efficiency can be easily reached[77]. Compared to O/W emulsion, W/O/W double emulsion is easier to get rupture or stratification[51] during the mixing or evaporation, since more dispersed phase are created which thus increases the interfacial energy, which leads to the loss of loaded contents. Typically, good E.E[18] (usually less than 30%) and loading ability[77] (usually

less than 1%)are hard to be both satisfied at meantime. Thus surfactants or emulsifiers are normally required to stabilize the PLA NPs and amphiphilic copolymer[75, 77] is also a preferred choice.

2.2.2.2 Reverse-phase-evaporation (REV)

Reverse-phase-evaporation technique was firstly created in 1978 by Francis Szoka et al[78]. An aqueous buffer is added into organic solvents with lipids and the volatile organic solvents are subsequently removed by evaporation under reduced pressure to form vesicles[79]. A considerable fraction of aqueous phase is then encapsulated by the vesicles with high efficiency[80]. Phosphatidylcholine[81], soybean phosphatidylcholine[82], cholesterol[83]and 1,2–dipalmitoyl–sn–glycerol–3-phospocholinemonohydrate (DPPC)[84] etc., and the mixture of them are commonly used to prepare large unilamellar and oligolamellar lipid vesicles.

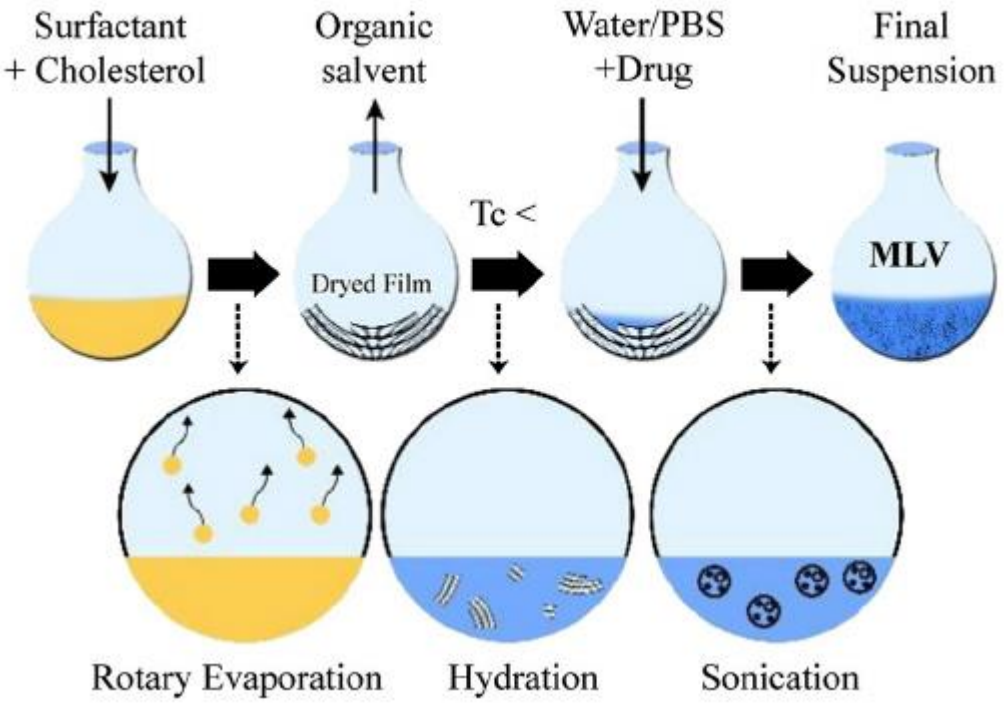

Figure 8. Protocol for niosome preparation through REV method[85]. MLV: Mulit-lamellar vesicles.

Now the REV procedure has been a popular drug encapsulation method, especially for hydrophilic drugs. Hosny[86] prepared ciprofloxacin liposomal hydrogel with soybean phosphatidylcholine (PC) and cholesterol (CH) for ocular treatments. It is found that the entrapment efficiency and permeability of the liposomes can be controlled by

changing the molar ratio of PC/CH. R.C.R. Beck et al[82]developed a novel redispersible liposomal-N-acetylcysteine powder for pulmonary administration. Besides, reverse-phase-evaporation could also be a supplementary method for LBL to encapsulate small neutral water-soluble compounds[87].

However, the controllability over the size and morphology of the vesicles is lacked, which is because vesicles could hardly remain stability after evaporation of organic solvents and coalesces and ruptures[81] of vesicles occur casually. The wide size distribution of the liposomes could lead to a huge loss of drug once the over-sized particles are excluded, e.g., the E.E. goes down from 54.2% to 5.2% when filtered by a 200nm membrane, and the mass loading decreases to 0.08%.[84] In addition, the complex operation procedure and easy permeability[86] of the liposomes may limit its application for long-term controlled release.

2.2.3 Versatile encapsulation methods for both hydrophilic and hydrophobic drugs

2.2.3.1 Layer-by-Layer assembly

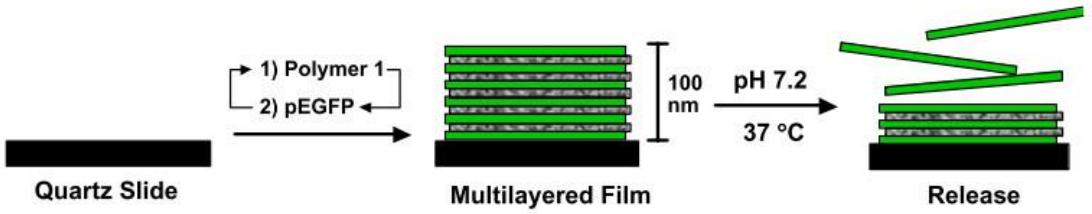

Figure 9. Example of Layer-by-Layer materials[14].

Layer-by-layer (LBL) assembly method is based on the electrostatic attraction[88] or hydrophobic forces[87] between polyelectrolytes, such as poly (ethylene imine)[89], poly-lysine[90], poly (arcylic acid)[91], chitosan, poly(styrene sulfonic acid) and so on. Different bioactive agents frequently play the role of the depositing species to grow a core-shell structure, like BSA, dextran sulfate, glucose oxidase; inorganic materials, e.g. nanodiamonds[90], gold nanoparticles[16], porous $CaCO_3$[92] or silica[93] microparticles can also be used. Then the particles are quenched into drug and polymer solutions step by step[94] to form NPs. The final step is the removal of the template core to make a hollow

structure for further absorption[17], or the drug contents can be encapsulated at the first step, like DNA[14] as the initial core of the NPs so that it could be coated with multi-layer polymers to modify its properties. By regulation of the conditions of LBL cycles[95], multi-layered NPs could be produced with a tunable particle size[96] and a controlled release rate[91].

The LBL method is suitable method for both hydrophilic and hydrophobic drugs since it doesn't depend on the solubility of the drugs to accomplish the encapsulation, but the electrostatic interaction between polymers and drugs. But in the other hand, it also limits the selection of neutral polymers and drugs[87, 97], and the density of the drug within the layers is usually as low as several micrograms per cm^2. Furthermore, the *in-vivo* toxicity, immune-responses[18], leaky shells[87], and the complex preparation process remain severe obstacles to be solved[97].

2.2.3.2 Spray-drying technique

The spray-drying technique was firstly invented by Pamujula et al[98] in 2004 to improve the entrapment efficiency of hydrophilic drugs (proteins[99, 100], ceftazidime, ciprofloxacin[101]). The polymer and lipids are normally dissolved in a volatile organic solvent (DCM, chloroform) and then mixed with aqueous solution which contains drugs to form a W/O emulsion[102]. In the second step, the suspensions are injected through a standard nozzle (0.70mm or 1.0mm) and blew into a chamber with hot nitrogen. By changing the flow rates, size-tunable[103] NPs could be easily obtained. Finally the NPs are collected and dried[104] to further characterization or release study[105].

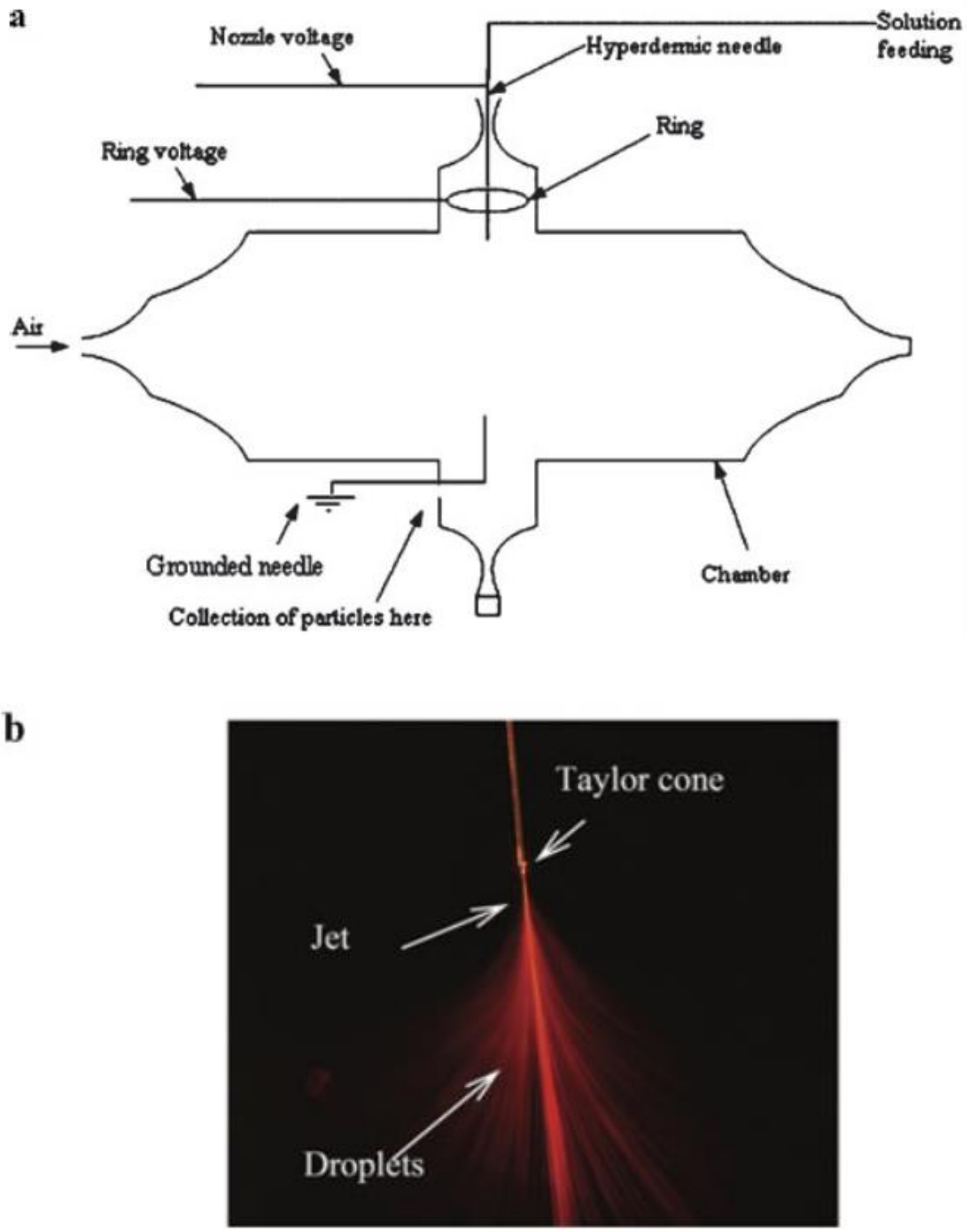

Figure 10. Construction of REV device. (a): schematic representation of the electrospray experimental setup. (b): The schematic of electrospray in the jet mode[99].

The current art-state of this method is more driven by electrospray (voltage difference[99, 103]) than conventional mechanical syringe pumps and NPs can be fabricated with a more narrow distribution (Figure 10). Furthermore, this method is modified and applied to encapsulation of hydrophobic drugs as well. For example, Hirvonen et al.[103]synthesized beclomethasone-dipropionate-loaded and salbutamol-

sulfate-loaded PLA NPs with a diameter around 200nm. However, due to the weaker affinity of hydrophilic drugs with polymer, the encapsulation efficiency of them is usually lower than that of hydrophobic drugs, though mass loading of the latter is just around 1%[82]. Besides, the low electrical conductivity of organic solvents requires additional electrolytes.

2.2.4 Summary

Here we have taken a quick and full view of different bulk encapsulation methods for hydrophobic/hydrophilic compounds. These conventional bulk methods have advantages of ease to operate, cheap costs, high encapsulation efficiency and long-term controlled release, etc. To point out, there is neither an absolutely clear boundary line between different methods, nor a restriction for one method being limited for one single use. With modifications and novel developments, the traditional protocols can be promoted to the area where they never applied before, and combination of different encapsulation methods is a popular trend[49, 56, 82]. The disadvantages of the conventional bulk methods are also obvious---They lack to ability to precisely control over the results: size, distribution, surface properties and drug loading ability of NPs; the wasted drugs and no-recycle increase the expenses; the mixing and evaporation of solvents usually take a period of time. Thus, new encapsulation methods are strongly needed--in a more tiny and precise scale, in a cheaper and faster way and with a safer and more-controllable product. Microfluidic technology is one of the most promising candidates to overcome these drawbacks and will be introduced in the following sections.

2.3 Microfluidic platform for drug delivery system

In this chapter we will introduce the basic concepts of microfluidics and why it is a promising technology in biomedical field. Commonly used materials for microfluidic fabrication and different microfluidic devices are going to be reviewed to compare their advantages and disadvantages. Recent achievements by microfluidics for drug delivery area will be discussed as well.

2.3.1 Introduction of Microfluidics

Microfluidics is the science and technology of systems to manipulate tiny amounts of fluids in an integrated chip having channels with dimensions of tens to hundreds micrometers[106]. The history of microfluidics can be traced back to 1980s and it was firstly adapted to help molecular biology analysis and got incredible development since then. Currently, microfluidics is contributing to various research areas, including biochemistry analysis[107], colloids and interfaces[108], fluid mechanics[109], in-situ synthesis of functional materials[110, 111], rapid screening of drug discovery[112, 113] and cell biology[114], etc. It offers us ability to analyze, separate[115] or synthesize materials by use of small quantities of samples with advantages of low costs, high resolution and sensitivity, good controllability and short experimental time.

A microfluidic system normally includes but not limited to 4 components: power source (syringe pumps, voltage difference), input ports (nanoport, tubing), microfluidic chip (channels, valves, junctions) and output ports (reservoir)[116]. Microfluidic chip is the core part of this system and can be built with different engineering materials, like polymer, glass and resins.

2.3.2 Materials for microfluidic fabrication

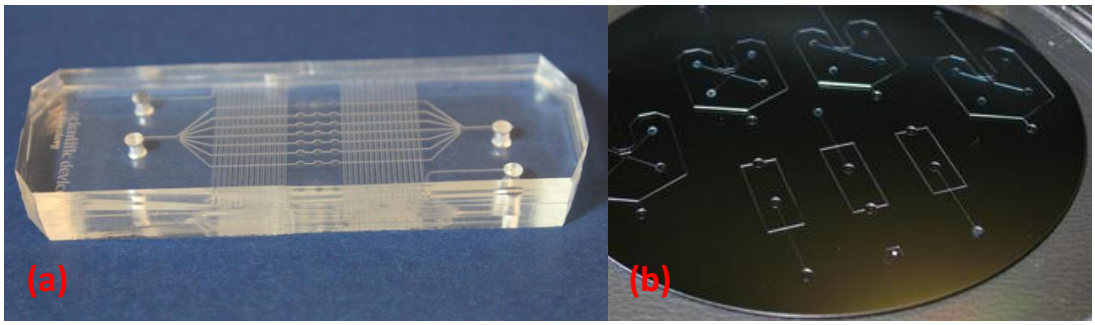

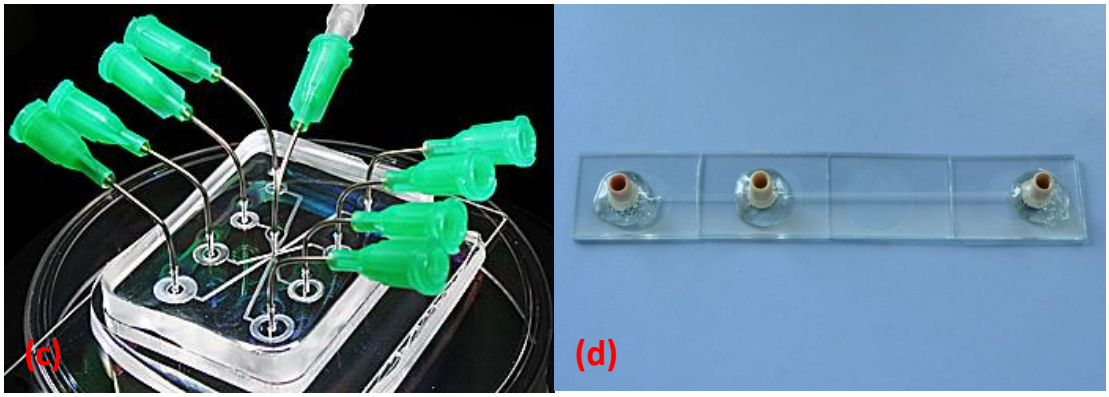

Figure 11. Examples of microfluidics devices. (a). PDMS chip. copyright ©scientific device laboratory. (b) SU-8 chip. copyright © Elveflow. (c). NOA chip copyright © the National Institute of Standards and Technology. (d). Glass microfluidic capillary

Poly (dimethylsiloxane) (PDMS) is the mostly used material to fabricate microfluidic devices[117], which is an optically transparent, elastic and non-toxic thermosetting polymer. Plus tunable flexibility, smooth surface, chemical inertia and ease to cut[118], PDMS is a superior platform to support most engineering components: valves, tubes, adhesives, electrodes, corrosive solvents and so on[119]. By changing the heating temperature molar ratio of curing agent and monomer, the bulk PDMS can be polymerized with different softness. With the development of soft lithography technique, hundreds of micron-scaled or even nano-scaled (nanofluidics) channels with a 3D structure could be easily built on a PDMS chip of less than 10 cm^2 (Figure 11a). However, the highly hydrophobic nature of PDMS[120], makes it normally requires surface modification by UV/ozone plasma[121, 122, 123] when applied to aqueous solution and leakage usually occurs under high pressure or after multiple-cycles of uses because of aging and permeability. In addition, the low elastic modulus of PDMS makes it hard to form effective tiny elements in a micron- or even millimeter-scales.

Families of SU-8 (2000 and 3000 series)[124, 125, 126, 127, 128] (Figure 11b), NOA (60, 70 and 80 series, etc.)[129, 130] (Figure 11c) thermoset polyester (TPE), polyurethane methacrylate (PUMA)[131] are widely used resins to build microfluidic channels. These resins can be UV or thermo-cured in a short time and form a geometric structure with a high aspect ratio. Because of good rigidity, transparency and chemical stability, they

offer excellent alternatives to PDMS[132], especially for microfluidic devices with high-pressure injections. The fabrication of these polymers are mainly done by soft lithography[133], which is a highly precise and replicable technique to build molds with a resolution of several microns. These resins are able to handle most solvents, however, may still suffer from swelling-effects. Due to the nature of the multiple steps of photolithography, dedicatedly designed devices usually have very low fault tolerance for solvent development and assembling, each tiny error or contamination perhaps lead to a re-start over, which indicates that the cost of resins should be more than it appears[131].

Silicon wafers and glass capillaries (Figure 11d) attract attentions because they have a superior solvents resistance to organic and acidic solvents compared to PDMS and resins. The establishment of microfluidic channels on glass wafer is written by laser[134] or craved by acid-etching with a resolution up to less than 1µm. The glass is rarely affected by solvents and hardly deforms because of its high elastic modulus. Thus glass-based microfluidic devices could offer an excellent platform to observe complex behaviors of microfluidics and nanofluidics. Capillaries are usually insert-set together and the inner one is tapered and cut to form a round orifice to finely focus the fluids, so that highly monodispersed droplets, bubbles and nanoparticles can be generated. The hydrophobic surface of capillary can be tuned by coating with 5% Hydroxypropyl cellulose (HPC) solution. Besides, unlike photo-cured polymers, which can't be split into single useful component again, capillaries-based devices can be disassembled easily to clean or recycle[135]. It should be noticed that the capillary phenomenon could lead to unexpected clogging and reflux and the fragile nature of glass restrains its robustness under extremely high pressure, like supercritical fluids, in which case stainless steels are mainly used[136].

2.3.3 Recent developments of microfluidics-assisted drug delivery system

The rapid development of drug delivery research requires the drug delivery carriers to be more controllable. Microfluidics technology offers a better platform than conventional methods in control of: particle size, drug loading efficiency, surface properties and release rate.

2.3.3.1 Nanoparticles

The impact of particle size has been found in many aspects of its functions: degradation, drug loading ability and release rate, hydrodynamic properties and smaller NPs are found have a less uptake by immune system[137]. Flow focusing (F.F.) microfluidics could provide a high-throughput platform to synthesize very small drug-loaded nanoparticles[42]in one step without external power supply.

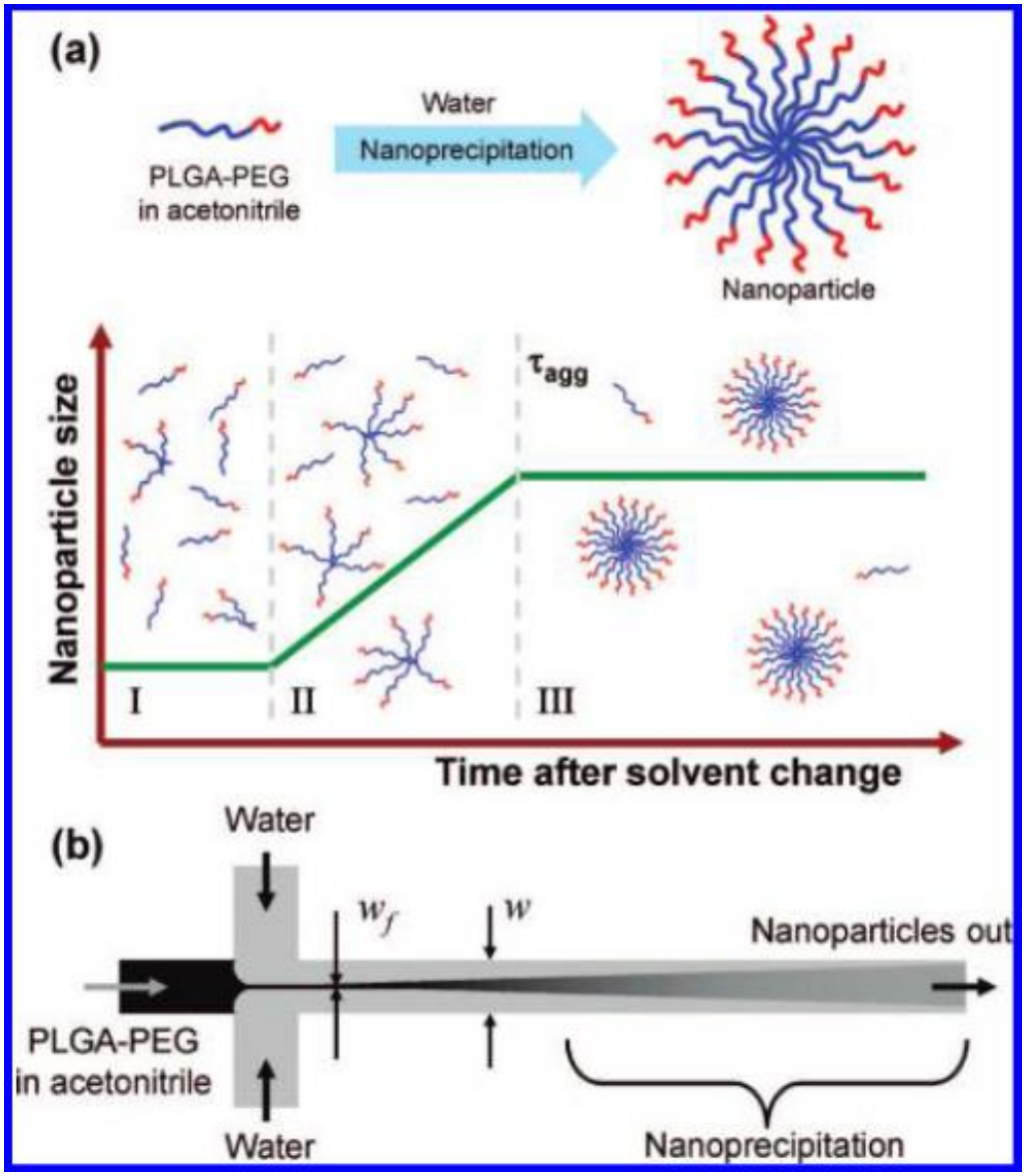

Figure 12. Nanoprecipitation of PLGA-PEG copolymers. (a) Self-assembly of PLGA-PEG diblock copolymers during nanoprecipitation. (b) The process of mixing in a microfluidic device[45].

Karnik et al[45] (See Figure 12) discovered smaller PLGA-PEG NPs can be fabricated

on a F.F. platform than bulk nanoprecipitation with the same O/W ratio because the microfluidic channel could offer higher mixing rate and then avoid large aggregation of polymers, with a E.E. around 50% and a mass loading less than 5%. By varying composition of polymers and precursors, both of morphology and surface charges of NPs can be easily controlled[138]. Monodispersed block copolymer vesicles with a tunable size from 40 nm to 2 μm are attained by Thiele et al[139]with a very narrow distribution. Commonly used polymers (PLA, PCL, PS, liposomes[140]) and drugs (doxorubicin, docetaxel, IFN-α[141], siRNA[1]) in bulk encapsulation methods can be replicated on microfluidic platforms and form drug-loaded NPs with a high encapsulation efficiency. Stimuli-responsive[142] (pH, thermo, glucose)NPs and can also be produced within microfluidic channels, which indicates the possibility of targeted drug delivery.

2.3.3.2 Microparticles/Microspheres

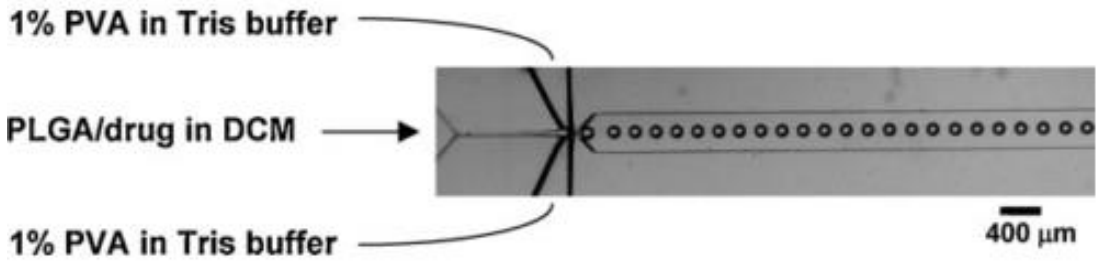

Figure 13. Optical microscopy image showing the orifice of the flow-focusing region generating droplets in water[143].

One key function of microfluidics is to generate discrete droplets which have excellent capability to encapsulate a series of drugs and form into microparticles. By playing with flow ratio, one could easily control the size of droplets and the production rate[135]. Compared to bulk emulsification method, in which mechanical shearing could lead to a broad size distribution, extremely monodispersed DEX-HEMA microgels can be easily fabricated in a co-flow chip[144] with an average diameter of 9.9 μm±0.3 μm. Shum et al[145]presents a droplet-based approach to produce highly uniformed double emulsion phospholipid vesicles on a glass-capillary microfluidic platform with a constant generation frequency round 500 Hz. The device exhibits a fantastic ability to

manipulate tiny amount of different fluid phases precisely so that the formation of each double emulsion droplet can be controlled individually. The sustained release of drugs also benefit from the on-chip production of monodispersed microparticles. Cumulative analysis shows that the release of bupivacaine from PLGA particles is slower than that from conventional single emulsion method of the similar average size but polydispersed. Furthermore, although this method has very similar mass loading ratio of drugs (around 20%) with the conventional bulk emulsion mixing protocols (around 18%), chip-produced PLGA microcapsules avoid an initial burst release which is observed with conventional particles[143]. This is because the microfluidics could offer a more homogenous mixing environment for the formation of drug-NPs, and less drug was adsorbed or trapped near the surface of the microparticles fabricated using the microfluidic device than those prepared using the conventional emulsification approach. Natural biomaterials can be fabricated into drug delivery carriers in microfluidic device as well, Breslauer et al[146]reconstituted silkworm cocoon silk as microspheres by laminar flow streams, which exhibit a characteristic β-sheet structure and remains the its nature of softness. Besides hydrodynamic production, droplets can also be prepared in other ways, like magnet-actuated microfluidics[147]. Once coupled with scaling-up, the microfluidic fabrication of large quantities of advanced microparticles will be enabled and assists in controlled drug release applications[148].

2.3.3.3 Multi-layer self-assembly

Self-assembly particles or matrix consist of multiple layers is a powerful cancer therapy media since different components can be encapsulated within one single compartment and the decoration of shells can offer more targeting sites with high specificity[149].

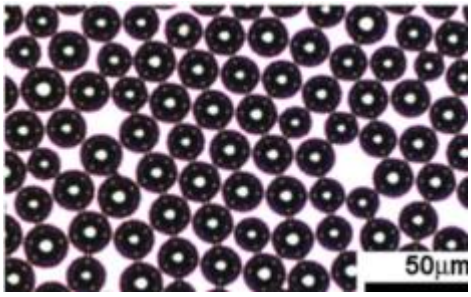

Figure 14. Images showing monodisperse multilayer gas lipospheres visible in bright field[150].

Hettiarachchi et al[150] (see Figure 14) used a droplet-based PDMS device to produce of micron-sized gas-cored lipospheres, the middle oil layer of which contains a high concentration of doxorubicin up to 15 mg/ml and the outside targeting ligands provide an effective binding with cancer cells. For production of lower-order (double, triple) emulsions, microfluidics technology shows a superior ability in controlling the numbers of inner drops and adjusting the thickness of shells, compared to mechanical mixing method, according to Deng et al.'s study[151, 152]. These multiphase emulsions are considered to be powerful tools for drug delivery applications[153]. Besides spherical shapes, hydrogels with non-spherical microarchitecture are synthesized on a microfluidic platform by Guo et al[154]. The formation of PAM/PEG core/shell droplets and hydrogels with rod-like, oval and triangle shapes can be realized by modifying the flow rate and polymerization temperature. The irregularly-shaped hydrogels exhibit significant anisotropy and different protein release rates which are highly shapes-dependent. 3-D mimic architecture of drug delivery potential can also be replicated by building multilayers of cell–matrix inside a microchannel and the thickness of each layer can be tailored with a resolution to microscale[155].

2.3.3.4 Janus particles

As the name indicates, Janus particles are a series of anisotropic particles with biphasic geometry[156]. The morphology and composition of Janus particles can be independently controlled to form various shapes and encapsulate different components so that they have great potential in drug delivery applications.

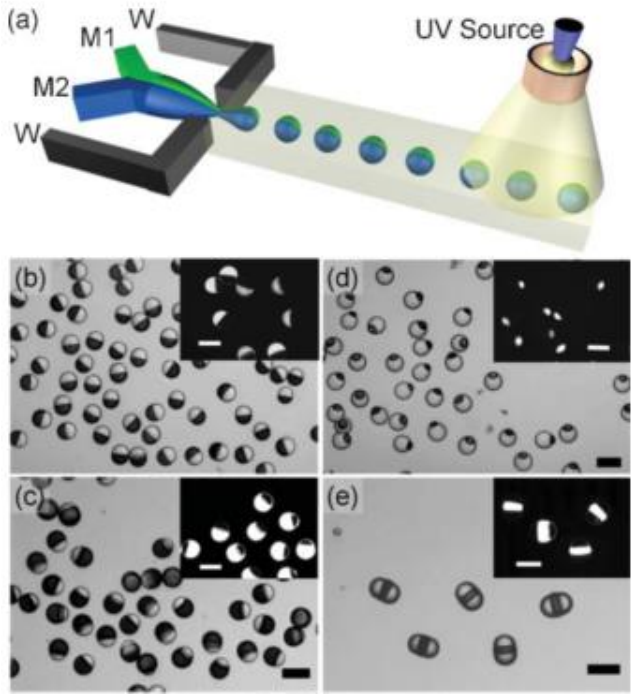

Figure 15. Fabrication of various Janus particles of different morphology. (a) Schematic of formation of droplets with different monomers M1 and M2. (b, c, d) Optical micro-scopy images of Janus particles. Bright and dark phases are polymers of M1 and M2, respectively. (e) Janus particles with ternary structures. Image reproduced from Prof. Huang's lab[157].

Dendukuri et al[158]reported a synthesis of rod-like PEG-diacrylate Janus particles with a length about 100um in a co-flowed microchannel with one end labeled by rhodamine. The two ends of Janus particles appear different colors under fluorescence microscopy and the width of each band can be altered by changing the flow rates of the streams, which can incorporate with other functional moieties like drugs. Monodispersed colloid-filled Janus spheres are produced by Shepherd et al[159]within a Y-junction chip and the shape of these hydrogel granules are be locked by in-situ photopolymerization. Weitz's group presents a series of methods to generate Janus particles, including from templates of double emulsion droplets[160], phase separation of homogenous droplets[161]and precursor solution of prefabricated cross-linkable polymers[162]and photoinitiators for UV-polymerization are usually required to solidify the morphology of the Janus particles. Janus particles could also encapsulate inorganic compounds (e.g., mass loading of Fe_3O_4 around 4%~7%) and incorporate with functional groups[163] which

reveals the possibility of co-delivery of different drugs or biomarkers within a single particle[157, 164].

2.3.3.5 Supercritical Fluid (SCF)

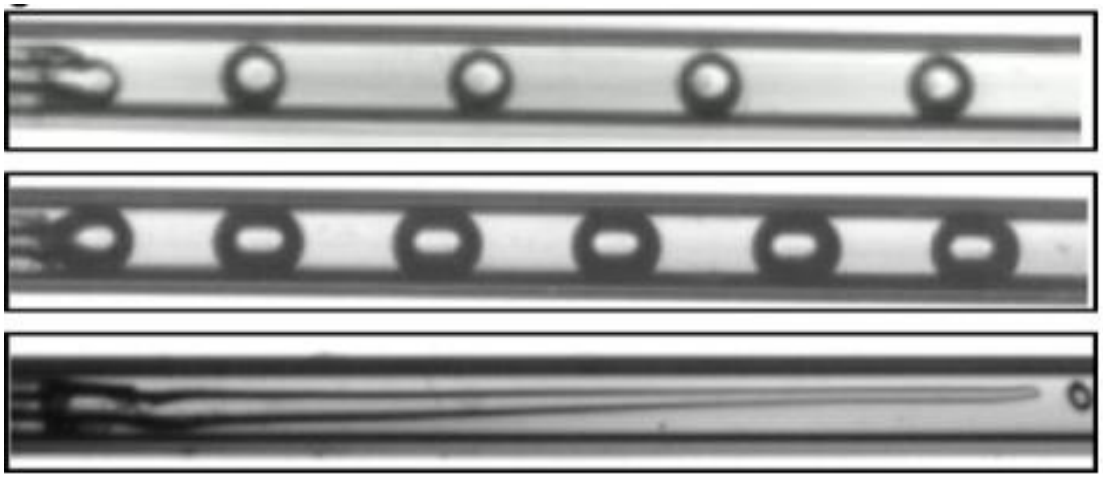

Figure 16. High pressure SCFs-liquid micro co-flows[136].

The SCF has been widely used for industry applications such as microreactors[165], extraction[166] and recently applied to drug delivery field because of their unique properties[167]. For example, the commonly used CO_2, is a non-toxic, transparent, chemically inert and economic material and its supercritical conditions are easy to be satisfied. The SCF could be an instead of organic solvents during the preparation of drug-loaded NPs[168] and the encapsulation occurs after a rapid decompression precipitation. Champeau et al[169]used supercritical CO_2 as a solvent to improve the entrapment of ketoprofen and aspirin into PEO platelets and the solubility of the drugs was found proportional to the pressure of CO_2 (from 0 to 12%, when the pressure increased from 5MPa to 15MPa), so that a gradually increase of drug loading efficiency was monitored with the increase of pressure. Another use of SCF is being applied to extract the inner phase of an existing emulsion as an "anti-solvent" to form microparticles or nanoparticles. With this method, Shekunov et al[170]fabricated nanoparticles of model hydrophobic drugs with a size range from 100nm to 1000nm. The concentration of residual solvents decreases to several ppm from the original 10%~30% (w/w) in a short time and the morphology of particles are found correlated to the drug concentration, emulsion droplet size and the molar ration of organic solvent.

From the research of Chattopadhyay et al[171], the original droplet size is thought as the major control parameter of the finial particle size and the kinetic dissolution coefficient for encapsulated drugs is observed being reduced by 2–4 orders of magnitude when compared to the unprocessed drug particles. For future perspective, the SCF only needs relatively mild conditions and has great potential for scaling-up. However, to design economic, safe, and robust microreactors capable of working at the desired working conditions compatible with the use of most supercritical fluids[172], remains to be a key issue to be solved.

2.4 Combination of chemotherapy and thermotherapy

Thermotherapy treats cancer and tumor cells by heating them physically to a specific temperature range and kill them. However, the clinical application of conventional hyperthermia were usually limited by its poor targeting ability, which caused severe side effects to nearby healthy tissues. Nanotechnology now offers a possibility to solve this problem.

Polymeric nanoparticles containing magnetic components like Fe_2O_3[5], Fe_3O_4[173] are mostly used for thermotherapy since the iron oxide particles can produce heat that is transferred from an external alternating magnetic field of a high frequency. Sanson[8] et al synthesized highly magnetic nanoparticles (loaded up to 70 wt%) and observed deformation of the vesicle membrane under an applied magnetic field, and conducting a magneto-chemotherapy.

Gold nanoparticles are another important series of ideal biomaterials for hyperthermia due to their non-toxicity, uniformity, and highly clearance through kidneys[174]. The radioenhancing effect[175] by irradiation was found and measured more than 30 years ago. Hainfled[174] et al performed an intravenous injection of 1.9 nm diameter gold particles and 250 kVp x-ray therapy. One-year survival of mice bearing subcutaneous EMT-6 mammary carcinomas was 86% versus 20% with x-rays alone and 0% with gold alone. Golden materials can also be active in the near-infrared (NIR) region of the radiation spectrum, which is called photo-thermal therapy and could

minimize the light extinction by intrinsic chromophores in native tissue[176, 177, 178, 179]. By conjugating to anti-epidermal growth factor receptor (anti-EGFR) monoclonal antibodies, Huang et al found that gold nanorods bind to targeted cells with a high affinity[178]. In addition, the scattered red light from gold nanorods made themselves easily visualized in dark field, so that both efficient cancer cell diagnostics and selective photothermal therapy are realized at the same time. Besides, other inorganic materials like quantum dots[180] can also be applied to hyperthermia due to their high photo-to-thermal conversion rate and high light absorption cross-sectional surface.

Compared with traditional thermotherapy, nanoparticles provide a more economic, safe, energy-concentrated method, with advantages of faster heating-up, non-invasive and shorter treatment period. Combination of chemotherapy and thermotherapy also open potential applications for spontaneous drug loading and *in-vivo/vitro* magnetic/photonic response imaging.

Chapter 3 Fabrication of Polymeric Nanoparticles using microfluidics for encapsulation and release of hydrophobic drugs

3.1 Summary

Here we present a novel microfluidic flow focusing method for synthesis of Doxorubicin (DOX)/Tamoxifen (TAM)-encapsulated PLGA nanoparticles (NPs), using a water-miscible precursor (Dimethyl Sulfoxide+Dichloromethane) solution. We achieved two major breakthroughs: (1) Extruding this partially water-miscible into an aqueous solution produced a previously unseen transformation phenomenon of the precursor fluid: jet to micro-droplets (emulsions) to nanoparticles; (2) Uniform PLGA NPs were synthesized with a considerable drug loading ratio, the size of which could be precisely tuned by changing the flow ratios, polymer concentration, and volume ratio of DCM (V_{DCM}/V_{DMSO}) in the precursor. We further investigated the mechanism of the evolution process of precursor fluid, and the effect of V_{DCM}/V_{DMSO} on the formation of NPs and drug release kinetics. Our work suggests that this rapid, facile, efficient and low-cost method is promising technology for NP fabrication and can be extended to benefit the fields like nanomedicine and cancer therapy.

3.2 Introduction

Poly(lactic-co-glycolic acid) (PLGA) nanoparticles and microparticles exhibit great potential for nanobiomedicine[71], and is one the most commonly used biopolymers approved by FDA because of its biosafety, biocompatibility, biodegradability[181]. Microfluidic technology has been developed for the synthesis of these series of NPs in past decades because of its advantages, including homogenous reaction environments from a single batch[45], enhanced reproducibility[182], non-excessive consumption of

expensive agents[106], and high, steady and fast throughput motored by mechanical valves and pumps[106], compared with bulk methods. Currently, two microfluidic methods are most frequently used for producing drug-loaded NPs: (1) rapid mixing and nanoprecipiation, and (2) droplet-based flow focusing. The conventional method of rapid mixing and nanoprecipitation, mixing one water-miscible fluid with an aqueous solution, could bring us small NPs (10~100 nm)[138, 183], however, with a relatively low encapsulation efficiency (E.E., usually less than 50%)[45] compared to the droplet-based method; on the other hand, the particles from droplets and emulsions formed by water-immiscible solvents are usually having a better drug loading ratio yet oversized (10^0 to 10^2 μm) [143, 144, 145, 146, 148, 184]. Efforts have been made to push forward the state of the art: Lee et al[185] used droplets fusion instead of direct convection of discrete and continuous fluids, but the low flow rates/ratios easily resulted in PLGA NPs larger than several hundred nanometers; Karnik et al[183] accelerated the micromixing in a twisted channel and synthesized hybrid PLGA-lipid-PEG NPs via a single-step process within a much smaller particle size less than 100nm , yet a low drug loading ability (w/w, less than 5%).

We are thus motived to decrease the NP size without sacrificing its drug loading ability by using a partially water-miscible mixture of Dimethyl Sulfoxide (DMSO) and Dichloromethane (DCM) instead of pure DMSO or pure DCM[143] as a dispersed phase at a microfluidic platform. In a co-axial glass capillaries-based microfluidic channel, thin stable jets of this partially water-miscible precursor transforms into microdroplets, and then to NPs under the action of the solubilization of DMSO into water. Strikingly, this method leads to high mass loading and high E.E for both hydrophobic drug (Tamoxifen) and hydrophilic drug (Doxorubicin).

With a hydrophobic drug Tamoxifen[17], E.E. has high of 88% were measured. Compared to previous bulk mixing using similar organic phases[62, 66], (Doxorubicin-Poly (D, L-lactide-co-glycolide) Acid) DOX-PLGA NPs synthesized by this microfluidic method were smaller(90~160nm), size-tunable, of an higher E.E (up to 66%) and mass loading ability (up to 26.3%), by adjusting the flow rates, polymer concentration and V_{DCM}/V_{DMSO}. The release properties are not affected by this procedure

and remain the same than the one obtained using pure DMSO. These characteristics imply that our approach provides a novel and valuable method producing NPs with a tunable size range, and significant drug loading ability under precise control, at a nanoscale level.

3.3 Experimental Section

3.3.1 Materials

Dichloromethane (HiPerSolv CHROMANORM for HPLC，VWR) and Dimethyl Sulfoxide (ACS grade, Amresco) were mixed at a volume ratio of 1/10 and 1/20 to prepare the precursor solutions. Poly (D, L-lactide-co-glycolide) acid (75:25, Mw 4000~15000, Sigma Aldrich) was dissolved in the dispersed phase, at different concentrations (5mg/ml, 15mg/ml) and Sodium dodecyl sulphate (SDS, GPR REACTPUR, VWR) was dissolved in DI water (0.5%, w/v) as the continuous phase. Phosphate buffered saline (PBS, pH=7.4 at 25 ℃, Sigma Aldrich).

3.3.2 Fabrication of the microfluidic platform

The microfluidic device (Figure 17) was constructed under the following protocols: (1) A round glass capillary (0.50mm ID×0.70mm OD, CM Scientific) was pulled by a micropipette puller and broken to a ~50μm ID tip (P-97, Sutter Instrument Company). (2) This tipped capillary was inserted into a square glass capillary (0.70mm ID, CM Scientific） to get a coaxial geometry. (3) The resulting coupled capillaries plus nanoports were stuck onto a glass platform using epoxy glues.

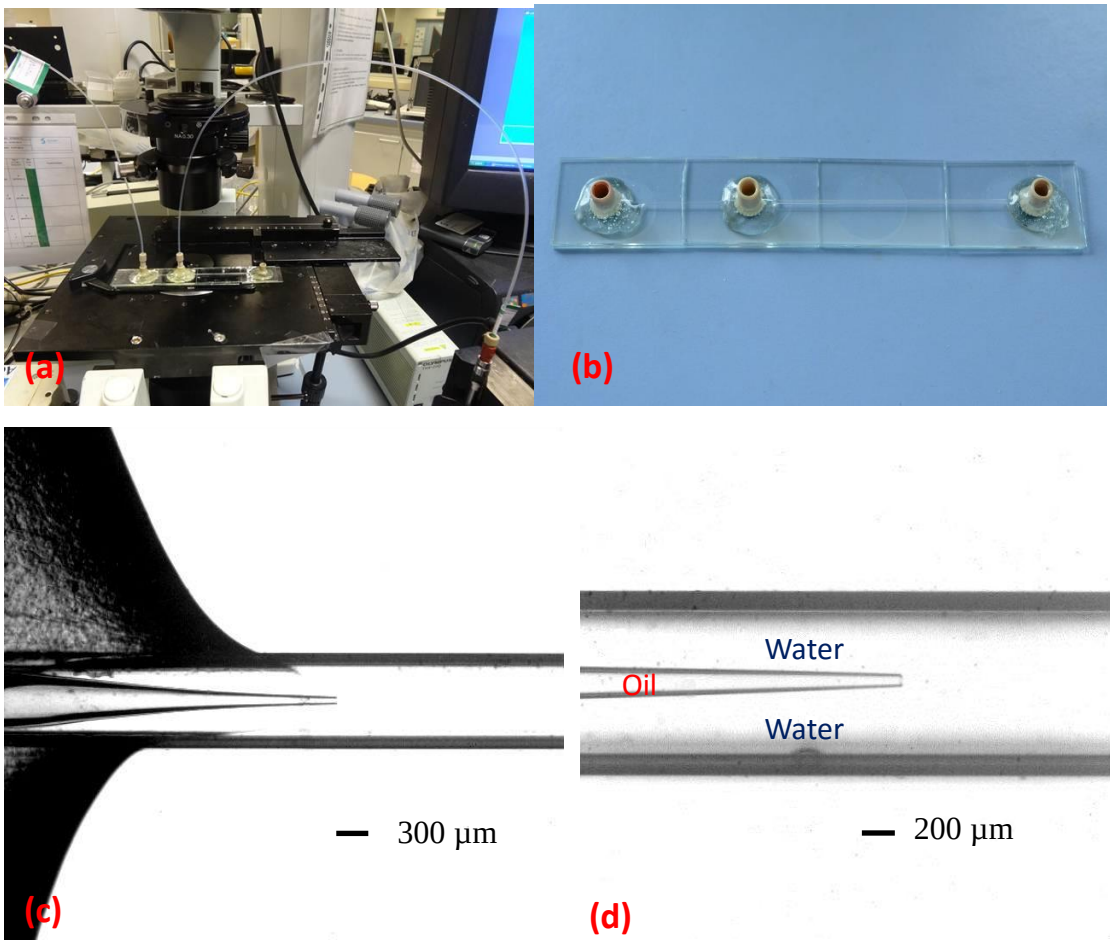

Figure 17. Coaxial microfluidic device fabricated with glass capillaries. (a) A microfluidic platform under operation; (b) A microfluidic chip constructed of glass capillaries and nanoports; (c) The nozzle of the inside round capillary under optical microscope; (d) The nozzle of the inside round capillary under optical microscope.

3.3.3 Synthesis of PLGA nanoparticles by microfluidic flow focusing

Two syringe pumps (Harvard Apparatus PHD 4000) are used to drive two fluid phases to flow in the same direction. The dispersed phase (PLGA solution) flows inside the round capillary, and the continuous phase (aqueous solution) flows between the round and square capillaries. A typical quantity flow rate of Q_{oil} is set as 10, 20, 30…to 60 µl/hr and Qw is set as 2000, 3000, 4000… to 10000 µl/hr. The solutions containing PLGA NPs are collected from the outlet and water-bath evaporated for 1 hour at 45°C to remove the DCM solvent. The PLGA NPs were characterized by Dynamic Lighting Scattering (Vasco particle size analyser, Cordouan Technologies) after solvent evaporation. Each measurement was repeated 3 times. (n = 3, mean ± S.D).

3.3.4 Drug Encapsulation by PLGA nanoparticles

The Doxorubicin (DOX) supplied by Discovery Fine Chemicals (Wimborne, UK) is commercially modified as Doxorubicin hydrochloride, so that Triethylamine (TEA, ≥99.5%, Sigma-Aldrich) was used to incubate DOX solution in DMSO overnight with 1:2 molar ratio to remove its hydrochloride group[186]. DOX (or Tamoxifen, Sigma Aldrich) and PLGA were dissolved in the precursor solution of 1 mg/ml and 5 mg/ml, respectively. A typical quantity flow rate of Q_{oil} is set as 50 µl/hr and Q_w is set as 5000 and 10000 µl/hr. 1 ml of microfluidic solution was collected from the capillary reservoir, and then transferred to an Amicon ultrafiltration tube (MWCO=3kDa, Amicon ultra-4) to centrifuge for 30 min at 8000 rpm to separate the drug-loaded NPs[47]. The filtered NPs was re-suspended and dissolved by 1 ml of DMSO. The concentration of the encapsulated drug by PLGA NPs was calculated by measuring the concentration of the doxorubicin in the mixture by obtaining the UV absorbance of the solution at 481 nm (SpectraMax M2). For tamoxifen, the filtered NPs was re-suspended and dissolved by 2 ml mixture of DMSO and Methanol[187] (*v:v*=1:1), and the encapsulation efficiency was determined by measuring the UV absorbance at λ=285 nm. Each measurement was repeated 3 times. (n = 3, mean ± S.D).

3.3.5 Drug Release by PLGA nanoparticles

The DOX-PLGA NPs solution was collected at Q_{oil}= 50 µl/hr and Q_w =5000 µl/hr (C_{DOX}=1 mg/ml, V_{DCM}/V_{DMSO}=1/10) for 20 ml, which was concentrated to 1 ml by ultrafiltration (4500 rpm, MWCO=10 kDa, Amicon ultra-15). The concentrated NPs solution was then transferred to a dialysis membrane (MWCO=25 kDa) against 40 ml PBS solution (pH=7.4) in a release bottle with magnetic stirring at T=37 °C. The cumulative released dose was determined by UV spectroscopy. DOX-PLGA NPs solution made with the same protocols but using pure DMSO was used as a control group.

3.4 Results and Discussions

3.4.1 Stability of the partially water-miscible fluid in a confined microfluidic channel

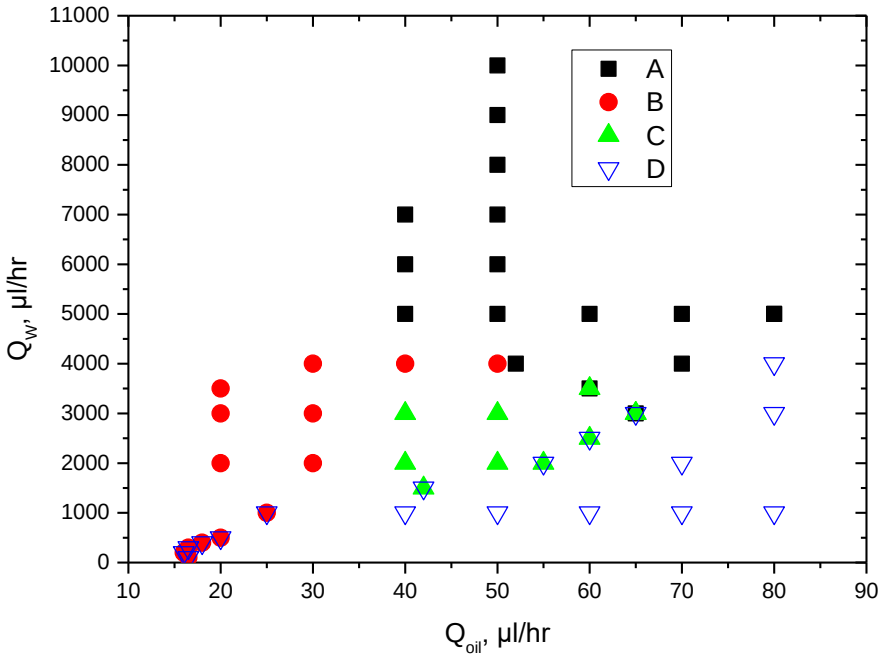

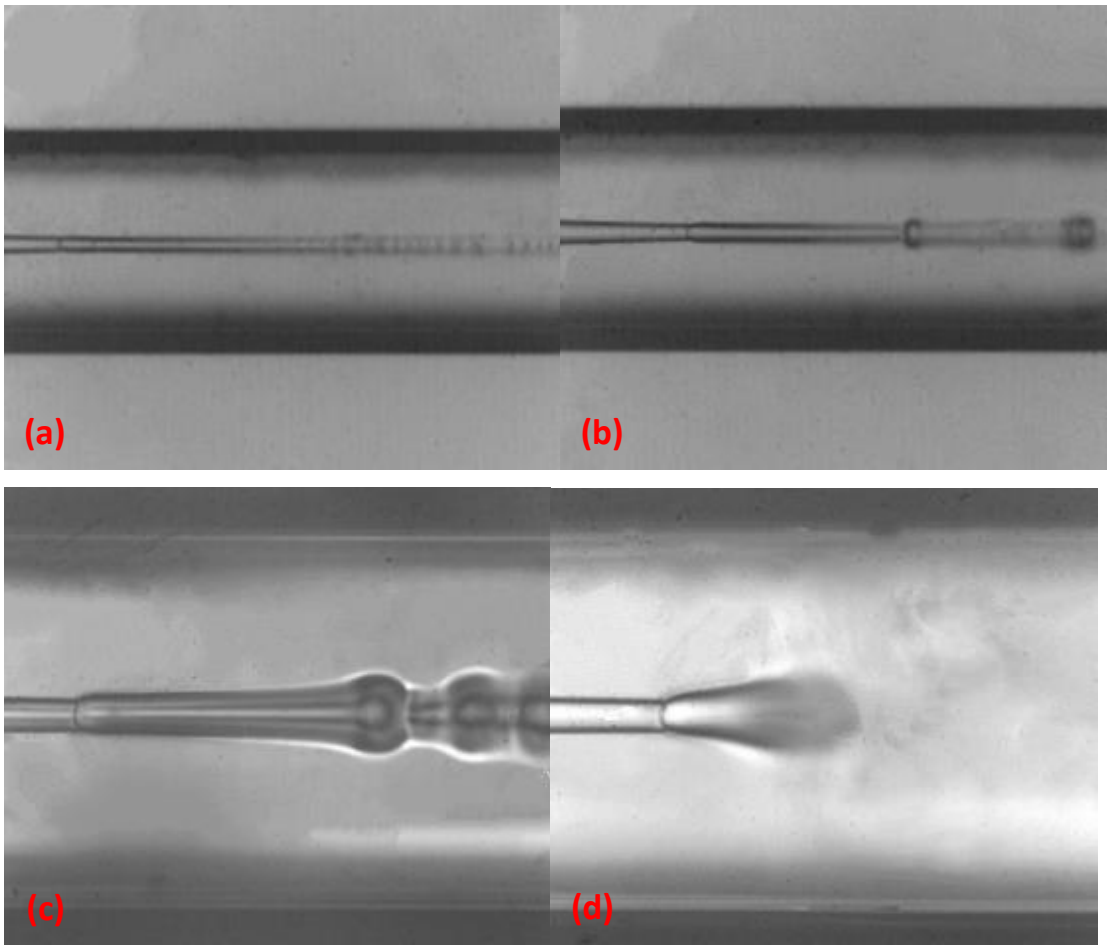

Figure 18. Map of flow behavior in the (Q_w, Q_{oil}) plane. Jets are observed as two forms: wide straight jets that are stable at nozzle and then diffuse with water through the channel (a, solid square); thin jets that break into tiny droplets at a well-defined location (d, open triangle); Droplets are observed with periodic modulations (b, solid circle; and c, solid square). V_{DCM}/V_{DMSO}=1/10 and 0.5% SDS in water.

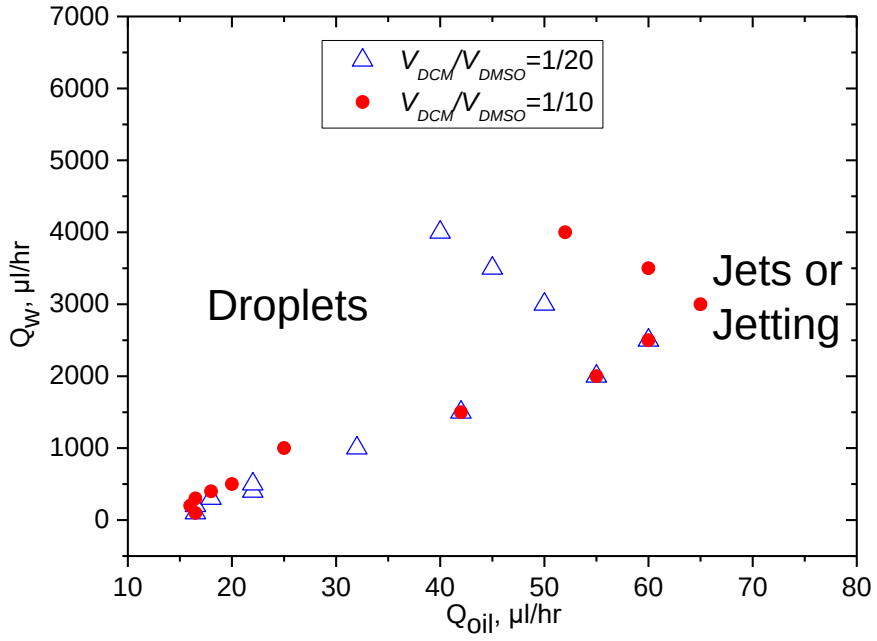

Figure 19. Boundary between droplets and jets shifts as the V_{DCM}/V_{DMSO} changes. Triangle and round scatters represent the critical (Q_w, Q_{oil}) conditions of the boundary between droplets and jets (or jetting) with V_{DCM}/V_{DMSO} =1/20 and 1/10, respectively. 0.5% SDS in water

Figure 18 displays different flow patterns of this partially water-miscible precursor with operational (Q_{oil}, Q_w) close to the nozzle (i.e at a distance shorter than the diameter of the external capillary tube). These patterns observed close to the nozzle are reminiscent from the one obtained using immisicible fluids[184]. To be more precise, we note no modification of the flow diagram. A droplet regime is basically found for very low (Q_{oil}, Q_w), with droplets emitted periodically with a size comparable to the nozzle radius (Figure 18 picture b and red circles) or larger droplets resulting from the instability of an emerging oscillating jet (Figure 18 picture c and green triangles)[184]. Large short jets are found close to the (Figure 18 picture d and blue triangle). In this case, no visible macroscopic droplets are formed. For large values of the external flow rate, we observed what we call jetting: thin and straight jets are produced (Figure 18

picture a and black squares).

The similarities between partially miscible and not miscible fluids are not surprising. Even though the fluids are partially miscible, they still have a surface tension. Jets of liquids displaying surface tension are linearly unstable due to Rayleigh-Plateau instability[144, 188]. The nature of the instability at the linear level (absolute or convective) controls whether drops or a jet are obtained. In the convective case, growing disturbances are simultaneously convected downstream and a continuous jet can persist in the system over some distance (which does not preclude the formation of droplets downstream). By contrast, in the absolute instability regime, no jet is stable, as any perturbation generates oscillations that grow and travel backwards to invade the whole capillary. This corresponds to the droplets and plugs regimes.

In our study, this process might be altered by the release of DMSO into water. This is in fact not the case close to the nozzle. The Péclet number (ie. the ratio of the convective time by the diffusion time) is very large, diffusion plays little role in the process and the liquids behave as if they were immiscible. The Péclet number is given by Pe=Q/DR where Q is the flow rate, D is the diffusion coefficient, and R is the size of the capillary tuble. Typical values Q=2000 µl/hr, D=10~10^2 m^2/s, and R=700 µm, leading to Pe=8000.

The boundaries of the various zones are varied by using a larger amount of DCM in the DMSO/DCM mixture (see Figure 19). At a given Q_w > 2500 µl/hr, the precursor of higher V_{DCM}/V_{DMSO} exhibited as droplets while the one of lower V_{DCM}/V_{DMSO} exhibited as jets at the same Q_{oil}, because the precursor of higher V_{DCM}/V_{DMSO} contains more insoluble component, which is inclined to give a higher interfacial tension and thus a larger domain of drops in the parameter plane (Q_{oil}, Q_w).

At first sight, our strategy seems thus inefficient to produce small nanoparticles since the flow diagram is unchanged. However, the originality of our work and the possibility to reach our aim relies in the long time evolution. The jet and the drops shrink as a function of time i.e. as a function of their displacement in the capillary tube. When using polymer solution instead of pure fluids, the shrinking of the jet and of the drops

induces the formation of nanoparticles or sub-micron particles.

Using Dynamic Light scattering (see Table 1), we point out that both size and polydispersity of the PLGA NPs decrease gradually when increasing Q_w. PLGA NPs from the jetting region (region A) exhibit advantages of smaller size, more narrow distribution, and of higher through-put, compared with other regions. So we focus on this jetting region for further study.

Region	**A**: $_{oil}$=50µl/hr Q_w=6000µl/hr	**B**: $_{oil}$=50µl/hr Q_w=4000µl/hr	**C**:Q_{oil}=50µl/hr Q_w=3000µl/hr	**D**:Q_{oil}=50µl/hr Q_w=1000µl/hr
Diameter (nm)	103	106	128	321
Polydispersity	0.046	0.084	0.105	0.27

Table 1. Size and distribution of PLGA NPs collected from reservoir. Concentration of PLGA (Mw=4000~15000) = 5mg/ml, V_{DCM}/V_{DMSO} = 1/10.

3.4.2 Generation of NPs in the jetting zone: Jet to Original Droplets to Nanoparticles

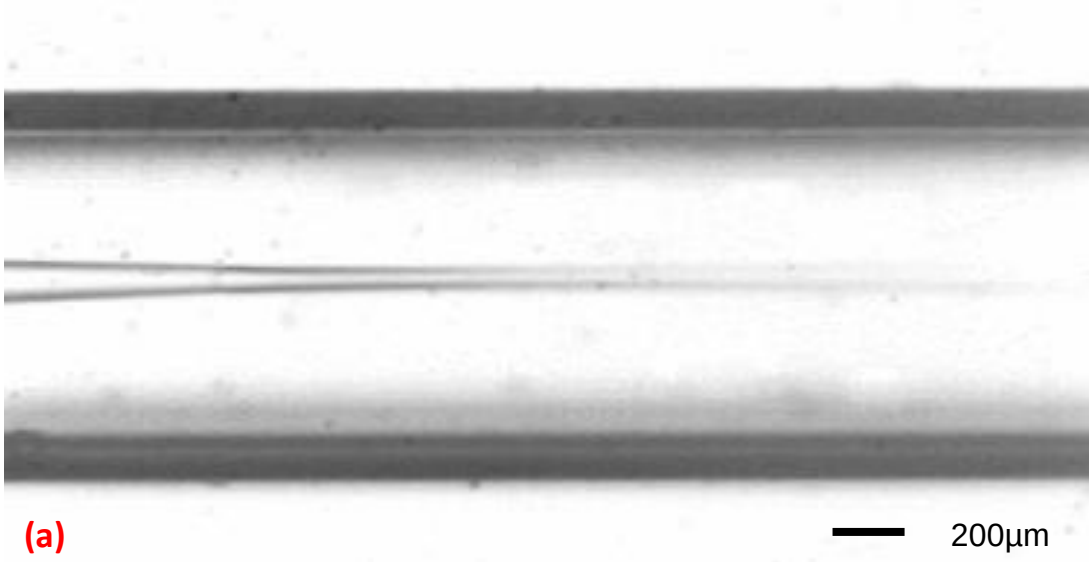

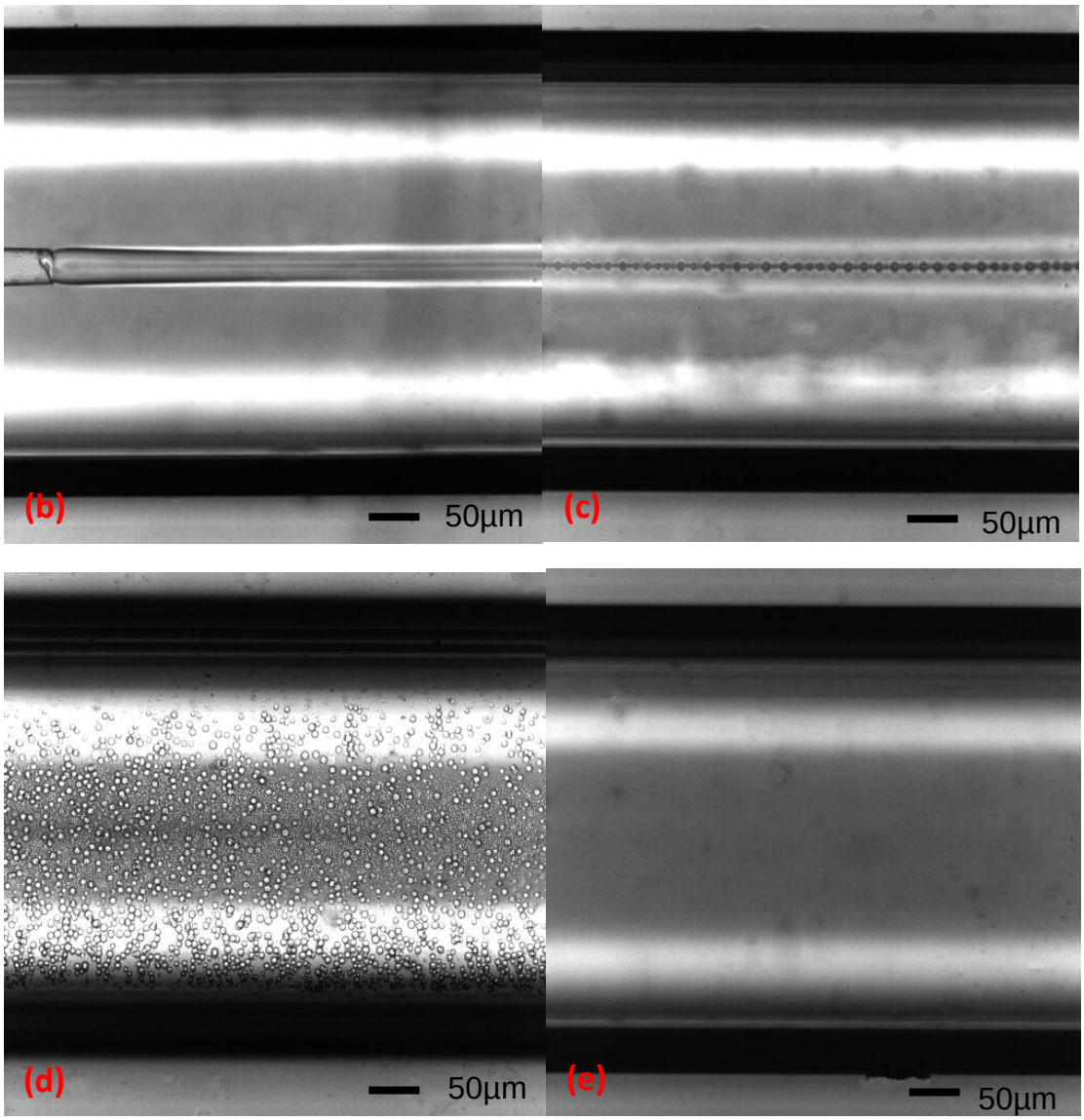

Figure 20. The evolution processes of different precursor fluids. (a) Flow focusing of water-miscible solvent (pure DMSO) and water, Q_w=3000 µl/hr, Qoil=50 µl/hr; (b-e) Flow focusing of partially water-miscible precursor (V_{DCM}/V_{DMSO}=1/10) and water, Q_w=10000 µl/hr, Q_{oil}= 100 µl/hr. Photos were taken at positions close to nozzle, 10 mm after nozzle, 20 mm after nozzle, 30 mm after nozzle, along the flows direction, successively.

In traditional flow focusing of water and water-miscible fluids like DMSO (Figure 20a), nanoparticles but no droplets form after rapid mixing and nanoprecipitation since there is no interfacial tension between these two fluids, which has been well studied and well-known[189]. However, in our experiments, when a water-immiscible component like DCM was added to DMSO and tuned the mixed fluid to partially water-miscible, a unique phenomenon was observed: a jet of fluid diffused into water (Figure 20b) and gradually perturbed into a steady stream of homogenous droplets (Figure 20c), which

spread among the whole microfluidic channel from the restricted central jetting zone, yet still flowing not stuck (Figure 20d), and finally shrinked as invisible nanoparticles under optical microscope (Figure 20e). The diameters of these original droplets by jetting are much less than that of the former jet, which can be used to produce monodispersed nanoparticles. This procedure consisted of three stages, having features of both conventional nanoprecipiation[183, 190, 191] and emulsion-based flow focusing[153, 188, 192]: (1) the soluble component (DMSO) diffuses into the water; (2) the surface tension of the precursor increases gradually since more insoluble component (DCM) was left, as a result of which a stream of tiny microdroplets are generated in place of the jetting away from the nozzle. This process can also be explained by Plateau-Rayleigh Instability that surface tension causes fluid stream break into a series of droplets eventually; (3) Although part of the DMSO residue within the microdroplets, and diffused into water, some remained as main component of the micro-emulsions, and further escaped into the water. The size of the particles decreased to a nanoscale level, which were invisible under microscope, however, detectable by DLS techniques. This evolution process--jet to original droplets to nanoparticles --occurred along the direction of the flow focusing and is clearly demonstrated by Figures 20b-e and following DLS results, which reveals a novel concept for synthesizing NPs.

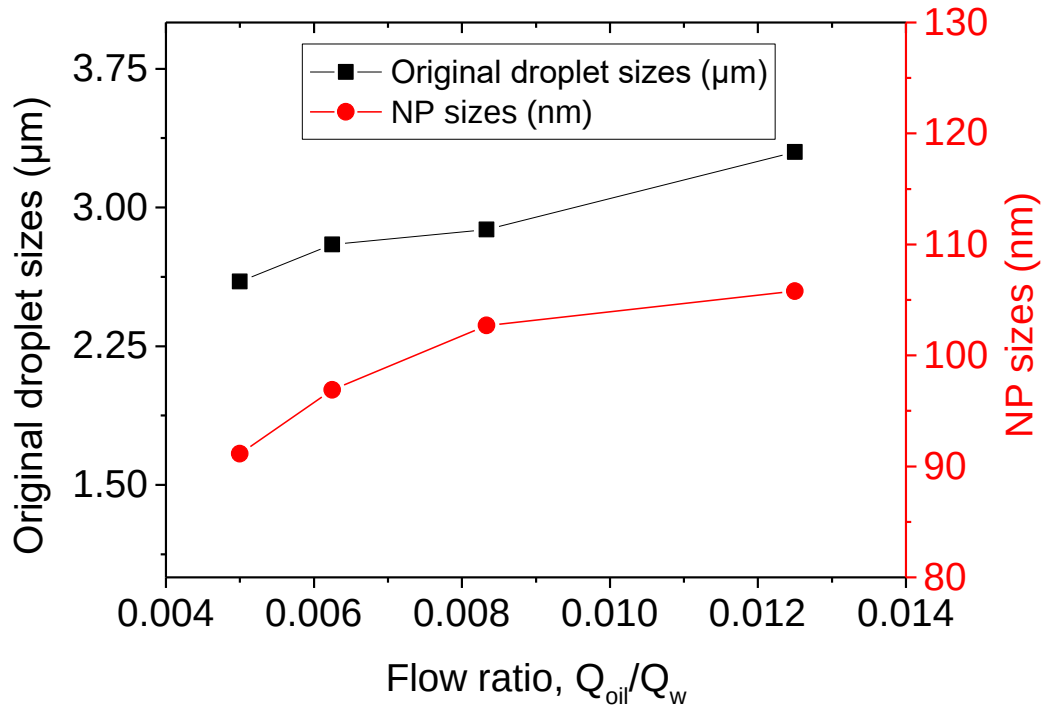

Figure 21. Relationship of original droplet diameter and PLGA NP diameter formed with different flow ratios from the jetting zone of fluid. Diameter of droplets was measured and calculated by using ImageJ software. Q_{oil}=50 μl/hr , Q_w was set as 1000 μl/hr,4000 μl/hr, 6000 μl/hr, 8000 μl/hr and 10000 μl/hr, respectively. Concentration of PLGA (Mw=4000~15000) = 5mg/ml, in water (*w/v*), V_{DCM}/V_{DMSO} =1/10.

In Figure 21, we found that at jetting zone, when flow ratio of Q_{oil}/Q_w increases from 50/10000 to 50/4000, the diameter of the original droplets increases under optical microscope. In addition, the sizes of synthesized PLGA NP exhibit a strong positive correlation with the sizes of original droplets. Thus, it is reasonable for us to conclude that the NP sizes are influenced by the original droplets sizes.

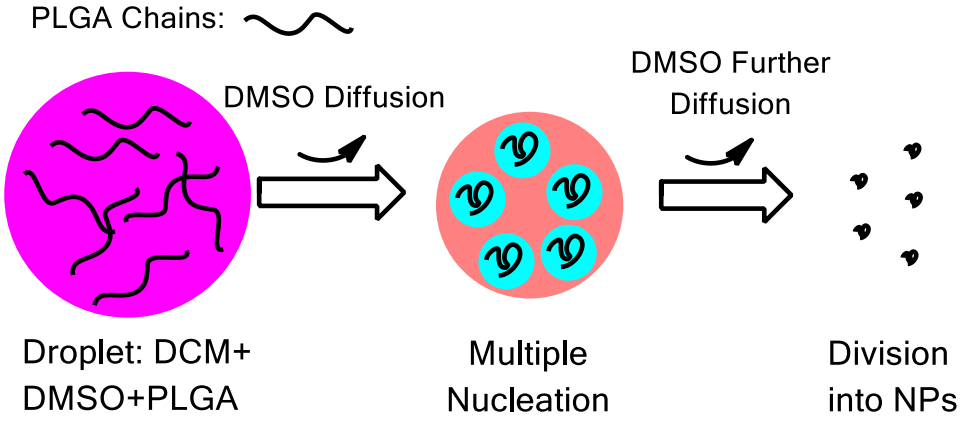

Figure 22. Mechanism of PLGA NPs formation from droplets. Purple color in the left circle

represents the mixture of DCM+DMSO; Red color in the middle circle represents the mixture of DCM+DMSO, yet less DCM content; Light blue color in the middle circle represents the mixture of DCM+DMSO, yet more DCM content; Solid black dots on the right side stand for PLGA NPs.

However, if we assume that one single droplet corresponds to one single nanoparticle in the final stage, and calculate the density of the PLGA NPs, given by the equation $\rho_o \frac{4}{3}\pi R^3 = \rho_f \frac{4}{3}\pi r^3$ (ρ_o stands for original polymer concentration=5mg/ml, ρ_f stands for final polymer concentration, R stands for the radius of original droplet≈1.5μm, r stands for the radius of final nanoparticle≈50nm), the final density ρ_o is around 135000kg/m^3. This value looks impossible for polymer materials by common sense, thus our previous assumption is overthrown and the most likely explanation should be: one single droplet will separate into a plurality of nanoparticles eventually.

The procedure of the evolution of NPs is probably like (see Figure 22): (1) A droplet forms by jetting, containing DCM, DMSO, and PLGA; (2) A multiple nucleation may happen within a single droplet. Since solvent environment for polymers turns bad due to the diffusion of DMSO into water, the PLGA chains are inclined to shrink and aggregate, with the remaining DCM content. (3) The polymer chains would further shrink and aggregate because of the change of solvent environment, and finally, numerous nanoparticles are split from the original droplets. Smaller the original droplet is, shorter the time it takes to shrink[193]. Under these rapid conditions the concentration of polymer inside the droplets increases rapidly and more nuclei are formed. We do thus observe smaller nanoparticles when the size of the initial droplet is smaller.

This mechanism is different from the NPs self-assembly by pure water-miscible fluid or pure water-immiscible fluid, since the formation of NPs in the jetting zone must experience a “transitional state” of droplets, and a multiple nucleation procedure. We can also use this theory to explain why higher V_{DCM}/V_{DMSO} leads to larger NPs. It is because that more DCM increases the surface tension between the fluid and water and increases the sizes of original droplets. Larger the original droplet is, longer the time it takes to shrink. Under these slow diffusion conditions, the concentration of polymers

inside the droplets does not increase too much, fewer nuclei are formed and polymers easily adsorb on them. We do thus observe larger nanoparticles when the volume ratio of DCM is higher.

3.4.3 Comparison of NPs synthesized by bulk and microfluidic methods

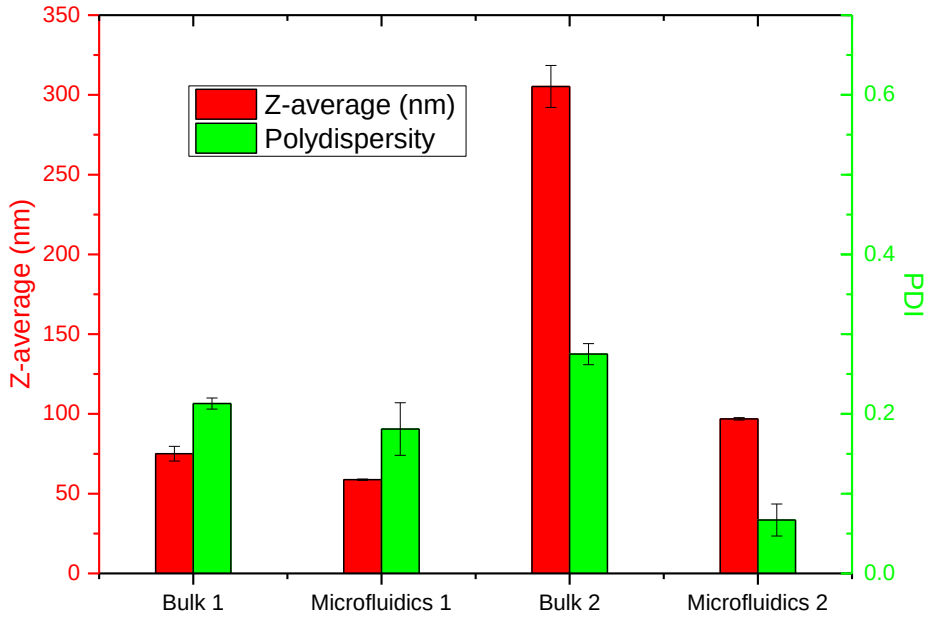

Figure 23. Size and polydispersity of PLGA NPs synthesized by bulk and microfluidic methods. Concentration of PLGA (Mw=4000~15000) = 5 mg/ml, Q_{oil}:Q_w=50 µl/hr : 8000 µl/hr for microfluidics and V_{oil}:V_w=0.05 ml:8 ml for bulk mixing. Bulk 1: pure DMSO, Bulk 2: V_{DCM}/V_{DMSO} =1/10, Microfluidics 1: pure DMSO, Microfluidics 2: V_{DCM}/V_{DMSO} =1/10. (n = 3; mean ± S.D.)

We synthesized PLGA NPs by using microfluidic and bulk mixing tools, individually (Figure 23). To prepare NPs by traditional synthesis via bulk mixing, 50ul of DCM/DMSO solution including PLGA was drop-wisely added into 8ml of water (0.5%SDS). The NPs synthesized by microfluidics using pure DMSO (Bulk 1 and Microfluidics 1) showed slight decreases in both size (from 75 nm to 59 nm) and polydispersity (from 0.213 to 0.181) compared to those from bulk mixing with the same flow ratio (Figure 13), which is consistent with the findings of previous report[138]. However, the NPs synthesized using mixed solvents of DCM/DMSO (Bulk 2 and

Microfluidics 2) using microfluidic flow focusing exhibited a much greater decrease in both size (from 305 nm to 97 nm) and polydispersity (from 0.275 to 0.067). These huge variations in size and polydispersity between bulk method and microfluidic method when using DCM/DMSO mixture, prove that this microfluidic technology can produce smaller and more homogenous NPs than bulk methods[13, 62, 66, 70]. Moreover, the size and distribution of NPs synthesized with the partially water-miscible solvent are more sensitive to the change of fluid mixing rates than those synthesized with the water-miscible precursor. Additionally, the NPs produced by microfluidics using DCM/DMSO precursor demonstrated a much narrower size distribution than NPs produced using pure DMSO precursor.

3.4.4 Effects of polymer concentration， flow ratio, and V_{DCM}/V_{DMSO} on the size of PLGA NPs in the jetting zone of fluid.

We further investigated the effects of different impact factors, specifically, polymer concentration, flow ratio, and V_{DCM} of the dispersed phases, on the size of PLGA NPs

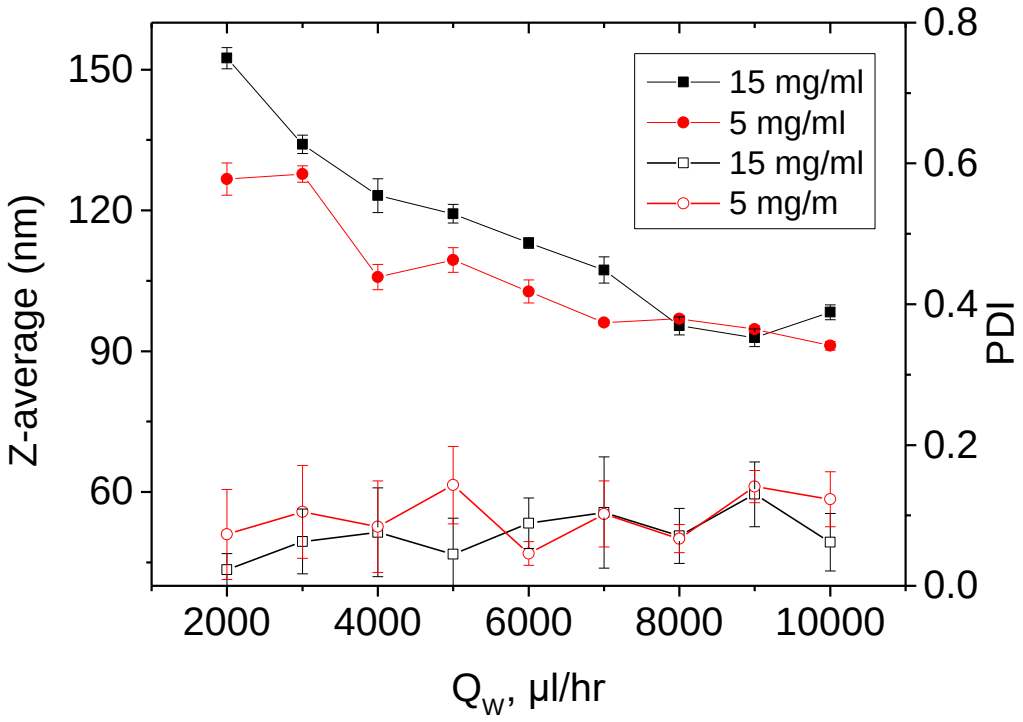

Figure 24. Size of PLGA NPs synthesized with different PLGA concentrations. Q_{oil}=50 µl/hr, V_{DCM}/V_{DMSO} =1/10. The solid icons represent the data of particle sizes and the open icons represent the date of particle dispersity. (n = 3; mean ± S.D.)

Comparing PLGA solutions of different concentrations, we found that polymer precursor of higher concentration lead to larger nanoparticles when with the same flow rates of Q_{oil} and Q_w (Figure 24), which is easy to be understood since in this case, more polymers would be absorbed or inserted into each nanoparticle so that its volume increased. We also observed that the change of particle size range of NPs from precursor of 15 mg/ml (152 nm to 93 nm) is more than that from precursor of 5mg/ml (104 nm to 74 nm) when Q_w increased from 2000 µl/hr to 10000 µl/hr. However, the polydispersity of PLGA NPs barely changed with the increase of the polymer concentration so that it provides us great potential to synthesize monodisperse nanoparticles with a concentrated precursor.

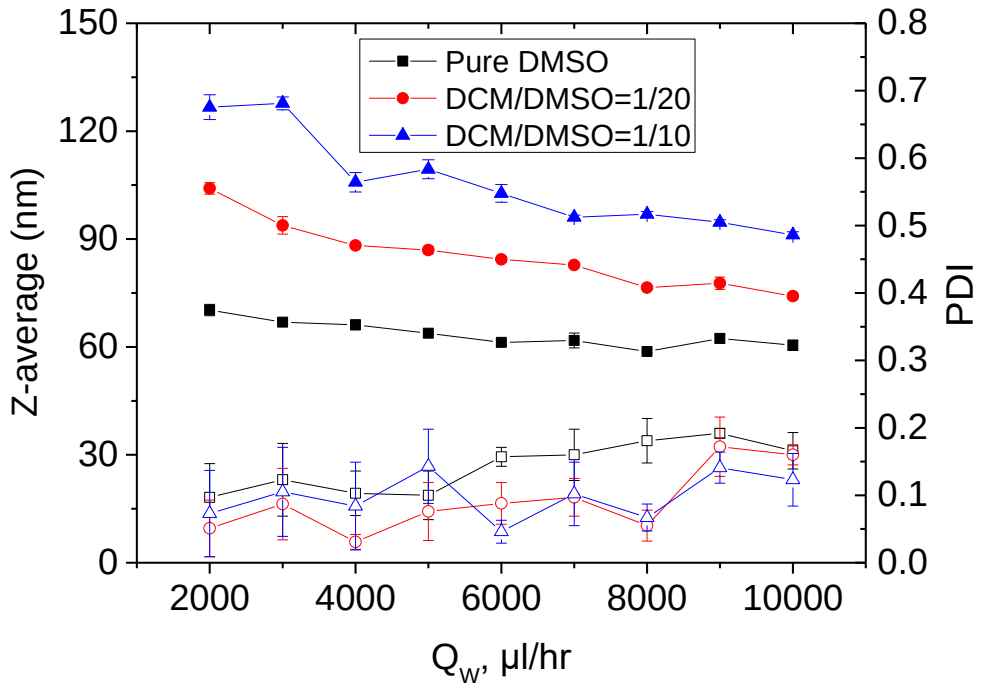

Figure 25. Size of PLGA NPs synthesized with precursors of different flow ratios and different V_{DCM}/V_{DMSO}. Q_{oil}=50 µl/hr, Concentration of PLGA (Mw=4000~15000) = 5 mg/ml. The solid icons represent the data of particle sizes (left Y axis) and the open icons represent the date of particle dispersity (right Y axis). (n = 3; mean ± S.D.)

It is found that at a given flow rate of $Q_{w,}$ larger PLGA NPs will be produced at a higher flow rate of Q_{oil}; and at a given flow rate of Q_{oil}, smaller PLGA NPs will be produced a t a higher flow rate of Q_w (Figure 15). It is reasonable for us to consider that higher flow ratio (Q_{oil}/Q_w) needs more time for solvent exchange (Equation 1). In this case, self-assembly of polymer occurs in an environment with less organic solvent[45], in which condition polymers cannot easily move, absorb or insert to a present nanoparticle, but nucleate new nanoparticles themselves of smaller sizes than those from flow focusing with more Q_{oil} fraction. Besides, the distribution of nanoparticles basically remains the same regardless change of flow rates of Q_{oil} and Q_w, which proves this microfluidic flow focusing a reliable technique to produce uniform nanoparticles with different flow rates.

$$\tau_{mix} \sim \frac{W_f^2}{4D} \approx \frac{w^2}{9D} \frac{1}{(1+\frac{1}{R})^2} \quad (1)$$

$\tau_{mix:}$ mixing time of hydrodynamic flow focusing

D: diffusivity of the solvent,

W_f: width of the focused stream,

w: width of the channel,

R: flow ratio, $Q_{oil}/Q_{w.}$

We next examined the effect of DCM on self-assembly of PLGA NPs by setting its volume ratio of DCM/DMSO in the dispersed phase as 0, 1/20 and 1/10 (Figure 15). At each given flow ratio of Q_{oil}/Q_w, the volume fraction of DCM is found to have a positive correlation with the diameter of the NPs. It can be explained in the Section 3.4.2 that the more DCM is introduced into the solution, the larger nanoparticles will be created. The size of PLGA NPs also changed as Q_w increasing from 2000 µl/hr to 10000 µl/hr, but with different ranges: 70 nm to 59 nm (no DCM), 104 nm to 74 nm (DCM/DMSO=1/20) and 128 nm to 91 nm (DCM/DMSO=1/10). Higher DCM fraction led to larger size range, in other word, different volume fraction of DCM brought the size range different sensitivities to the change of Q_w, which offers us a new controllable method to tune the size of nanoparticles with a broader range for selection by adding an immiscible component to dispersed phase and changing its volume fraction.

To be noticed, almost all of the PLGA NPs synthesized with DCM/DMSO precursor have a more narrow distribution than those with pure DMSO precursor, yet no significant correspondence to the volume fraction of DCM. This is because formation of nanoparticles from pure DMSO precursor and DCM/DMSO precursor are dominated by two different mechanism: with pure DMSO it is classical nanoprecipitation[45]; with DCM/DMSO, homogeneous micro droplets are firstly generated (Figure 20c) and then shrink to nanoparticles which inherited their homogeneity. Thus PLGA NPs evolved from highly uniform micro droplets are superior to those self-assembling from traditional nanoprecipitation in monodispersity.

3.4.5 Drug encapsulation and release

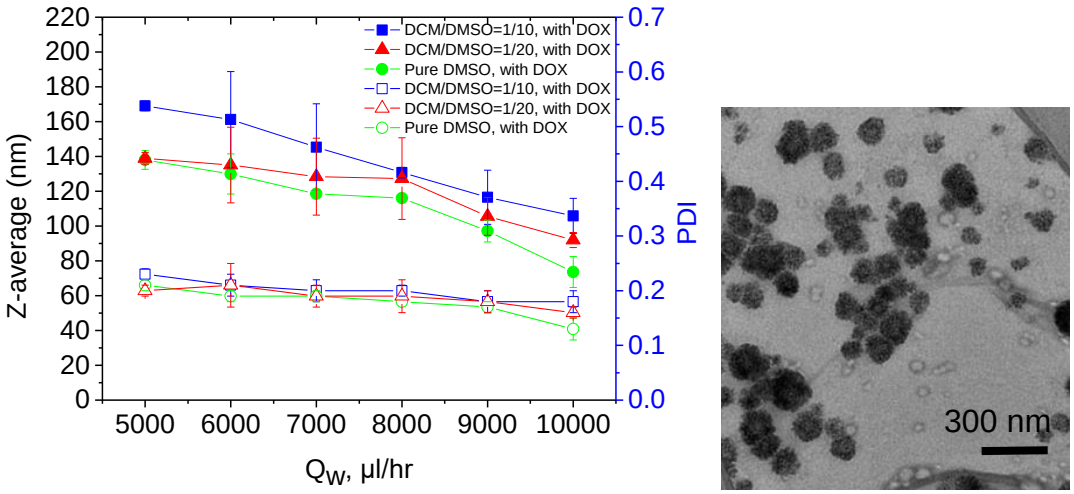

Figure 26. Size of DOX-encapsulated PLGA NPs synthesized with precursors of different flow ratios and different V_{DCM}/V_{DMSO}. The solid icons represent the data of particle sizes and the open icons represent the date of particle dispersity. Q_{oil}=50μl/hr. Concentration of PLGA (Mw=4000~15000) = 5mg/ml. Concentration of Doxorubicn = 1mg/ml. (n = 3; mean ± S.D.). TEM image of DOX-PLGA NPs (the scale bar is 100 nm) to demonstrate spherical shape of the nanoparticles.

Figure 26 illustrates the how the size of DOX-encapsulated NPs varies at different flow ratios and V_{DCM}/V_{DMSO}, the trend of which is basically consistent with the size of NPs without drugs (Figure 25). Generally, the sizes of drug-loaded NPs are larger than those without drugs. Noticeably, the DOX-PLGA NPs exhibited a good monodispersity, and the polydispersity gradually decreased as the flow ratio (Q_{oil}/Q_w) decreased, which proves that rapid mixing can offer a more homogenous environment for NPs formation.

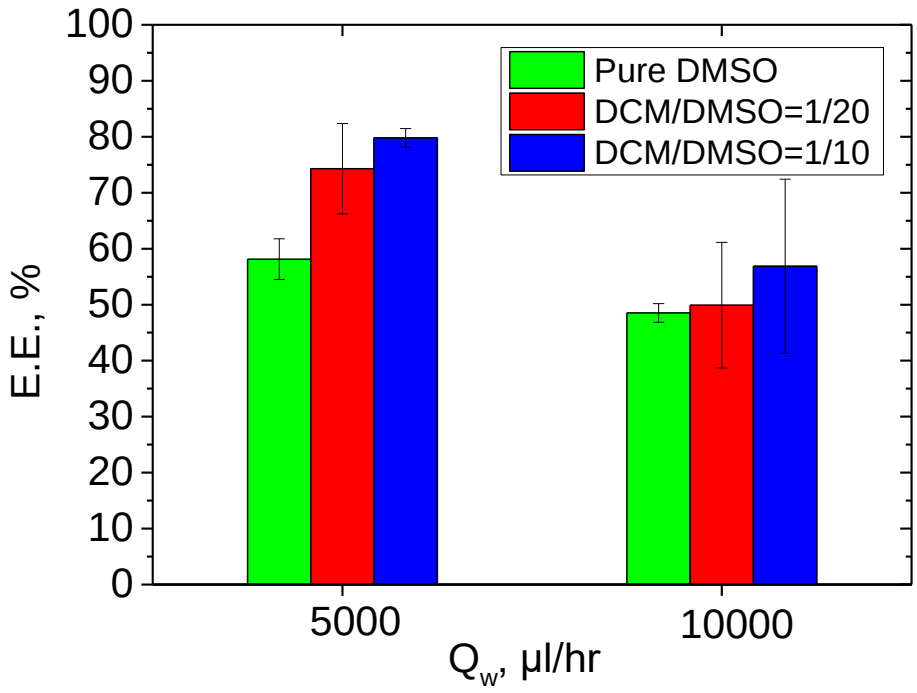

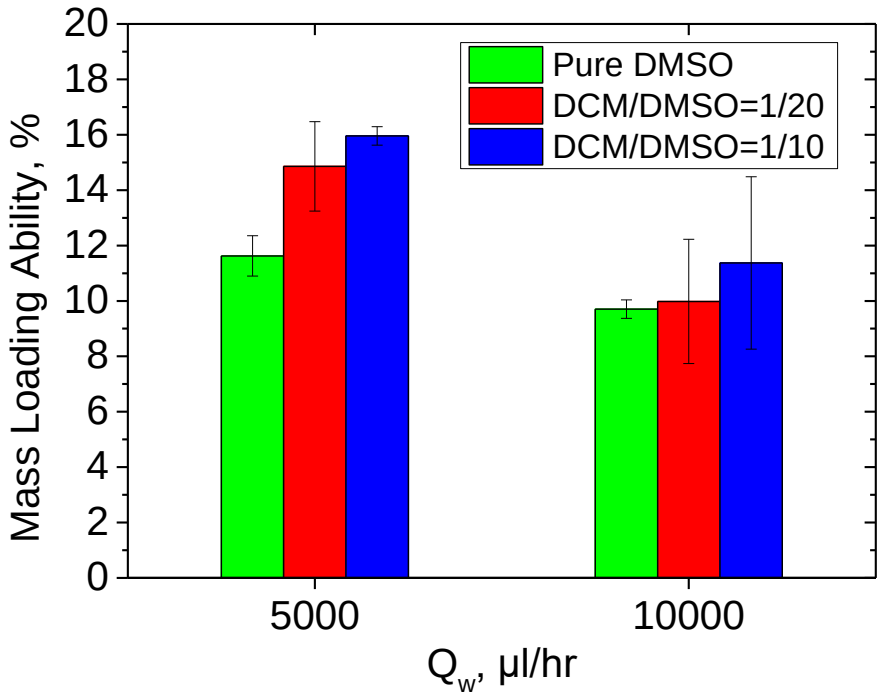

Figure 27. E.E. and mass loading ability of DOX-PLGA NPs of different flow ratios different V_{DCM}/V_{DMSO}. Q_{oil}=50 μl/hr, Concentration of PLGA (Mw=4000~15000) = 5 mg/ml. Concentration of Doxorubicin = 1 mg/ml. (n = 3; mean ± S.D.)

Drug encapsulation efficiency (E.E.) is defined as the fraction of the initial DOX that is encapsulated by PLGA NPs, whereas mass loading ability is defined as the mass

fraction of the encapsulated drug and nanoparticles. It is shown in Figure 27 that both E.E. and mass loading ability increased with the increase of V_{DCM}/V_{DMSO}, regardless of the flow ratio. With the addition of DCM from 0 to 1/20, and to 1/10, the E.E. increased from 48.5% to 49.9%, and to 56.9%, meanwhile the mass loading ability increased from 9.7% to 10.0%, and to 11.4%, at low flow ratio (Q_{oil}/Q_w =50/10000); the E.E. increased from 58.1% to 74.3%, and to 79.8%, meanwhile the mass loading ability increased from 11.6% to 14.9%, and to 16.0%, at high flow ratio (Q_{oil}/Q_w =50/5000). These results indicate that this partially water-miscible fluid could help to preserve drug within the NPs better than using pure DMSO and other classical water-miscible fluid in literature[49] by the introduction of DCM, which is mostly like due to the interfacial tension between the partially water-miscible fluid and water, as discussed in Section 3.4. 2, and help to "lock" the drug inside during their formation of NPs. The good affinity between DCM and DOX contributes to this effect as well. Higher V_{DCM}/V_{DMSO} led to higher E.E. can also be explained by that precursor of higher V_{DCM}/V_{DMSO} has larger interfacial tension with water so that more drug would be encapsulated.

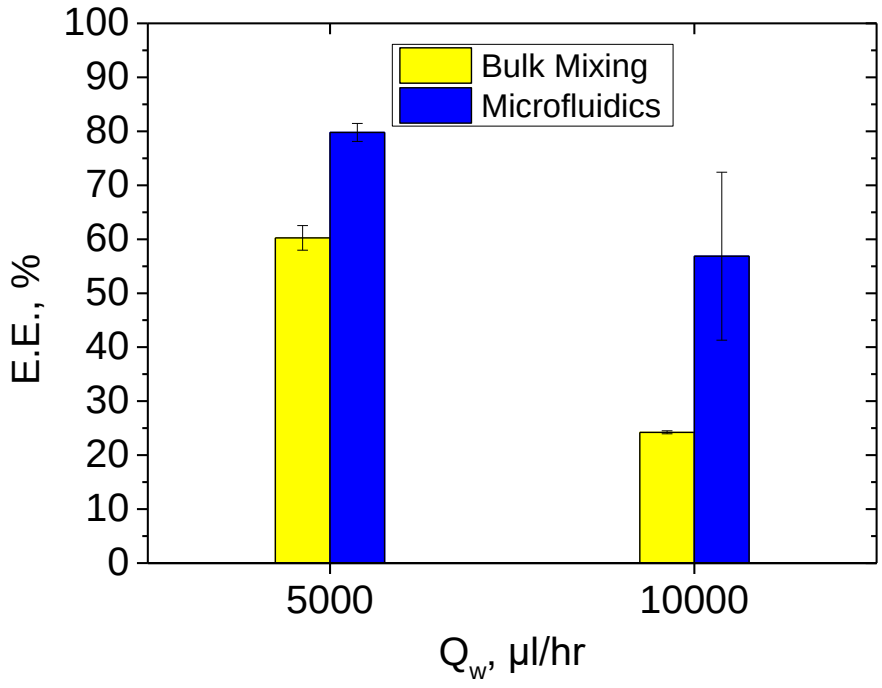

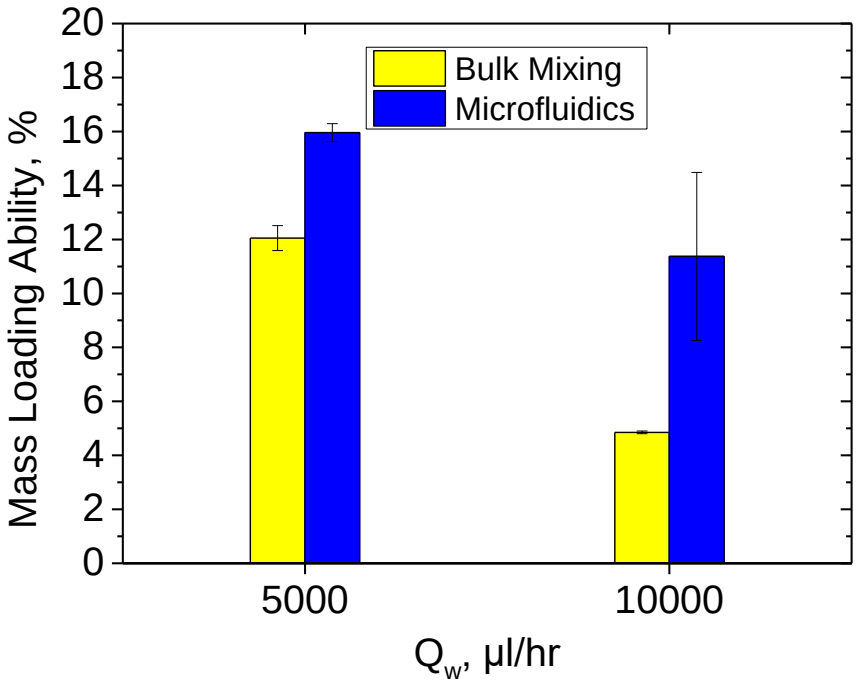

Figure 28. E.E. and mass loading ability of DOX-PLGA NPs by bulk mixing method and microfluidics method, respectively. V_{DCM}/V_{DMSO} =1/10. Concentration of Doxorubicin = 1 mg/ml. Q_{oil}=50 μl/hr, Concentration of PLGA (Mw=4000~15000) = 5 mg/ml. (n = 3; mean ± S.D.)

In addition, both of E.E. and mass loading ability of PLGA NPs by microfluidics have got improved (Figure 28) compared to bulk mixing protocols, especially at low flow ratio (Q_{oil}/Q_w). This feature is most likely due to the superior controllability of microfluidics to manipulate tiny volume of fluid[42, 135] while at rapid mixing.

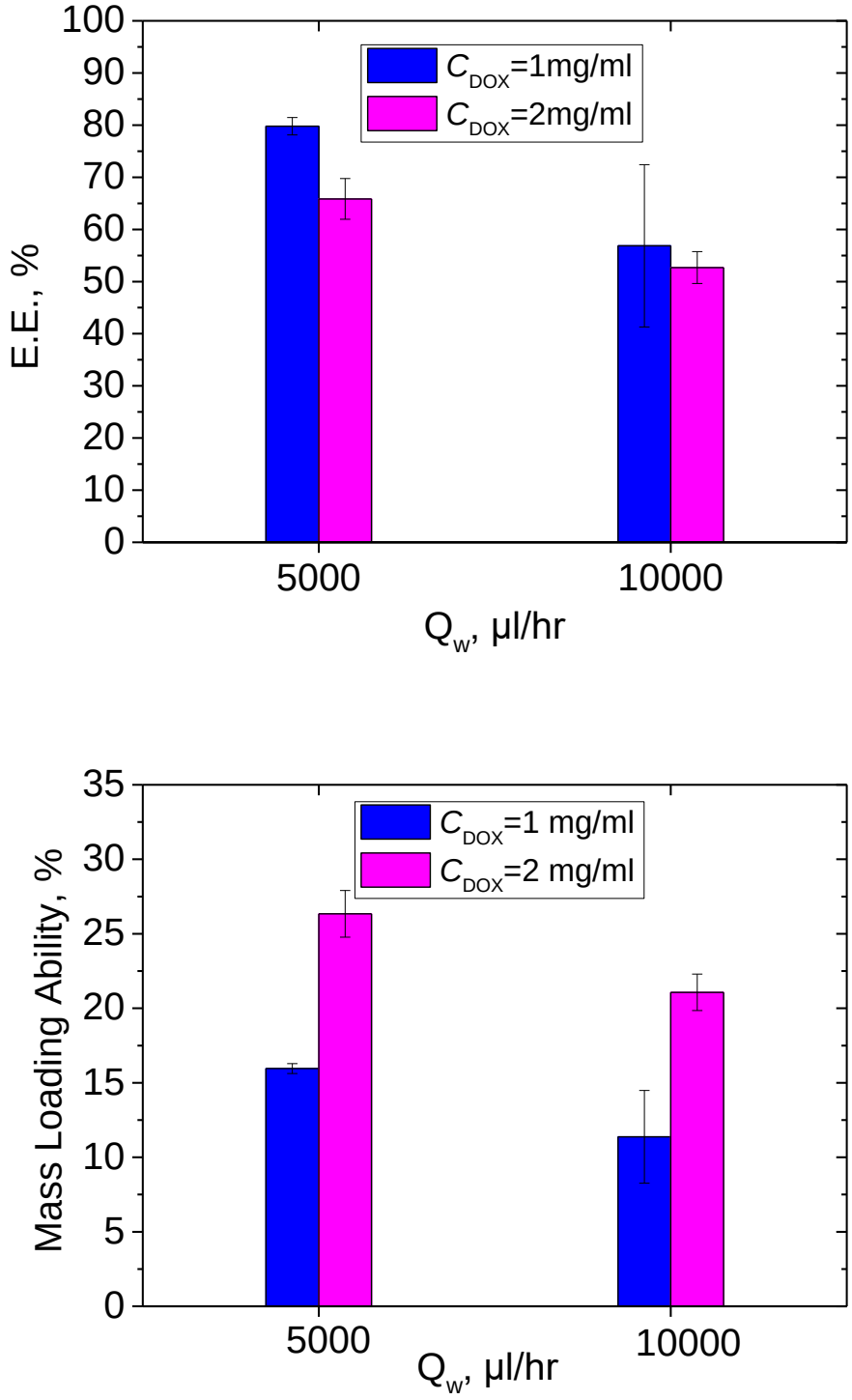

Figure 29. E.E. and mass loading ability of DOX-PLGA NPs of different flow ratios and initial drug concentrations. V_{DCM}/V_{DMSO} =1/10. Q_{oil}=50 μl/hr, Concentration of PLGA (Mw=4000~15000) = 5 mg/ml. (n = 3; mean ± S.D.)

We further investigated the effect of the initial DOX concentration on mass loading ability and E.E. (Figure 29). With a fixed V_{DCM}/V_{DMSO}=1/10, by doubling the drug feed

from 1mg/ml to 2mg/ml, we have got the mass loading ability greatly increased from 11.4% to 21.1%, and the E.E. just slightly decreased from 56.7% to 52.7%, at low flow ratio (Q_{oil}/Q_w =50/10000); and similarly, the mass loading ability greatly increased from 16.0% to 26.3%, and the E.E. just slightly decreased from 79.8% to 65.9%, at high flow ratio (Q_{oil}/Q_w =50/5000). This mass loading ratio shown by these PLGA NPs is not only significantly higher than former research using conventional synthesis[4, 41], but also comparable to droplets-based microfluidic method using pure water-miscible solvent[194, 195], and the relatively high E.E. ensures a low waste of drugs.

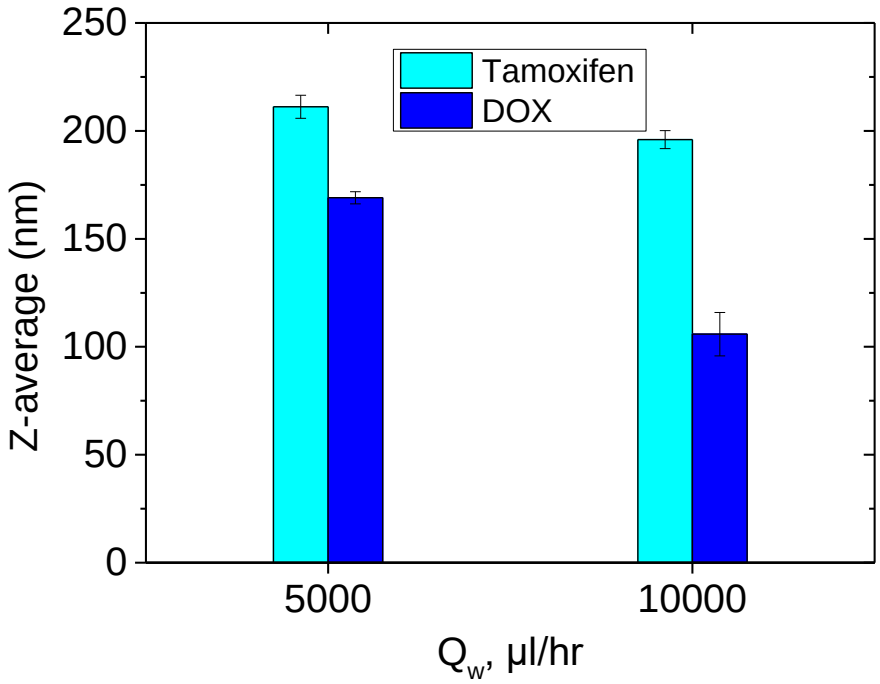

Figure 30. Size of DOX-PLGA NPs and Tamoxifen-PLGA NPs of different flow ratios. V_{DCM}/V_{DMSO} =1/10. Concentration of Doxorubicin and Tamoxifen= 1 mg/ml. Q_{oil}=50 µl/hr, Concentration of PLGA (Mw=4000~15000) = 5 mg/ml. (n = 3; mean ± S.D.)

When we switched the drug from Doxorubicin to Tamoxifen, it was also found that the affinity between drugs and solvents has a great effect on the size and encapsulation ability of NPs. The PLGA NPs containing Tamoxifen have larger sizes (Figure 30) compared to those containing Doxorubicin, since Tamoxifen is more hydrophobic than Doxorubicin, and could increase the surface tension of the transitional micro-droplets, which finally lead to larger NPs as discussed in Section 3.4.2.

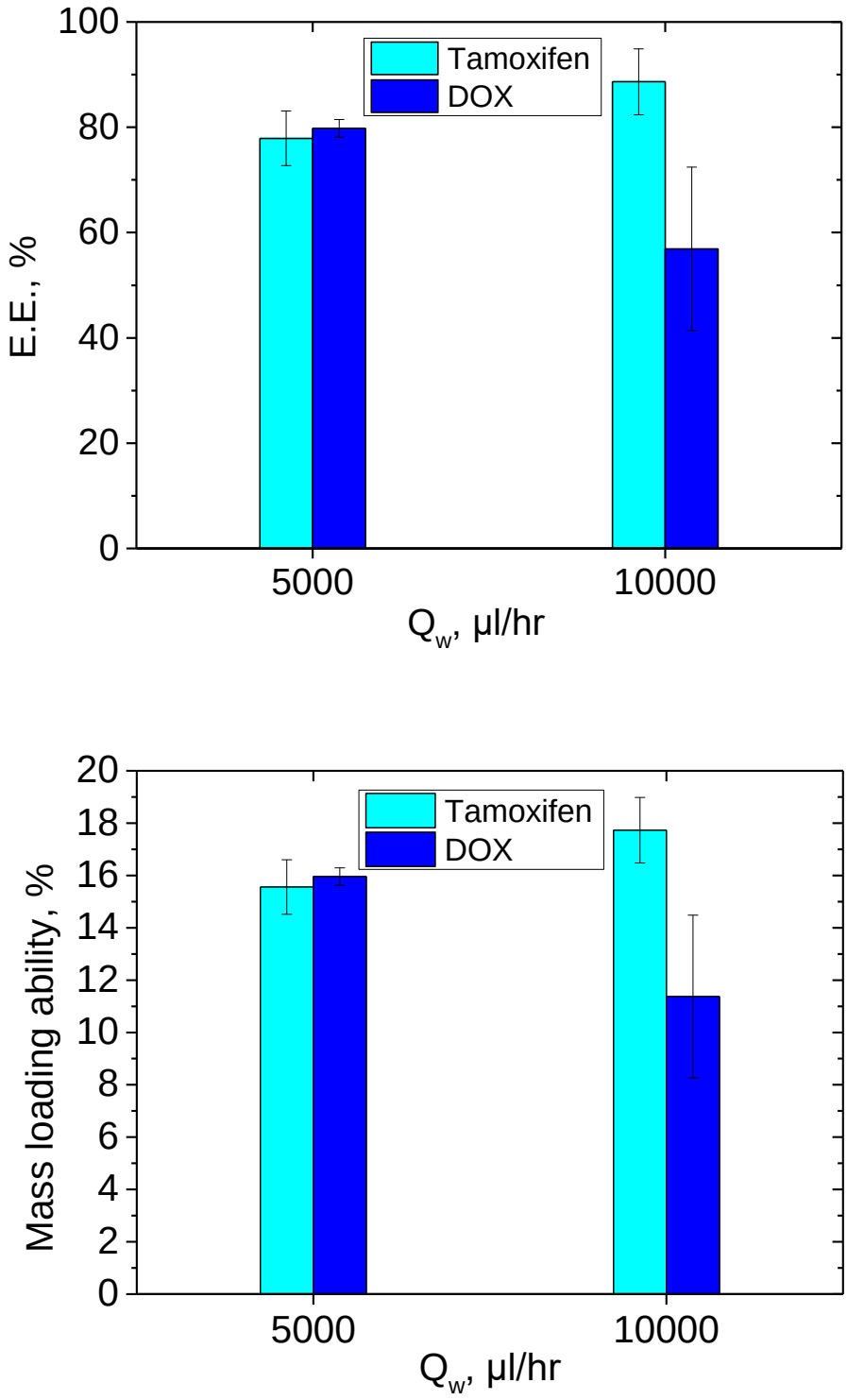

Figure 31. E.E. and mass loading ability of DOX-PLGA NPs and Tamoxifen-PLGA NPs of different flow ratios. Q_{oil}=50 µl/hr, Concentration of PLGA (Mw=4000~15000) = 5 mg/ml. V_{DCM}/V_{DMSO} =1/10. Concentration of Doxorubicin and Tamoxifen= 1mg/ml. (n = 3; mean ± S.D.)

In addition, the NPs exhibited a significantly improved E.E. and mass loading ability

with Tamoxifen than with Doxorubicin (Figure 31) at low flow ratio (Q_{oil}/Q_w =50/10000). It is most likely due to that Tamoxifen has higher affinity with DCM than Doxorubicin, so that more Tamoxifen can be preserved after the solvent replacement.

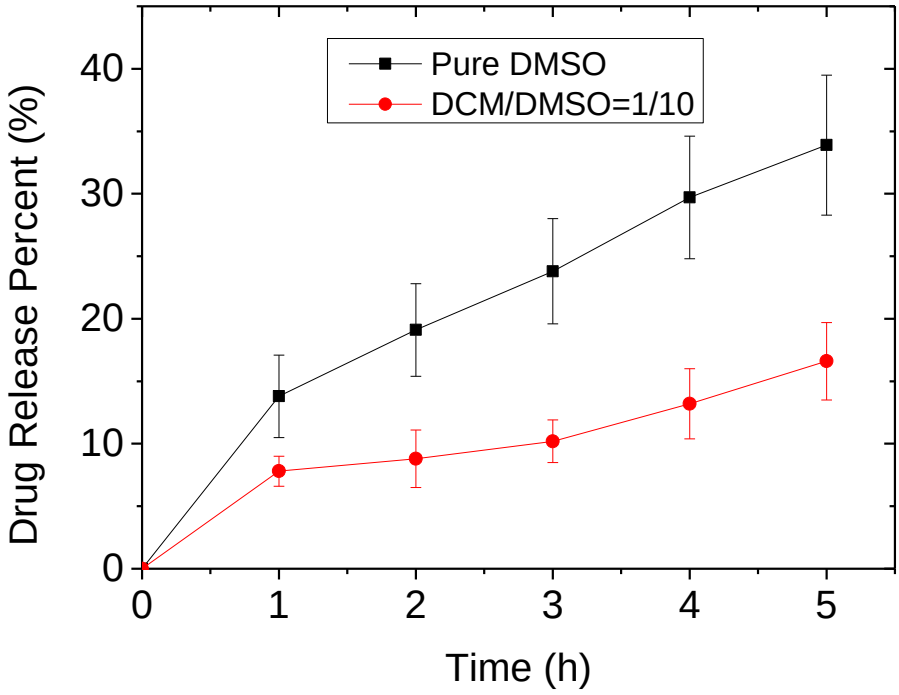

Figure 32. Comparison of *in-vitro* doxorubicin cumulative release profiles by PLGA NPs of different V_{DCM}/V_{DMSO}.

The role of V_{DCM}/V_{DMSO} played in the procedure of drug release was also studied: We found that DOX-PLGA NPs containing DCM during their formation exhibited a slower sustained release stage, compared to those without DCM during the formation (Figure 8). As previous research shown[196, 197, 198], DCM is inclined to shrink towards the core of NPs during its evaporation process, so that more drug is desired to be "dragged" to and embedded in the "deeper" part of the NPs. This feature of the partially miscible water imply that it could help to preserve more drug inside NPs and facilitate to a more sustained release.

3.5 CONCLUSION

Herein we have successfully developed a novel microfluidic flow focusing method for synthesis of DOX-PLGA NPs using a partially water-miscible solvent. We investigated the stability of the partially water-miscible under the confinement of the microfluidic channel and a transformation process, “Jet to Droplets to Nanoparticles”, of the precursor fluid in the jetting zone was observed for the first time. The PLGA NPs size can be precisely tuned by controlling the flow ratio, polymer concentration, and V_{DCM} of the dispersed phase. Furthermore, the NPs synthesized using the partially water-miscible microfluidic precursor exhibited much better drug loading loading ability and a longer sustained release stage than conventional microfluidic methods using water-miscible precursor.

Besides, our microfluidic method with excessive drug loading hasn’t caused any clogging effect or drug aggregation during the long-time flow focusing. All of these characteristics prove that this microfluidic method by partially water-miscible fluid is a clean, highly-efficient, and robust platform to produce drug-encapsulated NPs, and has great potential for further applications such as cosmetics industry, controlled release, and 3D printing, etc.

Chapter 4 Drug Content Tunable Encapsulation and Controlled Release of a Hydrophilic Drug by a Modified Drop-wise Nanoprecipitation Method

4.1 Summary

To improve the encapsulation efficiency of hydrophilic drugs by polymer nanoparticles (NPs) has been arising attentions from the controlled release research field[48]. Here we developed a novel simply-modified drop-wise nanoprecipitation method which separated hydrophilic drug and polymer into aqueous phase (continuous phase) and organic phase (dispersed phase), individually, and involved a mixing process. Using this method, we produced ciprofloxacin-loaded NPs by Poly (D, L-lactic acid)-Dextran (PLA-DEX) and PLGA-PEG successfully, with a considerable drug loading ability (18.6% by PLA-DEX, 27.2% by PLGA-PEG, w/w), which could be precisely tuned by changing the initial drug feed concentration of ciprofloxacin. *In-vitro* sustained release study of ciprofloxacin was achieved in stimulated tear fluid (STF). Up to 95.4% of encapsulated ciprofloxacin was released by PLA-DEX NPs and 96.9% of encapsulated ciprofloxacin was released by PLGA-PEG NPs, within 144h. These studies suggest that this novel modified nanoprecipitation method is a rapid, facile, and reproducible technique for making nano-scale drug delivery carriers of high drug loading ability.

4.2 Introduction

Nanoprecipitation technology has grown into a highly-efficient, easily-handled, and mature tool to fabricate drug-loaded NPs for biomedicine researchers since its late 1980s start by Fessi et al[41]. Polymer and hydrophobic drugs were dissolved in the same

organic solvents and then mixed with aqueous solution. By modifying the solution mixing speed, O/W ratio[42], pH[43], polymer/drug ratio[44], block ratio of block polymers[45], solvent selection[46], etc., the parameters of NPs including size, distribution, and drug encapsulation efficiency, could be tuned easily.

However, the conventional nanoprecipitation procedure has relatively limited potential to encapsulate hydrophilic compounds[199], given their poor solubility in organic solvents compared to most commonly used emulsion-based techniques[12, 76, 200, 201, 202], not to mention precisely control of the drug loading amount[203], though the latter methods usually include complex preparation process, and result in much larger (several hundreds to thousands nanometers) non-uniform nanoparticles[78].

Here we chose ciprofloxacin as our drug model, one of the most commonly used anti-infective agents for ocular treatment because of its low toxicity, broad-spectrum antimicrobial activity, and low resistance from bacteria[86]. Then we developed our novel modified nanoprecipitation method that separates drug and polymer into organic phase and aqueous phase, individually. Monodispersed ciprofloxacin-loaded NPs were formed with a tunable size via a simple drop-wise mixing process similar to conventional nanoprecipitation's[199]. The drug encapsulation efficiencies of NPs and their *in-vitro* release kinetics were assessed. In addition, a high linear correlation was found between the initial concentration of ciprofloxacin and the mass loading ability of PLA-DEX and PLGA-PEG NPs. This work provides new quantitative approach for producing polymeric NPs with high loading of hydrophilic drugs by facile one-step nanoprecipitation.

4.3 Experimental Section

4.3.1 Materials

Poly (D, L-lactic acid)-Dextran (PLA 20 kDa -DEX 10 kDa) was synthesized as previously reported[47] and PLGA (30~35 kDa)-PEG (6 kDa) was purchased from Lakeshore Biomaterials (Birmingham, AL, USA). Ciprofloxacin, Dimethyl sulfoxide

(DMSO), and Hydrochloric acid (HCl) were purchased from Sigma Aldrich (Oakville, Canada). Simulated tear fluid (STF) was prepared for the in vitro release experiment using a previously described formulation[204].

4.3.2 Synthesis of PLA-DEX and PLGA-PEG NPs.

1 ml PLA-DEX or PLGA-PEG solution (5 mg/ml in DMSO) was added into 10 ml HCl aqueous solution (1 mol/L) drop-wisely with gentle magnetic stirring for 10 min. Then the solution was filtered by 200 nm filters for further use. The size and polydispersity (PDI) of NPs were determined by dynamic lighting scattering (90Plus Particle Size Analyzer, Brookhaven, λ = 659 nm at 90°).

4.3.3 Transmission Electron Microscopy (TEM).

The particle morphology of PLA-DEX and PLGA-PEG NPs were further characterized using transmission electron microscopy (TEM, Philips CM 10) with a lanthanum hexaboride filament (LaB6). The NP solution was prepared as the protocols mentioned above and coated onto a copper grid. A drop of aqueous phosphotungstic acid solution (20 mg/ml) was used to briefly stain the NPs for 10s and was then removed by absorbent paper. The copper grid was dried at room temperature over night before TEM imaging.

4.3.4 Ciprofloxacin encapsulation by PLA-DEX and PLGA-PEG NPs.

PLA-DEX was dissolved in DMSO (5 mg/ml), and ciprofloxacin was dissolved in 1 mol/L HCl aqueous solution with concentration of 0.5, 1, 2, 4, 5, 6, 8 mg/ml, respectively. 1ml PLA-DEX solution was added into 10ml Ciprofloxacin solution drop-wisely with gentle magnetic stirring for 10 min. Then the solution was filtered by 200 nm filters for further use. 1 ml of filtered solution was centrifuged with an Amicon centrifuge tube (MWCO=3000) for 30 min at 8000 rpm. 1ml of 1mol/L HCl aqueous solution was used to resuspend the NPs, and another round of centrifugation (8000 rpm, 30 min) was done in order to wash away the un-bonded and loosely-associated

ciprofloxacin. Afterwards, the NPs were dissolved by a mixed solvent of 1mol/L HCl aqueous solution and DMSO (*v: v=1:1*) to release all encapsulated drugs for determination of encapsulation efficiency by UV spectroscopy. The same procedure was applied for encapsulation of ciprofloxacin by PLGA-PEG for comparative analysis. The encapsulation efficiency and mass loading ability of NPs were calculated by the following Eq. (2) and Eq. (3).

Encapsulation Efficiency = $\frac{Mass\ of\ the\ drug\ encapsulated}{Mass\ of\ the\ initial\ drug\ feed} \times 100\%$ (2)

Mass loading ability = $\frac{Mass\ of\ the\ drug\ encapsulated}{Mass\ of\ the\ polymer} \times 100\%$ (3)

4.3.5 Drug release study.

After the modified nanoprecipitation (1 ml 5 mg/ml PLA-DEX+10 ml 5 mg/ml ciprofloxacin), 4 ml filtered solution was centrifuged, washed and re-centrifuged per the procedure from previous sections. The NPs were resuspended by 10 ml Millipore water, and then transferred into a dialysis membrane (100 kDa, MWCO), against 400 ml simulated tear fluid (STF) in a release bottle with stirring at 37 ℃. 1 ml of each sample was collected at 2h, 4h, 6h, 8h, 10h, 12h, 24h, 48h...etc. to determine the cumulative released dose by UV spectroscopy. Comparative groups of free drug without NP carriers and of Ciprofloxacin-PLGA-PEG NPs were made with the same protocols.

4.4 Results and Discussion

4.4.1 Formation of Ciprofloxacin-loaded NPs by block polymers

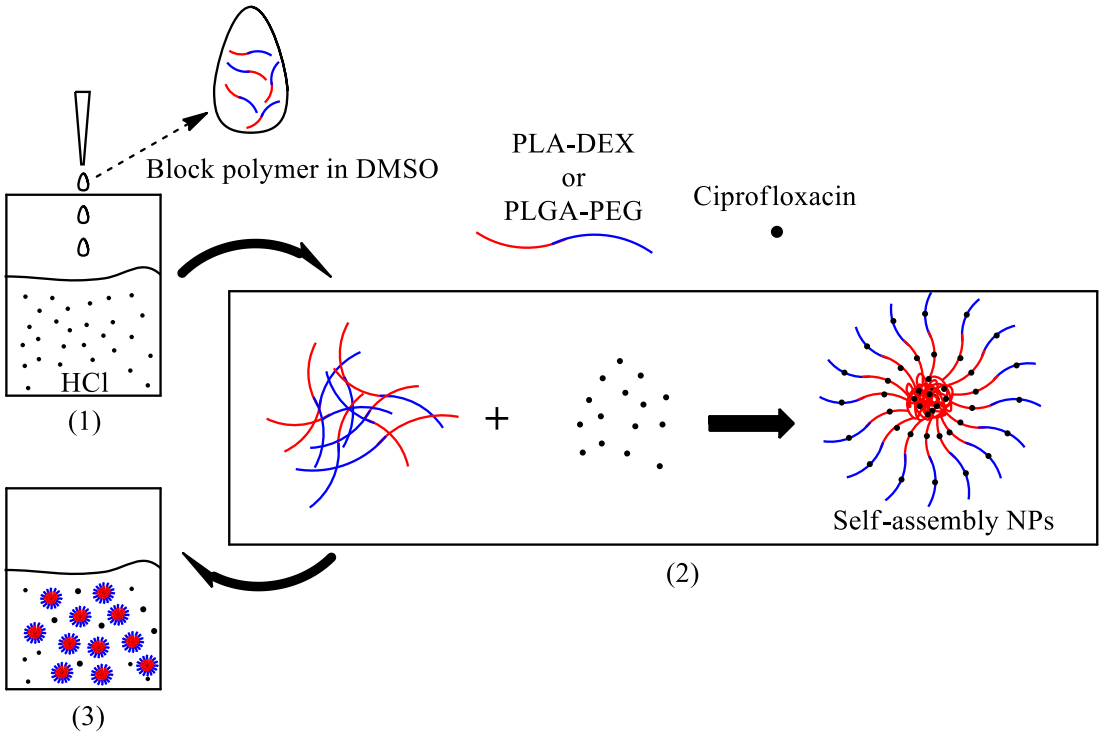

Figure 33. The formation procedure of ciprofloxacin-loaded NPs. (1) Drop-wise nanoprecipitation; (2) Block polymer self-assembled to form core-shell NPs with ciprofloxacin; (3) The NPs and non-encapsulated ciprofloxacin after nanoprecipitation.

Figure 33 shows a schematic of the formation process of ciprofloxacin-loaded NPs within the modified nanoprecipitation. It is known that in traditional nanoprecipitation the drug-loaded NPs form because of their co-nanoprecipitatian[205]due to the solvent displacement that turns one same "good" organic solvent into one same "bad" aqueous solvent. However, the difference of the modified nanoprecipitation is the ciprofloxacin and polymer were separated in two different "good" solvents at the beginning, which were then turned into one same "bad" solvent for both afterwards. The formation of drug-loaded NPs is due to the interfacial deposition of polymer and drug because of the interfacial solvent displacement between two different unstable liquid phases[41].

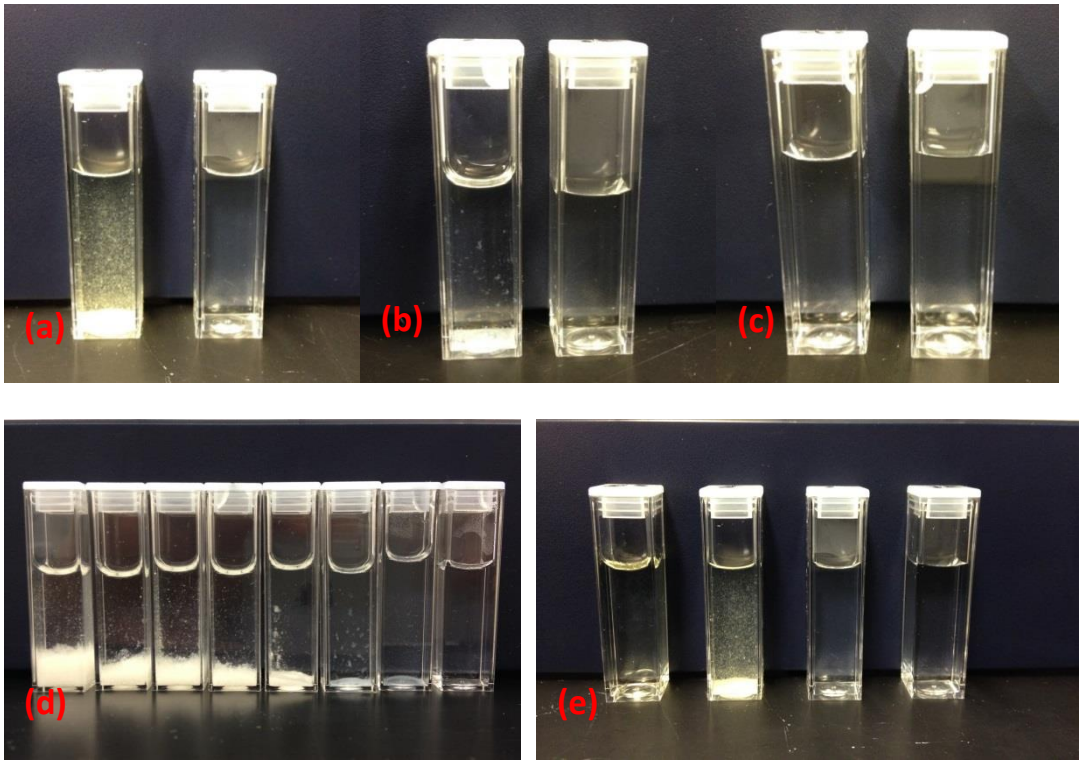

Figure 34. Nanoprecipitation of ciprofloxacin and PLA-DEX NPs. (a) A normal modified nanoprecipitation, Left: 1h after nanoprecipitation; Right: 0 min after nanoprecipitation. (b) Modified nanoprecipitation without PLA-DEX, Left: 1h after nanoprecipitation; Right: 0 min after nanoprecipitation. (c) Modified nanoprecipitation without Ciprofloxacin, Left: 1h after nanoprecipitation; Right: 0 min after nanoprecipitation. (d) Modified nanoprecipitation with different concentration of ciprofloxacin after 24h. Left to Right: 8, 6, 5, 4, 2, 1, 0.5, 0 mg/ml. (e) Solution of free drug and modified nanoprecipitation. Left to Right: ciprofloxacin in HCl solution, 1h after modified nanoprecipitation, 30 min after modified nanoprecipitation, 15 min after modified nanoprecipitation. (The protocol was drop-wisely adding 1 ml of 5 mg/ml PLA-DEX in DMSO into 8 mg/ml ciprofloxacin in 1 mol/L HCl aqueous if no additional statements).

Although only a little volume of dispersed phase (DMSO) was added into continuous phase (HCl aqueous solution), this tiny change of solvent environment was a driven force for the precipitation of ciprofloxacin, which is assessed in Figure 34b, the spontaneous aggregation of ciprofloxacin occurred without the PLA-DEX in the mixing process. Compared Figure 34a, b and c, we can see the PLA-DEX NPs had not precipitation, yet the existence of PLA-DEX in the solvents mixing promoted more precipitation of ciprofloxacin since the ciprofloxacin not only aggregated by itself, but also were absorbed or encapsulated by PLA-DEX, which is the mechanism of this modified nanoprecipitation. More concentrated the ciprofloxacin solution was, the more precipitation would be formed according to Figure 34d. It is also clearly

demonstrated in Figure 34e that how the precipitation of ciprofloxacin happened in a clear solution after nanoprecipitation by time. The solution turned slightly milky in 30 min and obvious precipitation formed in 1h, which indicated that the preparation to make NPs for use of characterization, encapsulation and release study should be done as fast as possible in case of severe aggregation.

4.4.2 Encapsulation of ciprofloxacin by NPs

Polymer	*C* of Cipro (mg/ml)	Size of NPs (nm)	PDI	Mass loading ability (%)
PLA-DEX	0.5	82.4±7.7	0.137±0.011	1.52±0.23
	1	89.2±3.2	0.129±0.015	3.33±0.84
	2	89.2±6.5	0.124±0.029	5.68±0.74
	4	93.2±7.3	0.141±0.020	8.45±0.31
	5	94.9±8.9	0.138±0.026	10.25±1.99
	6	94.4±9.3	0.133±0.014	12.06±1.90
	8	98.4±11.2	0.133±0.034	18.64±2.60
PLGA-PEG	0.5	174.4±1.2	0.125±0.014	3.29±1.00
	1	175.2±1.2	0.123±0.002	4.76±0.75
	2	177.8±7.6	0.123±0.007	5.97±1.60
	4	179.1±2.3	0.098±0.005	10.79±0.59
	5	182.8±4.6	0.124±0.007	13.71±1.25
	6	187.5±5.3	0.103±0.015	17.84±3.04
	8	205.4±15.2	0.112±0.022	27.24±4.79

Table 2. NP parameters of effective diameter, polydispersity, and mass loading ability for PLA-DEX and PLGA-PEG. (n = 3; mean ± S.D.)

As shown in Table 2, the effective diameters slightly increased from 82.4±7.7 nm to 98.4±11.2 nm by PLA-DEX NPs, and from 174.4±1.2 nm to 205.4±15.2 nm by PLGA-PEG NPs, respectively, with the increase of ciprofloxacin concentration from 0.5mg/ml to 8mg/ml. Given that other environmental conditions remained the same, this increase of NP size should be due to the increasing amount of encapsulated drug content within the NPs (Figure 35), which indicates that we could tune the NP size by controlling the concentration of ciprofloxacin. Moreover, with this modified nanoprecipitation method, the NPs remained a relatively low and similar polydispersity (Table 2) regardless of changes in ciprofloxacin concentration or NP size. This characteristic revealed that our

modified nanoprecipitation method has a superior controllability over the morphology of NPs.

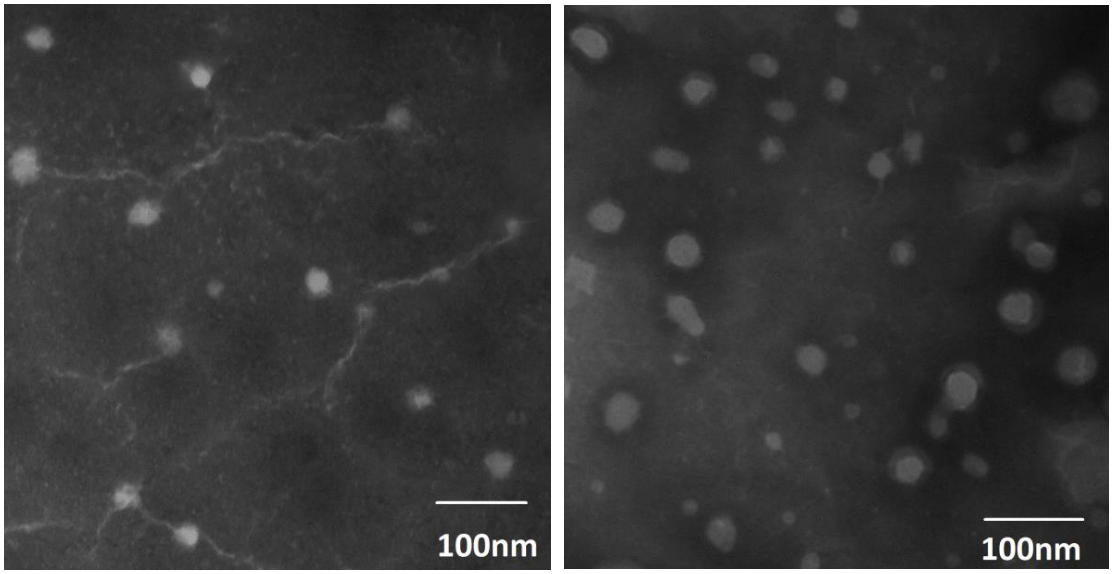

Figure 35. TEM image demonstrates the spherical shape of PLA–DEX NPs (Left) and PLGA-PEG NPs (Right).

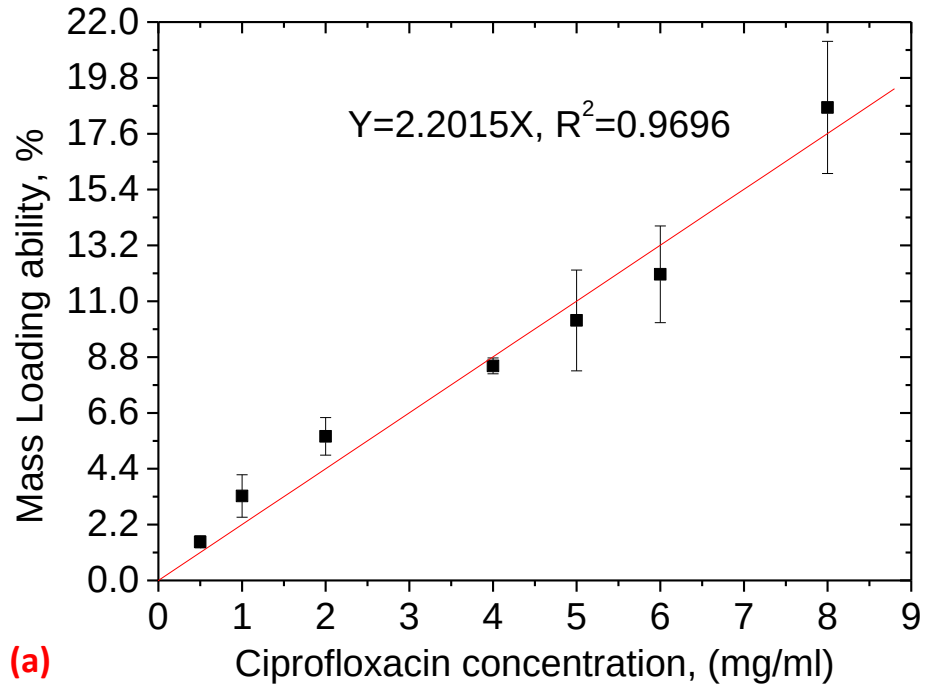

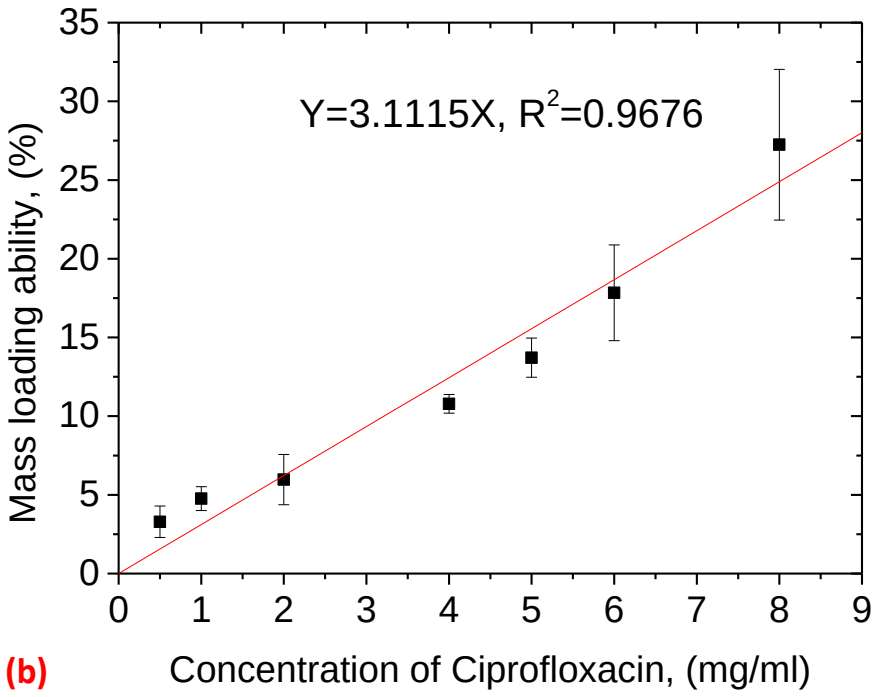

Figure 36. Relationship of NPs' mass loading ability and initial concentration of ciprofloxacin. (a) PLA-DEX NPs, y=2.2015x, R^2=0.9696; (b) PLGA-PEG NPs, y=3.1115x, R^2=0.9676. (n = 3; mean ± S.D.)

In addition, with this modified nanoprecipitation method, NPs presented a considerable mass loading ability, 18.6±2.6% by PLA-DEX and 27.2±4.8% by PLGA-PEG, respectively. Noticeably, one interesting phenomenon is that the mass loading ability of NPs, either PLA-DEX or PLGA-PEG, exhibited a very strong liner relationship with the concentration of ciprofloxacin by this modified nanoprecipitation. Both correlation coefficients were very close to 1 (R=0.9847 by PLA-DEX NPs and R =0.9837 by PLGA-DEX NPs) according to Figure 36, which indicates a quantitative approach that we could take to control the amount of the encapsulated ciprofloxacin[205] in the NPs by changing the concentration of original drug feed.

Furthermore, there is an interesting phenomenon to be noticed is that the mass loading ability of the PLA-DEX NPs exhibited a very strong liner relationship with the concentration of ciprofloxacin in the modified nanoprecipitation. The correlation coefficient R=0.9847 according to Figure 26, which indicates a quantitative approach that we could use to control the amount of the encapsulated ciprofloxacin[205] in the NPs

by changing the concentration of original drug feed.

Furthermore, the effective diameter of the NPs only increased by 1.2 times whereas its ability of drug loading had increased by more than 10 times, which means it could keep superior drug loading ability without significant change of its size.

The encapsulation efficiency of the PLA-DEX NPs slightly fluctuated, but all relatively low (1.05±0.17% to 1.97±0.54%) compared to the mass loading ability because there were much more ciprofloxacin than PLA-DEX in the solution. Perhaps we can use volatile solvents (e.g. acetone) instead of DMSO in the modified nanoprecipitation and perform a solvent evaporation[206] afterwards. After subtracting the NPs by centrifugation and filtration, we could re-use the filtered ciprofloxacin solution for another modified nanoprecipitation, or even multiple times. In this way, we may find a good balance between encapsulation efficiency and mass loading ability.

4.4.3 Ciprofloxacin Release Study

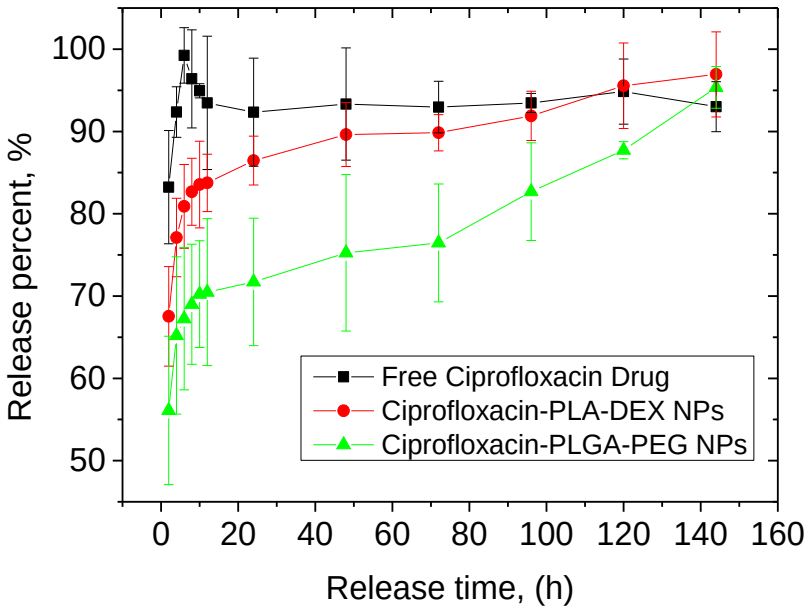

Figure 37. The cumulative release profiles of ciprofloxacin *in vitro* in STF at 37 °C as free drugs, by PLA-DEX NPs, and PLGA-PEG NPs. (n = 3; mean ± S.D.)

Figure 37 shows how the ciprofloxacin was released in simulated tear fluid (STF) as free drug, as encapsulated content by the PLA-DEX NPs, and by PLGA-PEG NPs,

respectively. The free drug group had a very quick release up to 83.2±6.9% within the initial 2h due to the free diffusion of the ciprofloxacin, and then the free diffusion nearly finished at 6h. In contrast, the ciprofloxacin encapsulated by both PLA-DEX and PLGA-PEG NPs had a slower burst-release within the initial 2h, up to 67.5±6.1% and 56.1±9.0%, respectively. These differences indicate that part of the encapsulated drugs was strongly associated to the NPs that were "covered" or "protected" well during the burst-release stage[207], compared to the free drug group. Both PLA-DEX NPs and PLGA-PEG NPs exhibited a much more controlled release profile than free drugs did. After the first 12h, a steady-release stage continued within both two groups, and ended up to 96.9±5.2% and 95.4±2.5%, respectively, at 144h. Noteworthy is that PLGA-PEG NPs released ciprofloxacin at a slower rate than PLA-DEX NPs did. This is perhaps because PLA-DEX NPs have more hydrophilic surfaces[23] which are less compact in an aqueous environment making it easier for ciprofloxacin drugs to detach[44]. Compared to the release profiles of free drug, both PLA-DEX and PLGA-PEG NPs prepared by this modified nanoprecipitation method showed great potential for a long time sustained release, which is needed for constant ocular treatments in clinical application[208].

4.5 CONCLUSION

A novel one-step drop-wise modified nanoprecipitation method was successfully developed, by which we could efficiently encapsulate the hydrophilic drug ciprofloxacin by PLA-DEX and PLGA-PEG NPs. NPs of considerable drug loading ability were synthesized with tunable sizes. We also found that the mass loading ability of the NPs varied as an excellent linear function of the concentration of ciprofloxacin, which demonstrates a possibility for an accurate control over the drug loading amount by NPs. Both of PLA-DEX and PLGA-PEG NPs exhibited great potential for a long-time sustained release compared to free drugs. By optimizing the formulation of NPs by changing the drug/polymer ratio and polymer composition, effective drug release rates and amounts for constant treatments in future clinical application[208] can be achieved. All of these characteristics make this modified nanoprecipitation method a

promising technique for encapsulation and release of hydrophilic drugs and preparation of functional NPs as drug delivery tools for further biomedical application.

Chapter 5 Investigation on possibility of combination of chemotherapy and magnetic therapy

5.1 Summary

We applied our modified flow focusing method using a partially water-miscible precursor to encapsulate magnetic iron oxide nanoparticles, within PTMC-*b*-PGA polymersomes, as a basis for future combination of chemotherapy and magnetic therapy. The modified flow focusing method showed better encapsulation efficiency (78%) and mass loading content of γ-Fe_2O_3 (43%) than conventional methods. The structure of PTMC-*b*-PGA polymersomes was characterized and confirmed by dynamic lighting scattering, static lighting scattering, and cryo-TEM. The influence of mixing methods (microfluidics and bulk) and flow ratio on the size and morphology of polymer vesicles were further investigated. This method successfully accomplished encapsulation of γ-Fe_2O_3 magnetic nanoparticles, prepared monodispersed polymer vesicles with considerable loading contents, thus, provided us a promising tool for fabricating multifunctional nanoparticle carriers for future multiple loading of anti-cancer drugs and inorganic therapeutics.

5.2 Introduction

Nanoparticles has been proved their effectiveness in cancer treatments over the past decades, no matter as the nano carrriers[9, 10, 71] of anti-cancer drugs, or as the metallic or inorganic hyperthermia nanoparticles[209, 210], or as diagnosis imaging probes[211, 212], etc. However, with the continuous research of the mechanisms of diseases and increasing treatment requirements, relying on a single type of drug or single therapy protocol usually could not solve the problem or meet patients' needs[1] completely. Thus, combinations of different nanotechnology cancer therapy methods[7, 213, 214] attract increasing attentions from researchers.

Dual loading of drug/ hyperthermia nanoparticles[6, 215, 216] has been arising interests of biomedical scientists recently, not only because of both nano-chemotherapy[36, 38] and nano-thermotherapy[174, 217] were tested effective in animal experiments, but also because of their combinations offer new advantages for cancer therapy strategies. For example, drug release from smart responsive polymer carriers[3, 37, 142] can be triggered by physical environmental stimulus like temperature and light, which can be shared with or offered by most commonly-used iron oxide nanoparticles[179, 218]. In addition, iron oxide nanoparticles can be used as theranostic signals[219], or to accelerate the drug release rate[8] in the chemotherapy systems, which further enhances the treatment effects.

However, the preparation of drug/iron oxide loading polymer vesicles by microfluidics at current stage are usually limited by the following drawbacks: (1) Oversized capsules (several hundred μm) by droplet-based microfluidics[220, 221], which brings obstacles for *in-vivo* study; (2) Poor loading ability of magnetic nanoparticles by flow-focusing based microfluidics, due to the poor solubility of iron oxide nanoparticles in common water-miscible organic solvents.

We are thus motivated to apply our modified microfluidic flow focusing method described in Chapter 3, in order to accomplish encapsulation of iron oxide nanoparticles first. In our experiments, we have successfully fabricated γ-Fe_2O_3- loaded PTMC-*b*-PGA polymersomes, with a respect to small and uniform vesicle size (dia.~200nm and PDI~0.2), and high loading ability of γ-Fe_2O_3 (mass loading > 40%). This modified microfluidic flow focusing method will provide huge potential for multiple encapsulation, imaging diagnosis, targeted therapy, and controlled drug release.

5.3 Experimental Section

5.3.1 Materials

PTMC (poly-trimethylenecarbonate, Mw=10000)-*b*-PGA-8(polyglycolic acid, Mw=3700) and γ-Fe_2O_3 nanoparticles (dia. 10~15 nm) were provided by collaborator Dr. Shusheng Zhang from Laboratoire de Chimie des Polymères Organiques,

University of Bordeaux. Dichloromethane (HiPerSolv CHROMANORM for HPLC，VWR), Dimethyl Sulfoxide (ACS grade, Amresco) Phosphate buffered saline (PBS, pH=7.4 at 25 ℃, Sigma Aldrich). Microfluidic capillary was fabricated as same protocols per the Section 3.2.2.

5.3.2 Preparation of polymersomes

PTMC-*b*-PGA (5 mg/ml) was dissolved in the mixed solvent of DCM/DMSO (V_{DCM}/V_{DMSO}=1/10) and filtered by 0.2 μm filter. The polymersomes were produced by a microfluidic flow focusing using the DCM/DMSO as a precursor and PBS buffer (0.01 mM) as a continuous phase at room temperature. The resulting dispersion was evaporated under a 37°C water-bath for one hour to remove DCM and then dialyzed against PBS buffer (0.01 mM, 1X) using a cellulose dialysis membrane (MWCO=3.5 kDa). The particle size and morphology were then measured and confirmed by DLS (dynamic lighting scattering) and SLS (static lighting scattering).

5.3.3 Fabrication of Fe_2O_3-loaded magnetic polymersomes by microfluidics

Doxorubicin, γ-Fe_2O_3, and PTMC-*b*-PGA (a typical weight ratio was: 1 mg/ml, 0.5 mg/ml, 5 mg/ml) were dissolved in the mixed solvent of DCM/DMSO (V_{DCM}/V_{DMSO}=1/10) and filtered by 0.22 μm PTFE membrane. A typical aqueous phase flow ratio was set as 10000 μL/hr and oil phase speed was set as 100 μL/hr. The aqueous phase was 0.01 mM PBS buffer with 0.02 wt % NaN3. The production solution was evaporated under a 45°C water-bath for one hour to remove DCM and then dialyzed against 1X PBS buffer using a cellulose dialysis membrane (MWCO=3.5 kDa) for 5h. Samples were then filtered by 0.8 μm membrane. The particle size and morphology were then measured and confirmed by DLS (dynamic lighting scattering) and SLS (static lighting scattering).

5.3.4 DLS andSLS characterization

DLS (dynamic lighting scattering) and SLS (static lighting scattering) were further performed using an ALV Laser goniometer, which consisted of a 35 mW HeNe linear polarized laser with a wavelength of 633nm and an ALV-5000/EPP Multiple Tau Digital correlator with 125 ns initial sampling time. Samples were collected after solvent evaporation and dialysis, and kept at 25.0 °C during all the experiments. The accessible scattering angle range was from 25° to 150°. Aliquots of samples (1 mL in 10 mm diameter cylindrical glass cell) were immersed in a filtered toluene bath. The data acquisition was done with the ALV-Correlator Control software. Polydispersity (PDI) was obtained by simple fit of 90° data.

5.3.5 Determination of encapsulation efficiency of Fe_2O_3

Iron oxide-loaded polymersomes were synthesized by microfluidics. After solvent evaporation and dialysis, 3.0 mL solution containing drug-loaded magnetic polymersomes was added into three Amicon® Ultra-15 centrifugal filter devices (MWCO=10000), respectively, and centrifuged at 4500 rpm for 30min. 3.0 mL DMSO/H_2O (80/20, *v/v*) was added into each tube to disrupt polymersomes and the solution was then transferred to a centrifuge tube (5mL, VWR) at 8000 rpm for 30min to induce aggregation of Fe_2O_3 nanoparticles.

Supernatant solution from each centrifuge tube was removed gently using a Pasteur pipette to leave Fe_2O_3 precipitation at the bottom of the centrifuge tube. 3.0 mL HCl solution (5 mol/L) was added into each tube to disrupt polymersomes and dissolve Fe_2O_3 nanoparticles. 0.3 mL solution from each centrifuge tube was transferred to three wells in a standard calibration UV 96 plate, respectively. The mean absorption at 350 nm was measured and the concentration of $Fe_2O_3$was calculated by using the standard calibration curve.

5.4 Results and Discussions

5.4.1 Effects of flow ratio on formation of polymersomes

Sample name	Q_w (μl/hr)	Q_{oil} (μl/hr)	Diameter (nm)	PDI
PTMC-*b*-PGA	5000	50	124±5.01	0.16±0.005
	10000	50	111.15±3.49	0.15±0.008
	10000	100	139.22±9.16	0.17±0.005
PTMC-*b*-PGA	10000	50	217.09±10.21	0.25±0.016
+γ-Fe_2O_3	10000	100	208.83±7.43	0.19±0.046

Table 3. Size of polymersomes with different flow ratios. (n = 3; mean ± S.D.)

Method	Sample name	Q_w (μl/hr)	Q_{oil} (μl/hr)	R_g (nm)	R_h (nm)	R_g/R_h	PDI
Microfluidics	PTMC-*b*-PGA	10000	100	52	51	1.03	0.17
	PTMC-*b*-PGA	10000	50	123	105	1.16	
	+γ-Fe_2O_3	10000	100	136	117	1.17	
Bulk	PTMC-*b*-PGA			108	68	1.60	0.344

Table 4. Comparison of PTMC-*b*-PGA polymersomes synthesized by microfluidics and bulk methods. Bulk experiment was performed as the same O/W volume ratio in a 100mL beaker.

We investigated the effects of flow ratio (Q_{oil}/Q_w) on the size and polydispersity of PTMC-*b*-PGA polymersomes. In Table 3, it is shown that increasing flow rates of oil phase led to increasing polymersome sizes, and flow rates of aqueous phase had a negative correlation with the polymersome sizes. This trend is consistent with the data of PLGA NPs in Chapter 3.

In addition, with addition of γ-Fe_2O_3 nanoparticles, the size of polymersomes increased greatly, yet the monodispersity just increased slightly. Furthermore, the shape factors (R_g/R_h) of PTMC-*b*-PGA polymersomes prepared by the microfluidics were very close to 1 (Table 4), regardless encapsulation of γ-Fe_2O_3, which indicates that much more PTMC-b-PGA vesicles were shaped as structures of polymersomes by the modified microfluidic method, compared to bulk method. These advantages prove that

this modified microfluidics method have a great controllability of particle size, distribution, and morphology, which can also be intuitively illustrated by the cryo-TEM picture. (Figure 38)

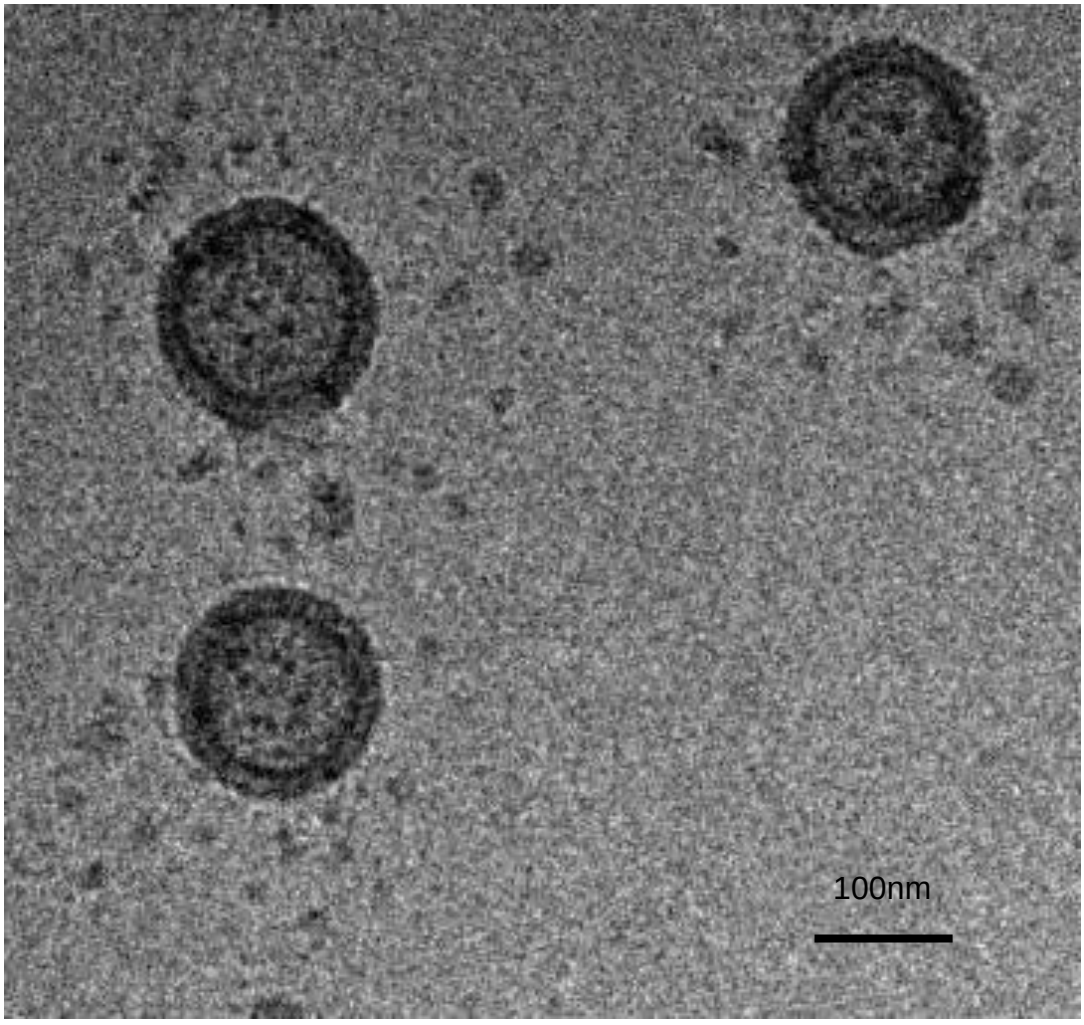

Figure 38. Morphology of PTMC-*b*-PGA polymersomes by Cryo-TEM

5.4.2 Encapsulation of iron oxide nanoparticles

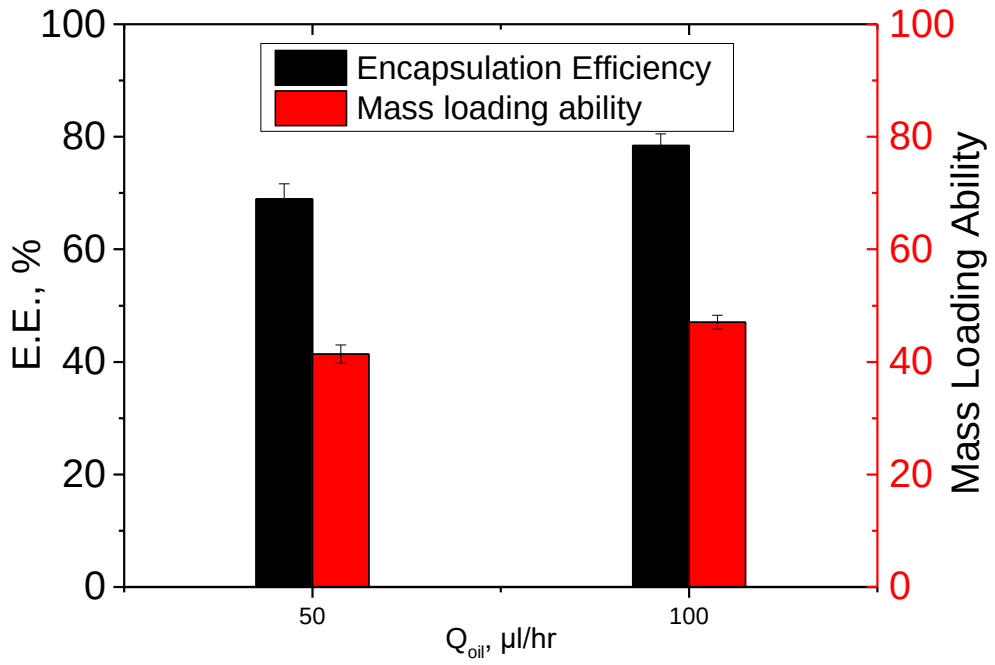

Figure 39. E.E. and mass loading ability of γ-Fe_2O_3 by PTMC-b-PGA polymersomes. V_{DCM}/V_{DMSO} =1/10. Q_w=10000 µl/hr, Concentration of PTMC-b-PGA=5mg/ml, γ-Fe2O3 =3mg/ml. DCM/DMSO=1/10, v/v, Q_w=10000 µl/hr. (n = 3; mean ± S.D.)

We successfully accomplished the encapsulation of γ-Fe2O3 within the PTMC-b-PGA polymersomes. By increasing the flow rate of oil phase from 50µl/hr to 100µl/hr, we improved the encapsulation efficiency from 69% to 78%, and the mass loading ability from 41% to 47%. To be noticed, the solubility of γ-Fe2O3 in DMSO is very poor so that most γ-Fe2O3 are dissolved within DCM component of the oil phase. Increase of oil phase led to the increase of the content of DCM, so that more γ-Fe2O3 could be preserved inside the particles. These data encapsulation efficiency and mass loading are highly comparable to previous literatures[8, 222], which means the novel microfluidic method has a superior ability for both organic drugs (Chapter 3) and inorganic therapeutics. This great property opens a door for further multiple encapsulation and cancer therapy.

5.5 Conclusion

Here we successfully applied our modified microfluidic flow focusing method to the encapsulation of inorganic γ-Fe_2O_3 nanoparticles. The morphology of PTMC-*b*-PGA polymersomes containing γ-Fe_2O_3 was confirmed by shape factor (R_h/R_g) and cryo-TEM. Higher flow ratio of Q_{oil}/Q_w could both increase particle size of polymersomes and Fe_2O_3 loading content inside the polymersomes. This method not only significantly improved the drug encapsulation efficiency and loading content, compared to the conventional bulk methods, but also provided a great potential for a combination of chemotherapy and magnetic therapy.

Chapter 6 Conclusions and Future Work

6.1 Encapsulation and controlled release of hydrophobic drugs by modified microfluidic flow focusing

(1) Summary

We have verified that the modified microfluidic flow focusing was able to generate smaller and uniform nanoparticles than conventional bulk methods and microfluidic flow focusing by adding DCM in the classical dispersed phase DMSO, to make a partially water-miscible precursor. This method helped improving the hydrophobic drug encapsulation efficiency and drug loading ability, and slower the sustained-release rate.

First of all, the modified microfluidic flow focusing method using a partially water-miscible precursor produced polymer NPs according to a novel fluidic mechanism: "Jet to Microdroplets to NPs". This mechanism was investigated that final particle sizes are directly influenced by the sizes of their original droplets.

Secondly, the formation of the NPs could be precisely controlled by tuning the flow rates, polymer concentration, and V_{Dcm}/V_{DMSO}. Higher flow ratio of Q_{oil}/Q_w was proved that could increase the NPs size and increase the drug content within the NPs. Higher polymer concentration was also proved that has a positive correlation with the final NPs size. Higher volume fraction ratio of DCM in the dispersed phase could also increase the particle size and the drug loading content. In addition, more hydrophobic the drug is, more drug will be encapsulated within the NPs by this method, at given parameters of flow rates, polymer concentration, and V_{Dcm}/V_{DMSO}.

Furthermore, *in-vitro* controlled release profiles of doxorubicin-loaded NPs fabricated from pure DMSO precursor and (DCM+DMSO) precursor were compared, and NPs from (DCM+DMSO) precursor was confirmed that has a more sustained-release procedure.

Generally, this microfluidic flow focusing method using a partially water-miscible

precursor is capable of fabricating uniform droplets and NPs, improving drug encapsulation efficiency and mass loading ability than classical methods, and slowing down the drug release rate. These important characteristics open a new door for preparation of droplets and nanoparticles, drug encapsulation and release, and cancer therapy.

(2) Future Work

The Map of flow behavior in the (Q_w, Q_{oil}) plane needs to be further extended and investigated, to understand whether the jet and jetting zones could remain their regime at higher flow rates. If not, a new phenomenon of flow behavior may be observed.

The choice of the partially water-miscible precursor can also be extended to other combination solvents: (1) Using THF, Acetone, alcohol, etc., as an instead of DMSO, since these solvents are easier to evaporate than DMSO; (2) Using ethyl acetate instead of DCM, since its low toxicity and low boiling point; (3) Using soybean oil instead of DCM, which is totally biocompatible and biodegradable solvent as important oil in our daily life. Noticeably, because of its non-volatile property, soybean oil may remain in the droplets and NPs for a long time, so micro-droplets or NPs perhaps could keep their shapes, “lock” more drugs inside, and release the drugs in a longer period; (4) Different combinations of solvents are worthy being tested to understand the effect of solvent choices on the NPs size, drug loading ability, and release profiles.

The role of DCM played in the drug encapsulation and release should be tested and the assumption proposed in Section 3.7 should be verified as well. The experiment can be designed like this: (1) A strongly fluorescent dye may be used as a drug model instead of doxorubicin or tamoxifen; (2) The formation of microdroplets and the distribution of dye in the microdroplets may be traced by confocal microscopes; the distribution of dye in the NPs may be detected by cyro-TEM; (3) A precursor using pure DMSO may be used as a control group, compared to a precursor using DCM+DMSO.

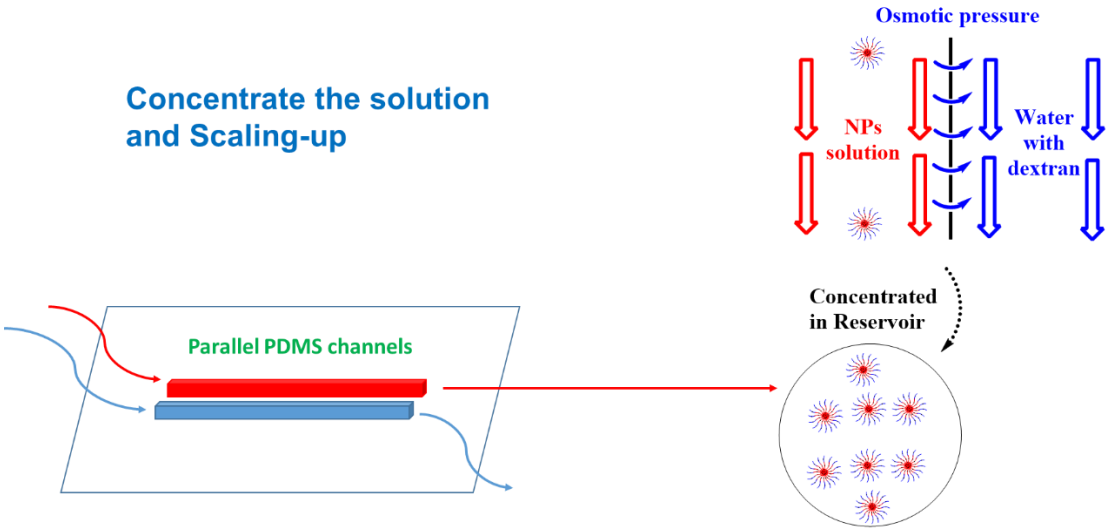

Figure 40. Scheme of the set-up of concentrating device for the NPs solution.

The major challenge of this method is to improve the concentration of NPs solution since it is very diluted (C_{PLGA}=0.05~0.1mg/mL) after being produced. We propose a PDMS chip with parallel channels to separate excessive water from the NPs solution, by co-flowing the NPs solution and aqueous solution with a high concentration of dextran. Due to the osmotic pressure between the two fluids and the good permeability of PDMS materials, the NPs solution can be gradually concentrated and collected in a reservoir for further use.

Hopefully, this method can be also further extended and optimized to be applied to industrial areas like cosmetics, fragrances, 3D printing and pharmacy

6.2 Improvement of the encapsulation efficiency of hydrophilic drugs by modified drop-wise nanoprecipitation

(1) Summary

We have successfully developed a novel simply-modified drop-wise nanoprecipitation method which separated hydrophilic drug and polymer into aqueous phase (continuous phase) and organic phase (dispersed phase), individually. Uniform nanoparticles with a considerable ciprofloxacin loading ability were synthesized acby two polymers, PLA-DEX and PLGA-PEG. The mass loading ability of both two

polymeric NPs which could be precisely tuned by changing the initial drug feed concentration of ciprofloxacin. *In-vitro* sustained release study of ciprofloxacin by both two polymeric NPs was achieved in stimulated tear fluid (STF) and the sustained-release could last for almost one week. These studies suggest that this novel modified nanoprecipitation method is a rapid, facile, and reproducible technique for making nano-scale drug delivery carriers of high drug loading ability.

(2) Future Work

The challenge of further improvement of the encapsulation efficiency still exist. Volatile solvent like acetone may be used as an instead of DMSO so that it could be easily removed by evaporation from the aqueous solution. So the rest of the aqueous solution which still contains considerable ciprofloxacin may be re-collected and recycled for another or more rounds of modified drop-wise nanoprecipitation. The encapsulation efficiency of ciprofloxacin perhaps will be greatly improved by repeating the nanoprecipitation procedure.

The effects of volume ratio of organic/aqueous phase and polymer concentration on the encapsulation efficiency and release profiles are going to be determined. Different polymer like polycarbonate and hydrophilic drug like insulin could be tested by this drug encapsulation system to see whether the linear correlation of mass loading ability and initial drug feed still valid, in order to extend it to a universal method, which could be combined with microfluidics as well. Optimizations of the phase ratio, polymer and drug concentration will be done in order to improve drug loading ability of the NPs with a respect to the encapsulation efficiency.

6.3 Improvement of the encapsulation efficiency of hydrophilic drugs by modified drop-wise nanoprecipitation

(1) Summary

We successfully applied our modified flow focusing method to encapsulate magnetic iron oxide nanoparticles, within PTMC-*b*-PGA polymersomes, as a basis for future

combination of chemotherapy and magnetic therapy. The modified flow focusing method showed good encapsulation efficiency (78%) and mass loading content of γ-Fe_2O_3 (43%). The morphology of the PTMC-*b*-PGA polymersomes and shape factor (R_h/R_g) were characterized by dynamic lighting scattering, static lighting scattering, and cryo-TEM. and cryo-TEM. Higher flow ratio of Q_{oil}/Q_w was found that could increase particle size of polymersomes and Fe_2O_3 loading content inside the polymersomes. This method successfully accomplished encapsulation of γ-Fe_2O_3 magnetic nanoparticles, prepared monodispersed polymer vesicles with considerable loading contents, thus, provided us a promising tool for fabricating multifunctional nanoparticle carriers for future multiple loading of anti-cancer drugs and inorganic therapeutics.

(2) Future Work

Our future work will be focused on accomplishing dual encapsulation of anti-cancer drug and iron oxide nanoparticles. Firstly, we are going to determine the loading contents of each compounds in the particles. Second, the formulation of the initial drug/Fe_2O_3/polymer ratio will be tuned to optimize the size and morphology of the polymer nanoparticles. Third, a magnetic field will be applied to the dual-encapsulated NPs in the *in-vitro* release or *in-vivo* release study.

6.4 Research plan/Milestones

The overall research timetable is tabulated below:

Research objectives	**2012**	**2013**			**2014**			**2015**			**2016**	
F: fall (Sep to Dec); W: winter (Jan to Apr); S: spring (May to Aug)	**F**	**W**	**S**	**F**	**W**	**S**	**F**	**W**	**S**	**F**	**W**	**S**
Courses												
Encapsulation and Controlled Release of Hydrophobic drugs												
Microfluidic method												
Literature review												
Fabrication of microfluidic platform												
Development of modified microfluidic flow focusing												
Microfluidic synthesis of PLGA NPs												
Microfluidic encapsulation of Doxorubicin												
In-vitro controlled release of Doxorubicin												
Investigation on mechanism of self-assembly behavior of NPs												
Extension to different hydrophobic drug Tamoxifen												
Optimization of drug-loaded NPs formations												
Encapsulation and Controlled Release of Hydrophilic drugs												
Literature review												
Development of modified drop-wise nanoprecipitation												
Synthesis and characterization of PLA-DEX NPs												
Encapsulation of Ciprofloxacin												
In-vitro controlled release of Ciprofloxacin												
Investigation on mechanism of self-assembly behavior of NPs												
Extension to different polymer PLGA-PEG												
Optimization of drug-loaded NPs formations												
Combination of Chemotherapy and Thermotherapy												
Literature review												
Dual encapsulation of Doxorubicin and Fe_2O_3												
In-vitro controlled release of Ciprofloxacin with magnetic field												
Thesis writing												
PhD defense												

Bibliography

1. Heath JR, Davis ME. Nanotechnology and cancer. In: *Annual Review of Medicine* (ed^(eds) (2008).

2. Wischke C, Schwendeman SP. Principles of encapsulating hydrophobic drugs in PLA/PLGA microparticles. *International Journal of Pharmaceutics* 364, 298-327 (2008).

3. LaVan DA, McGuire T, Langer R. Small-scale systems for in vivo drug delivery. *Nature Biotechnology* 21, 1184-1191 (2003).

4. Barichello JM, Morishita M, Takayama K, Nagai T. Encapsulation of hydrophilic and lipophilic drugs in PLGA nanoparticles by the nanoprecipitation method. *Drug Development and Industrial Pharmacy* 25, 471-476 (1999).

5. Ting-Yu Liua b, Shang-Hsiu Hub, Dean-Mo Liub, San-Yuan Chenb, I-Wei Chena,∗. Biomedical nanoparticle carriers with combined thermal and magnetic responses. *Nano Today*, (2008).

6. Fahima Dilnawaz AS, Chandana Mohanty, Sanjeeb K. Sahoo. Dual drug loaded superparamagnetic iron oxide nanoparticles for targeted cancer therapy. *Biomaterials*, (2010).

7. Santimukul Santra CK, Jan Grimm, J. Manuel Perez. Drug/Dye-Loaded, Multifunctional Iron Oxide Nanoparticles for Combined Targeted Cancer Therapy and Dual Optical/Magnetic Resonance Imaging. *Small*, (2009).

8. Sanson C. Doxorubicin Loaded Magnetic Polymersomes: TheranosticNanocarriers for MR Imaging and Magneto-Chemotherapy. *Acs Nano*, (2011).

9. Kataoka K, Harada A, Nagasaki Y. Block copolymer micelles for drug delivery: design, characterization and biological significance. *Advanced Drug Delivery Reviews* 47, 113-131 (2001).

10. Seigneuric R*, et al.* From Nanotechnology to Nanomedicine: Applications to Cancer Research. *Current Molecular Medicine* 10, 640-652 (2010).

11. Davis ME, Chen Z, Shin DM. Nanoparticle therapeutics: an emerging treatment modality for cancer. *Nature Reviews Drug Discovery* 7, 771-782 (2008).

12. Vila A, Sanchez A, Perez C, Alonso MJ. PLA-PEG nanospheres: New carriers for transmucosal delivery of proteins and plasmid DNA. *Polymers for Advanced Technologies* 13, 851-858 (2002).

13. Ravi Kumar MNV, Bakowsky U, Lehr CM. Preparation and characterization of cationic PLGA nanospheres as DNA carriers. *Biomaterials* 25, 1771-1777 (2004).

14. Jewell CM, Zhang JT, Fredin NJ, Lynn DM. Multilayered polyelectrolyte films promote the direct and localized delivery of DNA to cells. *Journal of Controlled Release* 106, 214-223 (2005).

15. Huang MJ*, et al.* One-step preparation of poly(epsilon-caprolactone)-polyethylene glycol)-poly(epsilon-caprolactone) nanoparticles for plasmid DNA delivery. *Journal of Biomedical Materials Research Part A* 86A, 979-986 (2008).

16. Guo S*, et al.* Enhanced Gene Delivery and siRNA Silencing by Gold Nanoparticles Coated with Charge-Reversal Polyelectrolyte. *Acs Nano* 4, 5505-5511 (2010).

17. Katas H, Cevher E, Alpara HO. Preparation of polyethyleneimine incorporated poly(D,L-lactide-co-glycolide) nanoparticles by spontaneous emulsion diffusion method for small interfering RNA delivery. *International Journal of Pharmaceutics* 369, 144-154 (2009).

18. Cun D, Foged C, Yang M, Frokjaer S, Nielsen HM. Preparation and characterization of poly(DL-lactide-co-glycolide) nanoparticles for siRNA delivery. *International Journal of Pharmaceutics* 390, 70-75 (2010).

19. Doerdelmann G, Kozlova D, Karczewski S, Lizio R, Knauer S, Epple M. Calcium phosphate increases the encapsulation efficiency of hydrophilic drugs (proteins, nucleic acids) into poly(D,L-lactide-co-glycolide acid) nanoparticles for intracellular delivery. *Journal of Materials Chemistry B* 2, 7250-7259 (2014).

20. Bhuchar N, Sunasee R, Ishihara K, Thundat T, Narain R. Degradable Thermoresponsive Nanogels for Protein Encapsulation and Controlled Release. *Bioconjugate Chemistry* 23, 75-83 (2012).

21. Xie S, Wang S, Zhao B, Han C, Wang M, Zhou W. Effect of PLGA as a polymeric emulsifier on preparation of hydrophilic protein-loaded solid lipid nanoparticles. *Colloids and Surfaces B-Biointerfaces* 67, 199-204 (2008).

22. Jain D, Banerjee R. Comparison of ciprofloxacin hydrochloride-loaded protein, lipid, and chitosan nanoparticles for drug delivery. *Journal of Biomedical Materials Research Part B-Applied Biomaterials* 86B, 105-112 (2008).

23. Gref R*, et al.* THE CONTROLLED INTRAVENOUS DELIVERY OF DRUGS USING PEG-COATED STERICALLY STABILIZED NANOSPHERES. *Advanced Drug Delivery Reviews* 16, 215-233 (1995).

24. Anderson JM, Shive MS. Biodegradation and biocompatibility of PLA and PLGA microspheres. *Advanced Drug Delivery Reviews* 28, 5-24 (1997).

25. Panyam J, Zhou WZ, Prabha S, Sahoo SK, Labhasetwar V. Rapid endo-lysosomal escape of poly(DL-lactide-co-glycolide) nanoparticles: implications for drug and gene delivery. *Faseb Journal* 16, (2002).

26. Otsuka H, Nagasaki Y, Kataoka K. PEGylated nanoparticles for biological and pharmaceutical applications. *Advanced Drug Delivery Reviews* 55, 403-419 (2003).

27. Cheng J*, et al.* Formulation of functionalized PLGA-PEG nanoparticles for in vivo targeted drug delivery. *Biomaterials* 28, 869-876 (2007).

28. Muller RH, Jacobs C, Kayser O. Nanosuspensions as particulate drug formulations in therapy Rationale for development and what we can expect for the future. *Advanced Drug Delivery Reviews* 47, 3-19 (2001).

29. Brannon-Peppas L, Blanchette JO. Nanoparticle and targeted systems for cancer therapy. *Advanced Drug Delivery Reviews* 56, 1649-1659 (2004).

30. Nishiyama N, Kataoka K. Current state, achievements, and future prospects of polymeric micelles as nanocarriers for drug and gene delivery. *Pharmacology & Therapeutics* 112, 630-648 (2006).

31. Oh JK, Drumright R, Siegwart DJ, Matyjaszewski K. The development of microgels/nanogels for drug delivery applications. *Progress in Polymer Science* 33, 448-477 (2008).

32. K. K. Upadhyay, 2,3*, et al.* Role of Block Copolymer Nanoconstructs in Cancer Therapy. (2009).

33. J. Thevenot HO, S. Lecommandoux. Polymersomes for theranostics (2013).

34. Hugo De Oliveira, 2 Julie Thevenot1,2 and S´ebastien, Lecommandoux1. Smart polymersomes for therapy and diagnosis: fast progress toward multifunctional biomimetic nanomedicines. (2012).

35. Discher DE, Eisenberg A. Polymer vesicles. *Science* 297, 967-973 (2002).

36. Bajpai AK, Shukla SK, Bhanu S, Kankane S. Responsive polymers in controlled drug delivery. *Progress in Polymer Science* 33, 1088-1118 (2008).

37. Ganta S, Devalapally H, Shahiwala A, Amiji M. A review of stimuli-responsive nanocarriers for drug and gene delivery. *Journal of Controlled Release* 126, 187-204 (2008).

38. Maeda H, Bharate GY, Daruwalla J. Polymeric drugs for efficient tumor-targeted drug delivery based on EPR-effect. *European Journal of Pharmaceutics and Biopharmaceutics* 71, 409-419 (2009).

39. De Jong WH, Borm PJA. Drug delivery and nanoparticles: Applications and hazards. *International Journal of Nanomedicine* 3, 133-149 (2008).

40. Petros RA, DeSimone JM. Strategies in the design of nanoparticles for therapeutic applications. *Nature Reviews Drug Discovery* 9, 615-627 (2010).

41. Fessi H, Puisieux F, Devissaguet JP, Ammoury N, Benita S. NANOCAPSULE FORMATION BY INTERFACIAL POLYMER DEPOSITION FOLLOWING SOLVENT DISPLACEMENT. *International Journal of Pharmaceutics* 55, R1-R4 (1989).

42. Martin-Banderas L*, et al.* Flow focusing: A versatile technology to produce size-controlled and specific-morphology microparticles. *Small* 1, 688-692 (2005).

43. Bo Q, Zhao Y. Double-hydrophilic block copolymer for encapsulation and two-way pH change-induced release of metalloporphyrins. *Journal of Polymer Science Part a-Polymer Chemistry* 44, 1734-1744 (2006).

44. Liu S, Jones L, Gu FX. Development of mucoadhesive drug delivery system using phenylboronic acid functionalized poly(D,L-lactide)-b-dextran nanoparticles. *Macromol Biosci* 12, 1622-1626 (2012).

45. Karnik R*, et al.* Microfluidic platform for controlled synthesis of polymeric nanoparticles. *Nano Letters* 8, 2906-2912 (2008).

46. Bilati U, Allemann E, Doelker E. Development of a nanoprecipitation method intended for the entrapment of hydrophilic drugs into nanoparticles. *European Journal of Pharmaceutical Sciences* 24, 67-75 (2005).

47. Verma MS, Liu S, Chen YY, Meerasa A, Gu FX. Size-tunable nanoparticles composed of dextran-b-poly(D,L-lactide) for drug delivery applications. *Nano Research* 5, 49-61 (2011).

48. Peltonen L, Aitta J, Hyvonen S, Karjalainen M, Hirvonen J. Improved entrapment efficiency of hydrophilic drug substance during nanoprecipitation of poly(l)lactide nanoparticles. *AAPS PharmSciTech* 5, E16-E16 (2004).

49. Astete CE, Sabliov CM. Synthesis and characterization of PLGA nanoparticles. *Journal of Biomaterials Science-Polymer Edition* 17, 247-289 (2006).

50. Freitas S, Hielscher G, Merkle HP, Gander B. Continuous contact- and contamination-free ultrasonic emulsification - a useful tool for pharmaceutical development and production. *Ultrasonics Sonochemistry* 13, 76-85 (2006).

51. Rosca ID, Watari F, Uo M. Microparticle formation and its mechanism in single and double emulsion solvent evaporation. *Journal of Controlled Release* 99, 271-280 (2004).

52. Dawes GJS, Fratila-Apachitei LE, Mulia K, Apachitei I, Witkamp GJ, Duszczyk J. Size effect of PLGA spheres on drug loading efficiency and release profiles. *Journal of Materials Science-*

Materials in Medicine 20, 1089-1094 (2009).

53. Choonara YE*, et al.* Polymeric emulsion and crosslink-mediated synthesis of super-stable nanoparticles as sustained-release anti-tuberculosis drug carriers. *Colloids and Surfaces B-Biointerfaces* 87, 243-254 (2011).

54. Zhu J, Hayward RC. Spontaneous generation of amphiphilic block copolymer micelles with multiple morphologies through interfacial instabilities. *Journal of the American Chemical Society* 130, 7496-7502 (2008).

55. Pan J, Feng S-S. Targeted delivery of paclitaxel using folate-decorated poly(lactide) - vitamin E TPGS nanoparticles. *Biomaterials* 29, 2663-2672 (2008).

56. Manchanda R, Fernandez-Fernandez A, Nagesetti A, McGoron AJ. Preparation and characterization of a polymeric (PLGA) nanoparticulate drug delivery system with simultaneous incorporation of chemotherapeutic and thermo-optical agents. *Colloids and Surfaces B-Biointerfaces* 75, 260-267 (2010).

57. Keum C-G*, et al.* Practical preparation procedures for docetaxel-loaded nanoparticles using polylactic acid-co-glycolic acid. *International Journal of Nanomedicine* 6, 2225-2234 (2011).

58. Zhang H, Bei J, Wang S. Multi-morphological biodegradable PLGE nanoparticles and their drug release behavior. *Biomaterials* 30, 100-107 (2009).

59. Cozar-Bernal MJ*, et al.* Insulin-loaded PLGA microparticles: flow focusing versus double emulsion/solvent evaporation. *Journal of Microencapsulation* 28, 430-441 (2011).

60. Puri S, Kallinteri P, Higgins S, Hutcheon GA, Garnett MC. Drug incorporation and release of water soluble drugs from novel functionalised poly(glycerol adipate) nanoparticles. *Journal of Controlled Release* 125, 59-67 (2008).

61. Niwa T, Takeuchi H, Hino T, Kunou N, Kawashima Y. PREPARATIONS OF BIODEGRADABLE NANOSPHERES OF WATER-SOLUBLE AND INSOLUBLE DRUGS WITH D,L-LACTIDE GLYCOLIDE COPOLYMER BY A NOVEL SPONTANEOUS EMULSIFICATION SOLVENT DIFFUSION METHOD, AND THE DRUG RELEASE BEHAVIOR. *Journal of Controlled Release* 25, 89-98 (1993).

62. Niwa T, Takeuchi H, Hino T, Kunou N, Kawashima Y. IN-VITRO DRUG-RELEASE BEHAVIOR OF D,L-LACTIDE/GLYCOLIDE COPOLYMER (PLGA) NANOSPHERES WITH NAFARELIN ACETATE PREPARED BY A NOVEL SPONTANEOUS EMULSIFICATION SOLVENT DIFFUSION METHOD. *Journal of Pharmaceutical Sciences* 83, 727-732 (1994).

63. QuintanarGuerrero D, Fessi H, Allemann E, Doelker E. Influence of stabilizing agents and preparative variables on the formation of poly(D,L-lactic acid) nanoparticles by an emulsification-diffusion technique. *International Journal of Pharmaceutics* 143, 133-141

(1996).

64. Quintanar-Guerrero D, Allemann E, Doelker E, Fessi H. Preparation and characterization of nanocapsules from preformed polymers by a new process based on emulsification-diffusion technique. *Pharmaceutical Research* 15, 1056-1062 (1998).

65. Leroux JC, Allemann E, Doelker E, Gurny R. NEW APPROACH FOR THE PREPARATION OF NANOPARTICLES BY AN EMULSIFICATION-DIFFUSION METHOD. *European Journal of Pharmaceutics and Biopharmaceutics* 41, 14-18 (1995).

66. Murakami H, Kobayashi M, Takeuchi H, Kawashima Y. Preparation of poly(DL-lactide-co-glycolide) nanoparticles by modified spontaneous emulsification solvent diffusion method. *International Journal of Pharmaceutics* 187, 143-152 (1999).

67. Trotta M, Debernardi F, Caputo O. Preparation of solid lipid nanoparticles by a solvent emulsitication-diffusion technique. *International Journal of Pharmaceutics* 257, 153-160 (2003).

68. Galindo-Rodriguez S, Allemann E, Fessi H, Doelker E. Physicochemical parameters associated with nanoparticle formation in the salting-out, emulsification-diffusion, and nanoprecipitation methods. *Pharmaceutical Research* 21, 1428-1439 (2004).

69. Quintanar-Guerrero D, Tamayo-Esquivel D, Ganem-Quintanar A, Allemann E, Doelker E. Adaptation and optimization of the emulsification-diffusion technique to prepare lipidic nanospheres. *European Journal of Pharmaceutical Sciences* 26, 211-218 (2005).

70. Kwon HY, Lee JY, Choi SW, Jang YS, Kim JH. Preparation of PLGA nanoparticles containing estrogen by emulsification-diffusion method. *Colloids and Surfaces a-Physicochemical and Engineering Aspects* 182, 123-130 (2001).

71. Zhang Y, Chan HF, Leong KW. Advanced materials and processing for drug delivery: The past and the future. *Advanced Drug Delivery Reviews* 65, 104-120 (2013).

72. M. R. Hussain TKM. Preparation of genipin cross-linked chitosan-gelatin microcapsules for encapsulation of Zanthoxylum limonella oil (ZLO) using salting-out method. *Journal of Microencapsulation*, (2008).

73. Ahmed N, Michelin-Jamois M, Fessi H, Elaissari A. Modified double emulsion process as a new route to prepare submicron biodegradable magnetic/polycaprolactone particles for in vivo theranostics. *Soft Matter* 8, 2554-2564 (2012).

74. Shi M*, et al.* Double walled POE/PLGA microspheres: encapsulation of water-soluble and water-insoluble proteins and their release properties. *Journal of Controlled Release* 89, 167-177 (2003).

75. Chognot D, Leonard M, Six J-L, Dellacherie E. Surfactive water-soluble copolymers for the preparation of controlled surface nanoparticles by double emulsion/solvent evaporation. *Colloids and Surfaces B-Biointerfaces* 51, 86-92 (2006).

76. Nihant N, Schugens C, Grandfils C, Jerome R, Teyssie P. POLYLACTIDE MICROPARTICLES PREPARED BY DOUBLE EMULSION/EVAPORATION TECHNIQUE .1. EFFECT OF PRIMARY EMULSION STABILITY. *Pharmaceutical Research* 11, 1479-1484 (1994).

77. Morlock M, Kissel T, Li YX, Koll H, Winter G. Erythropoietin loaded microspheres prepared from biodegradable LPLG-PEO-LPLG triblock copolymers: protein stabilization and in-vitro release properties. *Journal of Controlled Release* 56, 105-115 (1998).

78. Szoka F, Papahadjopoulos D. PROCEDURE FOR PREPARATION OF LIPOSOMES WITH LARGE INTERNAL AQUEOUS SPACE AND HIGH CAPTURE BY REVERSE-PHASE EVAPORATION. *Proceedings of the National Academy of Sciences of the United States of America* 75, 4194-4198 (1978).

79. Nagata T, Okada K, Takebe I, Matsui C. DELIVERY OF TOBACCO MOSAIC-VIRUS RNA INTO PLANT-PROTOPLASTS MEDIATED BY REVERSE-PHASE EVAPORATION VESICLES (LIPOSOMES). *Molecular & General Genetics* 184, 161-165 (1981).

80. Duzgunes N*, et al.* PHYSICOCHEMICAL CHARACTERIZATION OF LARGE UNILAMELLAR PHOSPHOLIPID-VESICLES PREPARED BY REVERSE-PHASE EVAPORATION. *Biochimica Et Biophysica Acta* 732, 289-299 (1983).

81. Paternostre MT, Roux M, Rigaud JL. MECHANISMS OF MEMBRANE-PROTEIN INSERTION INTO LIPOSOMES DURING RECONSTITUTION PROCEDURES INVOLVING THE USE OF DETERGENTS .1. SOLUBILIZATION OF LARGE UNILAMELLAR LIPOSOMES (PREPARED BY REVERSE-PHASE EVAPORATION) BY TRITON X-100, OCTYL GLUCOSIDE, AND SODIUM CHOLATE. *Biochemistry* 27, 2668-2677 (1988).

82. Ourique AF, Chaves PdS, Souto GD, Pohlmann AR, Guterres SS, Ruver Beck RC. Redispersible liposomal-N-acetylcysteine powder for pulmonary administration: Development, in vitro characterization and antioxidant activity. *European Journal of Pharmaceutical Sciences* 65, 174-182 (2014).

83. Tabaei SR*, et al.* Formation of Cholesterol-Rich Supported Membranes Using Solvent-Assisted Lipid Self-Assembly. *Langmuir* 30, 13345-13352 (2014).

84. Xu H*, et al.* Development of High-Content Gemcitabine PEGylated Liposomes and Their Cytotoxicity on Drug-Resistant Pancreatic Tumour Cells. *Pharmaceutical Research* 31, 2583-2592 (2014).

85. Saeid Moghassemi AH. Nano-niosomes as Nanoscale Drug Delivery Systems: An Illustrated Review. *Journal of Controlled Release*, (2014).

86. Hosny KM. Ciprofloxacin as Ocular Liposomal Hydrogel. *Aaps Pharmscitech* 11, 241-246 (2010).

87. Garello F, Stefania R, Aime S, Terreno E, Castelli DD. Successful Entrapping of Liposomes in Glucan Particles: An Innovative Micron-Sized Carrier to Deliver Water-Soluble Molecules. *Molecular Pharmaceutics* 11, 3760-3765 (2014).

88. Jiang CY, Tsukruk VV. Freestanding nanostructures via layer-by-layer assembly. *Advanced Materials* 18, 829-840 (2006).

89. DeLongchamp DM, Hammond PT. High-contrast electrochromism and controllable dissolution of assembled Prussian blue/polymer nanocomposites. *Advanced Functional Materials* 14, 224-232 (2004).

90. Huang H, Pierstorff E, Osawa E, Ho D. Protein-mediated assembly of nanodiamond hydrogels into a biocompatible and biofunctional multilayer nanofilm. *Acs Nano* 2, 203-212 (2008).

91. Kim B-S, Park SW, Hammond PT. Hydrogen-bonding layer-by-layer assembled biodegradable polymeric micelles as drug delivery vehicles from surfaces. *Acs Nano* 2, 386-392 (2008).

92. Wang CY, He CY, Tong Z, Liu XX, Ren BY, Zeng F. Combination of adsorption by porous CaCO3 microparticles and encapsulation by polyelectrolyte multilayer films for sustained drug delivery. *International Journal of Pharmaceutics* 308, 160-167 (2006).

93. Wang Y*, et al.* Encapsulation of Water-Insoluble Drugs in Polymer Capsules Prepared Using Mesoporous Silica Templates for Intracellular Drug Delivery. *Advanced Materials* 22, 4293-+ (2010).

94. Ji Q, Yoon SB, Hill JP, Vinu A, Yu J-S, Ariga K. Layer-by-Layer Films of Dual-Pore Carbon Capsules with Designable Selectivity of Gas Adsorption. *Journal of the American Chemical Society* 131, 4220-+ (2009).

95. Poon Z, Chang D, Zhao X, Hammond PT. Layer-by-Layer Nanoparticles with a pH-Sheddable Layer for in Vivo Targeting of Tumor Hypoxia. *Acs Nano* 5, 4284-4292 (2011).

96. Kumar CSSR, Mohammad F. Magnetic nanomaterials for hyperthermia-based therapy and controlled drug delivery. *Advanced Drug Delivery Reviews* 63, 789-808 (2011).

97. De Koker S, Hoogenboom R, De Geest BG. Polymeric multilayer capsules for drug delivery. *Chemical Society Reviews* 41, 2867-2884 (2012).

98. Sarala Pamujula RAG, Thomas Freeman, Venkataraman Srinivasan, Levon A. Bostanian, Vimal

Kishore and Tarun K. Mandal. Oral delivery of spray dried PLGA/amifostinenanoparticles. *Journal of pharmacy and pharmacology* (2004).

99. Xie J, Wang C-H. Encapsulation of proteins in biodegradable polymeric microparticles using electrospray in the Taylor Cone-Jet mode. *Biotechnology and Bioengineering* 97, 1278-1290 (2007).

100. Luck M, Pistel KF, Li YX, Blunk T, Muller RH, Kissel T. Plasma protein adsorption on biodegradable microspheres consisting of poly(D,L-lactide-co-glycolide), poly(L-lactide) or ABA triblock copolymers containing poly(oxyethylene) - Influence of production method and polymer composition. *Journal of Controlled Release* 55, 107-120 (1998).

101. Tsifansky MD, Yeo Y, Evgenov OV, Bellas E, Benjamin J, Kohane DS. Microparticles for inhalational delivery of antipseudomonal antibiotics. *Aaps Journal* 10, 254-260 (2008).

102. Schwendeman SP, Tobio M, Joworowicz M, Alonso MJ, Langer R. New strategies for the microencapsulation of tetanus vaccine. *Journal of Microencapsulation* 15, 299-318 (1998).

103. Valo H*, et al.* Electrospray Encapsulation of Hydrophilic and Hydrophobic Drugs in Poly(L-lactic acid) Nanoparticles. *Small* 5, 1791-1798 (2009).

104. Ungaro F*, et al.* Dry powders based on PLGA nanoparticles for pulmonary delivery of antibiotics: Modulation of encapsulation efficiency, release rate and lung deposition pattern by hydrophilic polymers. *Journal of Controlled Release* 157, 149-159 (2012).

105. Sweeney LG, Wang ZL, Loebenberg R, Wong JP, Lange CF, Finlay WH. Spray-freeze-dried liposomal ciprofloxacin powder for inhaled aerosol drug delivery. *International Journal of Pharmaceutics* 305, 180-185 (2005).

106. Whitesides GM. The origins and the future of microfluidics. *Nature* 442, 368-373 (2006).

107. Ohno K-i, Tachikawa K, Manz A. Microfluidics: Applications for analytical purposes in chemistry and biochemistry. *Electrophoresis* 29, 4443-4453 (2008).

108. Bonn D, Eggers J, Indekeu J, Meunier J, Rolley E. Wetting and spreading. *Reviews of Modern Physics* 81, 739-805 (2009).

109. Ottino JM, Wiggins S. Introduction: mixing in microfluidics. *Philosophical Transactions of the Royal Society of London Series a-Mathematical Physical and Engineering Sciences* 362, 923-935 (2004).

110. Liu D*, et al.* Microfluidic assisted one-step fabrication of porous silicon@acetalated dextran nanocomposites for precisely controlled combination chemotherapy. *Biomaterials* 39, 249-259 (2015).

111. Watanabe T, Lopez CG, Douglas JF, Ono T, Cabral JT. Microfluidic Approach to the Formation of Internally Porous Polymer Particles by Solvent Extraction. *Langmuir* 30, 2470-2479 (2014).

112. Dittrich PS, Manz A. Lab-on-a-chip: microfluidics in drug discovery. *Nature Reviews Drug Discovery* 5, 210-218 (2006).

113. Weigl BH, Bardell RL, Cabrera CR. Lab-on-a-chip for drug development. *Advanced Drug Delivery Reviews* 55, 349-377 (2003).

114. Li N, Tourovskaia A, Folch A. Biology on a chip: microfabrication for studying the behavior of cultured cells. *Critical reviews in biomedical engineering* 31, 423-488 (2003).

115. Gijs MAM. Magnetic bead handling on-chip: new opportunities for analytical applications. *Microfluidics and Nanofluidics* 1, 22-40 (2004).

116. Kleinstreuer C, Li J, Koo J. Microfluidics of nano-drug delivery. *International Journal of Heat and Mass Transfer* 51, 5590-5597 (2008).

117. Duffy DC, McDonald JC, Schueller OJA, Whitesides GM. Rapid prototyping of microfluidic systems in poly(dimethylsiloxane). *Analytical Chemistry* 70, 4974-4984 (1998).

118. McDonald JC*, et al.* Fabrication of microfluidic systems in poly(dimethylsiloxane). *Electrophoresis* 21, 27-40 (2000).

119. McDonald JC, Whitesides GM. Poly(dimethylsiloxane) as a material for fabricating microfluidic devices. *Accounts of Chemical Research* 35, 491-499 (2002).

120. Berdichevsky Y, Khandurina J, Guttman A, Lo YH. UV/ozone modification of poly(dimethylsiloxane) microfluidic channels. *Sensors and Actuators B-Chemical* 97, 402-408 (2004).

121. Hillborg H, Tomczak N, Olah A, Schonherr H, Vancso GJ. Nanoscale hydrophobic recovery: A chemical force microscopy study of UV/ozone-treated cross-linked poly(dimethylsiloxane). *Langmuir* 20, 785-794 (2004).

122. Olah A, Hillborg H, Vancso GJ. Hydrophobic recovery of UV/ozone treated poly(dimethylsiloxane): adhesion studies by contact mechanics and mechanism of surface modification. *Applied Surface Science* 239, 410-423 (2005).

123. Ye HK, Gu ZY, Gracias DH. Kinetics of ultraviolet and plasma surface modification of poly(dimethylsiloxane) probed by sum frequency vibrational spectroscopy. *Langmuir* 22, 1863-1868 (2006).

124. Carlier J*, et al.* Integrated microfluidics based on multi-layered SU-8 for mass spectrometry analysis. *Journal of Micromechanics and Microengineering* 14, 619-624 (2004).

125. Agirregabiria M*, et al.* Fabrication of SU-8 multilayer microstructures based on successive CMOS compatible adhesive bonding and releasing steps. *Lab on a Chip* 5, 545-552 (2005).

126. Tuomikoski S, Franssila S. Free-standing SU-8 microfluidic chips by adhesive bonding and release etching. *Sensors and Actuators a-Physical* 120, 408-415 (2005).

127. Ruano-Lopez JM*, et al.* A new SU-8 process to integrate buried waveguides and sealed microchannels for a Lab-on-a-Chip. *Sensors and Actuators B-Chemical* 114, 542-551 (2006).

128. Abgrall P, Conedera V, Camon H, Gue A-M, Nguyen N-T. SU-8 as a structural material for labs-on-chips and microelectromechanical systems. *Electrophoresis* 28, 4539-4551 (2007).

129. Dupont EP, Luisier R, Gijs MAM. NOA 63 as a UV-curable material for fabrication of microfluidic channels with native hydrophilicity. *Microelectronic Engineering* 87, 1253-1255 (2010).

130. Tsai L-F, Dahlquist WC, Kim S, Nordin GP. Bonding of polydimethylsiloxane microfluidics to silicon-based sensors. *Journal of Micro-Nanolithography Mems and Moems* 10, (2011).

131. Sollier E, Murray C, Maoddi P, Di Carlo D. Rapid prototyping polymers for microfluidic devices and high pressure injections. *Lab on a Chip* 11, 3752-3765 (2011).

132. Madadi H, Mohammadi M, Casals-Terre J, Castilla Lopez R. A novel fabrication technique to minimize poly(dimethylsiloxane)-microchannels deformation under high-pressure operation. *Electrophoresis* 34, 3126-3132 (2013).

133. Xia YN, Whitesides GM. Soft lithography. *Angewandte Chemie-International Edition* 37, 550-575 (1998).

134. Cheng Y, Sugioka K, Midorikawa K. 3D integration of microoptics and microfluidics in glass using femtosecond laser direct writing. In: *Fifth International Symposium on Laser Precision Microfabrication* (ed^(eds Miyamoto I, Helvajian H, Itoh K, Kobayashi KF, Ostendorf A, Sugioka K) (2004).

135. Lorber N*, et al.* Some recent advances in the design and the use of miniaturized droplet-based continuous process: Applications in chemistry and high-pressure microflows. *Lab on a Chip* 11, 779-787 (2011).

136. Marre S, Aymonier C, Subra P, Mignard E. Dripping to jetting transitions observed from supercritical fluid in liquid microcoflows. *Applied Physics Letters* 95, (2009).

137. Champion JA, Katare YK, Mitragotri S. Particle shape: A new design parameter for micro- and

nanoscale drug delivery carriers. *Journal of Controlled Release* 121, 3-9 (2007).

138. Valencia PM*, et al.* Single-Step Assembly of Homogenous Lipid - Polymeric and Lipid - Quantum Dot Nanoparticles Enabled by Microfluidic Rapid Mixing. *Acs Nano* 4, 1671-1679 (2010).

139. Thiele J, Steinhauser D, Pfohl T, Foerster S. Preparation of Monodisperse Block Copolymer Vesicles via Flow Focusing in Microfluidics. *Langmuir* 26, 6860-6863 (2010).

140. Jahn A, Vreeland WN, DeVoe DL, Locascio LE, Gaitan M. Microfluidic directed formation of liposomes of controlled size. *Langmuir* 23, 6289-6293 (2007).

141. Lesinski GB, Sharma S, Varker KA, Sinha P, Ferrari M, Carson WE. Release of biologically functional interferon-alpha from a nanochannel delivery system. *Biomedical Microdevices* 7, 71-79 (2005).

142. Chaterji S, Kwon IK, Park K. Smart polymeric gels: Redefining the limits of biomedical devices. *Progress in Polymer Science* 32, 1083-1122 (2007).

143. Xu Q*, et al.* Preparation of Monodisperse Biodegradable Polymer Microparticles Using a Microfluidic Flow-Focusing Device for Controlled Drug Delivery. *Small* 5, 1575-1581 (2009).

144. De Geest BG, Urbanski JP, Thorsen T, Demeester J, De Smedt SC. Synthesis of monodisperse biodegradable microgels in microfluidic devices. *Langmuir* 21, 10275-10279 (2005).

145. Shum HC, Lee D, Yoon I, Kodger T, Weitz DA. Double emulsion templated monodisperse phospholipid vesicles. *Langmuir* 24, 7651-7653 (2008).

146. Breslauer DN, Muller SJ, Lee LP. Generation of Monodisperse Silk Microspheres Prepared with Microfluidics. *Biomacromolecules* 11, 643-647 (2010).

147. Long Z, Shetty AM, Solomon MJ, Larson RG. Fundamentals of magnet-actuated droplet manipulation on an open hydrophobic surface. *Lab on a Chip* 9, 1567-1575 (2009).

148. Duncanson WJ, Lin T, Abate AR, Seiffert S, Shah RK, Weitz DA. Microfluidic synthesis of advanced microparticles for encapsulation and controlled release. *Lab on a Chip* 12, 2135-2145 (2012).

149. Shum HC*, et al.* Droplet Microfluidics for Fabrication of Non-Spherical Particles. *Macromolecular Rapid Communications* 31, 108-118 (2010).

150. Hettiarachchi K, Lee AP, Zhang S, Feingold S, Dayton PA. Controllable Microfluidic Synthesis of Multiphase Drug-Carrying Lipospheres for Site-Targeted Therapy. *Biotechnology Progress* 25, 938-945 (2009).

151. Deng N-N, Wang W, Ju X-J, Xie R, Weitz DA, Chu L-Y. Wetting-induced formation of controllable monodisperse multiple emulsions in microfluidics. *Lab on a Chip* 13, 4047-4052 (2013).

152. Deng N-N, Mou C-L, Wang W, Ju X-J, Xie R, Chu L-Y. Multiple emulsion formation from controllable drop pairs in microfluidics. *Microfluidics and Nanofluidics* 17, 967-972 (2014).

153. Zhao C-X. Multiphase flow microfluidics for the production of single or multiple emulsions for drug delivery. *Advanced Drug Delivery Reviews* 65, 1420-1446 (2013).

154. Guo S, Yao T, Ji X, Zeng C, Wang C, Zhang L. Versatile Preparation of Nonspherical Multiple Hydrogel Core PAM/PEG Emulsions and Hierarchical Hydrogel Microarchitectures. *Angewandte Chemie-International Edition* 53, 7504-7509 (2014).

155. Tan W, Desai TA. Layer-by-layer microfluidics for biomimetic three-dimensional structures. *Biomaterials* 25, 1355-1364 (2004).

156. Roh KH, Martin DC, Lahann J. Biphasic Janus particles with nanoscale anisotropy. *Nature Materials* 4, 759-763 (2005).

157. Yang S*, et al.* Microfluidic synthesis of multifunctional Janus particles for biomedical applications. *Lab on a Chip* 12, 2097-2102 (2012).

158. Dendukuri D, Pregibon DC, Collins J, Hatton TA, Doyle PS. Continuous-flow lithography for high-throughput microparticle synthesis. *Nature Materials* 5, 365-369 (2006).

159. Shepherd RF*, et al.* Microfluidic assembly of homogeneous and janus colloid-filled hydrogel granules. *Langmuir* 22, 8618-8622 (2006).

160. Chen C-H, Shah RK, Abate AR, Weitz DA. Janus Particles Templated from Double Emulsion Droplets Generated Using Mcrofluidics. *Langmuir* 25, 4320-4323 (2009).

161. Shah RK, Kim J-W, Weitz DA. Janus Supraparticles by Induced Phase Separation of Nanoparticles in Droplets. *Advanced Materials* 21, 1949-1953 (2009).

162. Seiffert S, Romanowsky MB, Weitz DA. Janus Microgels Produced from Functional Precursor Polymers. *Langmuir* 26, 14842-14847 (2010).

163. Yuet KP, Hwang DK, Haghgooie R, Doyle PS. Multifunctional Superparamagnetic Janus Particles. *Langmuir* 26, 4281-4287 (2010).

164. Loget G, Kuhn A. Bulk synthesis of Janus objects and asymmetric patchy particles. *Journal of Materials Chemistry* 22, 15457-15474 (2012).

165. Kobayashi J, Mori Y, Kobayashi S. Hydrogenation reactions using scCO(2) as a solvent in

microchannel reactors. *Chemical Communications*, 2567-2568 (2005).

166. Luther SK, Braeuer A. High-pressure microfluidics for the investigation into multi-phase systems using the supercritical fluid extraction of emulsions (SFEE). *Journal of Supercritical Fluids* 65, 78-86 (2012).

167. Lima AC, Sher P, Mano JF. Production methodologies of polymeric and hydrogel particles for drug delivery applications. *Expert Opinion on Drug Delivery* 9, 231-248 (2012).

168. Tandya A, Mammucari R, Dehghani F, Foster NR. Dense gas processing of polymeric controlled release formulations. *International Journal of Pharmaceutics* 328, 1-11 (2007).

169. Champeau M, Thomassin JM, Jerome C, Tassaing T. In situ investigation of supercritical CO2 assisted impregnation of drugs into a polymer by high pressure FTIR micro-spectroscopy. *The Analyst* 140, 869-879 (2015).

170. Shekunov BY, Chattopadhyay P, Seitzinger J, Huff R. Nanoparticles of Poorly Water-Soluble Drugs Prepared by Supercritical Fluid Extraction of Emulsions. *Pharmaceutical Research* 23, 196-204 (2006).

171. Chattopadhyay P, Huff R, Shekunov BY. Drug encapsulation using supercritical fluid extraction of emulsions. *J Pharm Sci* 95, 667-679 (2006).

172. Marre S, Roig Y, Aymonier C. Supercritical microfluidics: Opportunities in flow-through chemistry and materials science. *Journal of Supercritical Fluids* 66, 251-264 (2012).

173. Chalermchai Khemtong CWKaJG. Polymeric nanomedicine for cancer MR imaging and drug delivery. *Chemical Communications*, (2009).

174. James F Hainfeld DNS, Henry M Smilowitz. The use of gold nanoparticles to enhance radiotherapy in mice. *PHYSICS INMEDICINE AND BIOLOGY*, (2004).

175. Matsudaira H UAM, Furuno Iodine contrast medium sensitizes cultured mammalian cells to x-rays but not to γ rays. *Radiat Res* 84 144–8, (1980).

176. Huiyul Park JY, Jaemin Lee, Seungjoo Haam, In-Hong Choi,Kyung-Hwa Yoo. Multifunctional Nanoparticles for Combined Doxorubicin and Photothermal Treatments. *Acs Nano*, (2009).

177. Christopher Loo*, et al.* Nanoshell-Enabled Photonics-Based Imaging and Therapy of Cancer. *Technology in Cancer Research and Treatment*, (2004).

178. Xiaohua Huang IHE-S, Wei Qian, and Mostafa A. El-Sayed. Cancer Cell Imaging and Photothermal Therapy in the Near-Infrared Region by Using Gold Nanorods. *journal of the American Chemical Society*, (2006).

179. Kuo-Wei Hu T-ML, Kuei-Yi Chung,Keng-Shiang Huang, Chien-Tai Hsieh, Chi-Kuang Sun, and Chen-Sheng Yeh. Efficient Near-IR Hyperthermia and Intense Nonlinear Optical Imaging Contrast on the Gold Nanorod-in-Shell Nanostructures. *J Am Chem Soc*, (2009).

180. Seydel* C. Quantum dots get wet. *Science*, (2003).

181. Lim MPA, Lee WL, Widjaja E, Loo SCJ. One-step fabrication of core-shell structured alginate-PLGA/PLLA microparticles as a novel drug delivery system for water soluble drugs. *Biomaterials Science* 1, 486-493 (2013).

182. Ganan-Calvo AM, Gordillo JM. Perfectly monodisperse microbubbling by capillary flow focusing. *Physical Review Letters* 87, (2001).

183. Valencia PM, Pridgen EM, Rhee M, Langer R, Farokhzad OC, Karnik R. Microfluidic Platform for Combinatorial Synthesis and Optimization of Targeted Nanoparticles for Cancer Therapy. *Acs Nano* 7, 10671-10680 (2013).

184. Guillot P, Colin A, Ajdari A. Stability of a jet in confined pressure-driven biphasic flows at low Reynolds number in various geometries. *Physical Review E* 78, (2008).

185. Hung LH, Teh SY, Jester J, Lee AP. PLGA micro/nanosphere synthesis by droplet microfluidic solvent evaporation and extraction approaches. *Lab on a Chip* 10, 1820-1825 (2010).

186. Mohan P, Rapoport N. Doxorubicin as a molecular nanotheranostic agent: effect of doxorubicin encapsulation in micelles or nanoemulsions on the ultrasound-mediated intracellular delivery and nuclear trafficking. *Mol Pharm* 7, 1959-1973 (2010).

187. I. Brigger PCVM, M. Appel, M. Besnard,R. Gurny, M. Renoir, P. Couvreur. Tamoxifen encapsulation within polyethylene glycol-coated nanospheres. A new antiestrogen formulation. (2001).

188. Ke Y*, et al.* Size Controlling of Monodisperse Carboxymethyl Cellulose Microparticles via a Microfluidic Process. *Journal of Applied Polymer Science* 131, (2014).

189. Lim J-M*, et al.* Parallel microfluidic synthesis of size-tunable polymeric nanoparticles using 3D flow focusing towards in vivo study. *Nanomedicine-Nanotechnology Biology and Medicine* 10, 401-409 (2014).

190. Andar AU, Hood RR, Vreeland WN, DeVoe DL, Swaan PW. Microfluidic Preparation of Liposomes to Determine Particle Size Influence on Cellular Uptake Mechanisms. *Pharmaceutical Research* 31, 401-413 (2014).

191. He J*, et al.* Vesicular Self-Assembly of Colloidal Amphiphiles in Microfluidics. *Acs Applied*

Materials & Interfaces 5, 9746-9751 (2013).

192. Vladisavljevic GT*, et al.* Industrial lab-on-a-chip: Design, applications and scale-up for drug discovery and delivery. *Advanced Drug Delivery Reviews* 65, 1626-1663 (2013).

193. A. J. Webster MEC. Stabilization of Emulsions by Trapped Species. *Langmuir*, (1998).

194. Liu D*, et al.* Microfluidic Assembly of Monodisperse Multistage pH-Responsive Polymer/Porous Silicon Composites for Precisely Controlled Multi-Drug Delivery. *Small* 10, 2029-2038 (2014).

195. Khan IU*, et al.* Microfluidic conceived drug loaded Janus particles in side-by-side capillaries device. *International Journal of Pharmaceutics* 473, 239-249 (2014).

196. P.Chang E. Controlled Emulsion Droplet Solvent Evaporation for Particle Production. (2013).

197. Routh ADEaAF. Evaporation of Pinned Droplets Containing Polymer – An Examination of the Important Groups Controlling Final Shape. (2015).

198. Roland H. Staff DS, Andrey Turshatov , Davide Donadio ,, Hans-Jürgen Butt KL, Kaloian Koynov , * and Daniel Crespy *. Particle Formation in the Emulsion-Solvent Evaporation Process (2013).

199. Schubert S, Delaney JT, Jr., Schubert US. Nanoprecipitation and nanoformulation of polymers: from history to powerful possibilities beyond poly(lactic acid). *Soft Matter* 7, 1581-1588 (2011).

200. Bilati U, Allemann E, Doelker E. Nanoprecipitation versus emulsion-based techniques for the encapsulation of proteins into biodegradable nanoparticles and process-related stability issues. *AAPS PharmSciTech* 6, E594-604 (2005).

201. Huang X, Lowe TL. Biodegradable thermoresponsive hydrogels for aqueous encapsulation and controlled release of hydrophilic model drugs. *Biomacromolecules* 6, 2131-2139 (2005).

202. Gallarate M, Trotta M, Battaglia L, Chirio D. Preparation of solid lipid nanoparticles from W/O/W emulsions: Preliminary studies on insulin encapsulation. *Journal of Microencapsulation* 26, 394-402 (2009).

203. Pramod PS, Takamura K, Chaphekar S, Balasubramanian N, Jayakannan M. Dextran Vesicular Carriers for Dual Encapsulation of Hydrophilic and Hydrophobic Molecules and Delivery into Cells. *Biomacromolecules* 13, 3627-3640 (2012).

204. Shen J, Deng Y, Jin X, Ping Q, Su Z, Li L. Thiolated nanostructured lipid carriers as a potential ocular drug delivery system for cyclosporine A: Improving in vivo ocular distribution. *International Journal of Pharmaceutics* 402, 248-253 (2010).

205. Capretto L, Cheng W, Carugo D, Katsamenis OL, Hill M, Zhang X. Mechanism of co-nanoprecipitation of organic actives and block copolymers in a microfluidic environment. *Nanotechnology* 23, (2012).

206. Farago PV, Raffin RP, Pohlmann AR, Guterres SS, Zawadzki SF. Physicochemical characterization of a hydrophilic model drug-loaded PHBV microparticles obtained by the double emulsion/solvent evaporation technique. *Journal of the Brazilian Chemical Society* 19, 1298-1305 (2008).

207. Magenheim B, Levy MY, Benita S. A NEW IN-VITRO TECHNIQUE FOR THE EVALUATION OF DRUG-RELEASE PROFILE FROM COLLOIDAL CARRIERS - ULTRAFILTRATION TECHNIQUE AT LOW-PRESSURE. *International Journal of Pharmaceutics* 94, 115-123 (1993).

208. Gaudana R, Jwala J, Boddu SHS, Mitra AK. Recent Perspectives in Ocular Drug Delivery. *Pharmaceutical Research* 26, 1197-1216 (2009).

209. Andreas Jordan RS, Peter Wust, Horst Fähling, Roland Felix. Magnetic fluid hyperthermia (MFH): Cancer treatment with AC magnetic field induced excitation of biocompatible superparamagnetic nanoparticles. *Journal of Magnetism and Magnetic Materials*, (1999).

210. Rudolf Hergt SD, Robert Müller and Matthias Zeisberger. Magnetic particle hyperthermia: nanoparticle magnetism and materials development for cancer therapy. *Journal of Physics: Condensed Matter*, (2006).

211. Liang Cheng KY, Yonggang Li, Jianhua Chen, Chao Wang, Mingwang Shao, Shuit-Tong Lee, Zhuang Liu. Facile Preparation of Multifunctional Upconversion Nanoprobes for Multimodal Imaging and Dual-Targeted Photothermal Therapy. *Angewandte Chemie-International Edition*, (2011).

212. Reju Thomas I-KP, Yong Yeon Jeong Magnetic Iron Oxide Nanoparticles for Multimodal Imaging and Therapy of Cancer. *International Journal of Molecular Sciences*, (2013).

213. Mi Kyung Yu YYJ, Jinho Park, Sangjin Park, Jin Woong Kim, Jung Jun Min,Kyuwon Kim, Sangyong Jon. Drug-Loaded Superparamagnetic Iron Oxide Nanoparticles for Combined Cancer Imaging and Therapy In Vivo. *Angewandte Chemie-International Edition*, (2008).

214. Timothy A Larson JB, Jesse Aaron and Konstantin Sokolov. Hybrid plasmonic magnetic nanoparticles as molecular specific agents for MRI/optical imaging and photothermal therapy of cancer cells. *Nanotechnology*, (2007).

215. Eddington DT, Beebe DJ. Flow control with hydrogels. *Advanced Drug Delivery Reviews* 56, 199-210 (2004).

216. Tapan K. Jain JR, Michelle Strand, Diandra L. Leslie-Pelecky, Chris A. Flask, Vinod Labhasetwar.

Magnetic nanoparticles with dual functional properties: Drug delivery and magnetic resonance imaging. *Biomaterials*, (2008).

217. Manfred Johannsen， Uwe Gneveckow BT, Kasra TaymoorianChie Hee Chob, Norbert Waldofner , Regina Scholz , Andreas Jordan, Stefan A. Loening, Peter Wustb. Thermotherapy of Prostate Cancer Using Magnetic Nanoparticles Feasibility, Imaging, and Three-Dimensional Temperature Distribution. *European Urology*, (2007).

218. Jaeyun Kim SP, Ji Eun Lee, Seung Min Jin,Jung Hee Lee, In Su Lee, Ilseung Yang, Jun-Sung Kim,Seong Keun Kim, Myung-Haing Cho, andTaeghwan Hyeon. Designed Fabrication of Multifunctional Magnetic Gold Nanoshells and Their Application to Magnetic Resonance Imaging and Photothermal Therapy. *Angewandte Chemie-International Edition*, (2006).

219. Xiang-Hong Peng XQ, Hui Mao, Andrew Y Wang, Zhuo (Georgia) Chen, Shuming Nie, Dong M Shin. Targeted magnetic iron oxide nanoparticles for tumor imaging and therapy. *International Journal of Nanomedicine*, (2008).

220. Esther Amstad S-HK, and David A. Weitz. Photo- and Thermoresponsive Polymersomes for Triggered Release. *Angewandte Chemie-International Edition*, (2012).

221. C.-H. Yang K-SH, Y.-S. Lin, K. Lu, C.-C. Tzeng,E.-C. Wang, C.-H. Lin,W.-Y. Hsua and J.-Y. Chang. Microfluidic assisted synthesis of multi-functional polycaprolactone microcapsules: incorporation of CdTe quantum dots, Fe3O4 superparamagnetic nanoparticles and tamoxifen anticancer drugs†. *Lab on a Chip*, (2008).

222. N. Schleich PS, P. Danhier, B. Ucakar, S. Laurent, R.N. Muller, C. Jérôme, B. Gallezc, V. Préat, F. Danhier. Dual anticancer drug/superparamagnetic iron oxide-loaded PLGA-based nanoparticles for cancer therapy and magnetic resonance imaging. *International Journal of Pharmaceutics*, (2013).